ACS OMEGA

http://pubs.acs.org/journal/acsodf

Review

Heteroatom Codoped Graphene: The Importance of Nitrogen

Pablo A. Denis*

Cite This: *ACS Omega* 2022, 7, 45935−45961

Read Online

ACCESS | Metrics & More | Article Recommendations

ABSTRACT: Although graphene has exceptional properties, they are not enough to solve the extensive list of pressing world problems. The substitutional doping of graphene using heteroatoms is one of the preferred methods to adjust the physicochemical properties of graphene. Much effort has been made to dope graphene using a single dopant. However, in recent years, substantial efforts have been made to dope graphene using two or more dopants. This review summarizes all the hard work done to synthesize, characterize, and develop new technologies using codoped, tridoped, and quaternary doped graphene. First, I discuss a simple question that has a complicated answer: When can an atom be considered a dopant? Then, I briefly discuss the single atom doped graphene as a starting point for this review's primary objective: codoped or dual-doped graphene. I extend the discussion to include tridoped and quaternary doped graphene. I review most of the systems that have been synthesized or studied theoretically and the areas in which they have been used to develop new technologies. Finally, I discuss the challenges and prospects that will shape the future of this fascinating field. It will be shown that most of the graphene systems that have been reported involve the use of nitrogen, and much effort is needed to develop codoped graphene systems that do not rely on the stabilizing effects of nitrogen. I expect that this review will contribute to introducing more researchers to this fascinating field and enlarge the list of codoped graphene systems that have been synthesized.

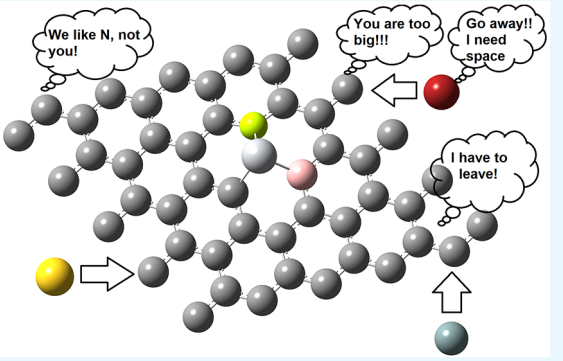

1. INTRODUCTION

Humanity is facing a point of no return because if most of the planet's population does not change their lifestyle, we will unchain the sixth extinction event on Earth. Chemistry alone cannot solve all the problems; it cannot stop wars or end racism or religious conflicts. However, chemistry can help humanity solve many pressing difficulties that urgently need to be circumvented, such as energy production, conversion, and storage, water purification, development of CO_2 capture systems, drug design, and food production, to mention just a few. To that end, discovering new materials with tailored properties has become an obsession. Graphene[1,2] is one of the rising stars in science. Nonetheless, despite its fantastic natural properties, the pristine form of graphene has limited use. Up to now there is not a flagship product derived from graphene as there is the transistor derived from silicon.

Several methods have been designed to modify graphene: it can be chemically functionalized,[3,4] external stress or electrical fields can be applied, and some of the carbon atoms of the graphene framework can be replaced by heteroatoms, a process that introduces an impurity in the system.[5−12] The latter will be the focus of this review. Although significant advances have been made in the preparation of single atom doped graphene, and the properties induced by elemental doping are fascinating,[5−12] a new research direction has been opened: the introduction of more than one dopant type in the graphene framework. This transformation is known as the codoping of graphene or sometimes as the dual doping of graphene when it exclusively refers to introducing two foreign atoms. Experimental research and theoretical research have demonstrated that the introduction of at least two dopants can dramatically alter the physicochemical properties of graphene. As an example, I mention the adsorption of lithium on mono- and codoped graphene with 2p and 3p elements.[13] As we can appreciate in Table 1, the adsorption energies of Li on N and S doped graphene are −0.72 and −1.25 eV, respectively. Interestingly, when the N and S dopants are introduced simultaneously, the adsorption energy of Li becomes −2.99 eV, about 1 eV larger than the sum of the adsorption energies of Li on N and S doped graphene.[13] This is not an isolated example of the dramatic effects that codoping can induce, as I will describe in this review.

Several examples in the literature that evidence the advantage of introducing two, three, or even four different heteroatoms will be reported below. The present review is organized in the following way: I first discuss in section 2 what can be considered

Received: September 17, 2022
Accepted: November 17, 2022
Published: December 5, 2022

https://doi.org/10.1021/acsomega.2c06010
ACS Omega 2022, 7, 45935−45961

Table 1. Interaction Energies, Magnetic Moments, Li−X Distances and Charges Determined for XY Dual Doped Graphene Interacting with a Single Lithium Atom, at the VDW-DF/DZP Level of Theory

		IE (eV)			
XY	position of Li	XY ortho[a]	XY para[b]	d_{Li-X} (Å) XY ortho	Q (μ_B) XY ortho
AlB	below Al	−2.11	−2.52	2.75	1.0
AlN	below Al	−2.16	−2.03	2.66	1.0
AlO	below Al	−2.27	−2.23	2.83	0.0
SiB	below Si	−2.41	−2.59	2.62	0.62
SiN	below Si	−2.18	−2.14	2.70	0.0
SiO	below Si	−1.97	−1.90	2.77	0.0
PB	below P	−1.89	−1.45	2.67	0.06
PN	below P	−1.44	−1.41	2.65	0.19
PO	below P	−2.30	−1.34	2.73	0.0
SB	below S	−1.79	−1.87	2.81	0.06
SN	below S and bonded to N	−2.99	−1.35	2.77	0.0
SO	below S	−1.84	−1.38	2.74	0.0
B	below B-hex	−2.41		2.33	0.0
N	below N-hex	−0.72		2.34	0.0
graphene	over hex	−1.11		2.32	0.0

[a]Ortho disposition of dopants. [b]Para disposition of dopants.

a dopant since there is no consensus in the literature, and then I briefly inform in section 3 which dopants have been introduced in the graphene framework. In section 4, I advocate commenting on the codoped graphene systems that have been studied, and finally, to conclude the review, in section 5 I indicate the challenges that need to be surmounted for the title field to mature. Finally, I apologize for all the articles that have not been included in this review. The literature about doped graphene contains over 1 million articles, thesis, books, and technical reports. Including all of them in a single review would be impossible. Nevertheless, I expect that the nearly 500 works included cover most of the examples available in the literature and contribute to developing this fascinating research area.

2. WHEN CAN A HETEROATOM BE CONSIDERED A DOPANT?

In this review, heteroatom doping of graphene is considered to be attained when at least one carbon atom of graphene is replaced by another element. Although this definition seems straightforward, when reading the literature, it is possible to become confused. For example, several publications claim to have doped graphene with fluorine atoms.[14−21] Considering that fluorine has a strong tendency to form only single bonds because it has seven valence electrons, it is not easy to imagine this element embedded in the graphene framework replacing a carbon atom, as it will bind only with one carbon atom. Vineesh et al.[14] reported that N and F codoped graphene displays "enhanced electrocatalytic efficiency than the 'N' and 'F' individually doped graphene" for the oxygen reduction reaction (ORR). In Vineesh's work,[14] nitrogen was introduced by thermal treatment of fluorinated graphene in the presence of melamine. The amounts of N and F introduced were 2 and 4 atom %, respectively. XPS confirmed the presence of nitrogen in several forms—pyrrolic, pyridinic, and graphitic—while in the case of fluorine C−F and F−C−F bonds were confirmed. Along the same line, Jiang et al.[15] prepared N and F codoped graphene by thermal treatment of graphene oxide/polyaniline composites and NH_4F. It was proposed as an efficient metal-free ORR catalyst in fuel cells. XPS confirmed the presence of N and F. Nitrogen was found in the same configuration discussed above. However, fluorine was proposed to be present in ionic and semi-ionic C−F bonds. Liu et al.[16] also reported the preparation of N and F codoped graphene. The method was simple: they fluorinated N-doped reduced graphene oxide using XeF_2 at 180 °C. XPS confirmed C−F covalent bonding, and two more peaks corresponding to $CF-CF_n$ and CF_2 were determined. The material exhibited interesting photoluminescence properties. Although the presented results represented a significant advance over the existing literature, it is hard to accept that the fluorine atoms are dopants. Instead, in my opinion it is fairer to consider fluorine a functional group covalently attached to graphene but not a member of the graphene framework because, once a fluorine atom is added, nothing more can be bonded.

Fluorine is not the only halogen reported to accompany nitrogen or phosphorus dopants. There are reports in the literature of nitrogen and halogen codoped graphene, with particular attention to iodine,[22−24] and P−X codoped graphene with X = Cl, Br, and I.[25] In general, the amount of iodine is small, below 1%, and XPS is not conclusive on the nature of the iodine dopant. Wu et al.[22] determined that, in PI codoped graphene, the high resolution of the XPS signal corresponded to I_3 and I_5. Thus it is unlikely that iodine was introduced in the graphene framework. Instead, it is more likely to be adsorbed between graphene layers. Nevertheless, it should be remembered that halogens heavier than fluorine have the capability to form multiple bonds and may be able to replace carbon atoms. Finally, it is essential to mention that, despite being adsorbed, halogens can effectively "dope" graphene because they are natural σ-donors and π-electron withdrawers.[25] Therefore, despite the nature of the halogen dopant, i.e., adsorbed or embedded, it works as a dopant, but adsorbed halogens will not be covered in this review.

Finally, it is interesting to mention the case of oxygen. First, it is crucial to consider that it is a common practice to obtain graphene sheets by reducing graphene oxide. In some cases, the reduction is not complete, and also during this process, dopants are introduced using a suitable gas. Considering that in some cases oxygen is not 100% eliminated, in practice, two dopants are present—the one whose introduction was pursued using a gas (for example) and oxygen—so many cases of single atom doping are truly codoped graphene systems. Zhan et al.[23] observed the O 1s peak when preparing the I and N codoped graphene nanocomposite described above. The codoping with iodine and nitrogen better facilitated oxygen bonding than the single atom doping of nitrogen or iodine.[23] Therefore, caution should be taken when doping is claimed because doping may have been achieved by functionalization, adsorption, or substitution. The latter process is the one that I discuss herein. I considered that an atom is a dopant if it is embedded in the graphene framework replacing one or more carbon atoms.

3. BRIEF SUMMARY OF SINGLE-ATOM-DOPED GRAPHENE

When replacing a carbon atom with a dopant, it is not surprising to find that, as early as 2009, Panchakarla et al.[26] reported the preparation of boron[26−28] and nitrogen[26,28−35] doped graphene. These two elements present atomic radii of 85 and 65 pm, respectively, very close to the value of carbon, 70 pm. Therefore, the graphene sheet will not suffer excessive stress if these elements are embedded in the graphene framework. The

https://doi.org/10.1021/acsomega.2c06010
ACS Omega 2022, 7, 45935−45961

influence of precursors and synthesis conditions on the preparation of N-doped graphene have been established in the milestone investigation by Wang et al.[30] as early as 2014. Also, for a detailed review of the different strategies available to synthesize N-doped graphene, we refer the readers to the excellent review by Vesel et al.[35] In particular, Table 1 of the latter summarizes the postsynthesis of N-doped graphene while Table 2, of the same reference, provides an overview of the literature on the direct synthesis of N-doped graphene. A slightly different situation is observed for Be-doped graphene. Although this element has only four electrons, theoretical calculations have shown that the Be atom does not lie in the graphene but bulges out of the sheet.[36,37] The protrusion is significant; for example, in a 5 × 5 graphene sheet, the Be atom is located 0.78 Å above the carbon atoms. Although this system is stable, it is waiting to be synthesized. It is expected to have outstanding properties that may render it valid as an anode material for lithium ion batteries.[37] Moving down in the periodic table, Al-doped graphene was studied for more than 10 years by theoretical materials scientists.[38−44] It was not until recently that Al-doped graphene was prepared.[45−47] It was the last 3p element used to dope graphene. Ullah et al.[46] successfully prepared a large area Al-doped graphene by chemical vapor deposition. Zagler et al.[47] showed that the Al dopants were found in 3- and 4-fold coordinated configurations. Occasionally N dopants were found to be embedded in the graphene framework and bonded to Al, as predicted by us.[48,49]

On the contrary, Si-doped graphene[50−56] was prepared earlier. In 2012, Zhou et al.[50] reported that Si atoms could be found in mono- and divacancies in the graphene layer. When Si is bonded to three atoms, it prefers sp^3 hybridization, but if it is bonded to four atoms, sp^2 d-like hybridization is adopted. As observed for Al, nitrogen was sometimes found to replace one of the carbon atoms bonded to the Si impurities, again in agreement with our findings.[48,49] Si-doped graphene is expected to have outstanding mechanical,[52] electronic,[53−55] and optical properties.[54,55] Also, I have demonstrated that, when it is present in the graphene layer, it can promote cycloaddition reactions,[56] which can be difficult to attain on perfect graphene.[57] The main effect of the Si dopant is to reduce the enormous deformation energy required to form a covalent bond with the diene or dienophile. It has the same effect as a functional group[58] present before the cycloaddition reaction or the SiC surface in which graphene can grow.[59]

The doping of graphene with phosphorus[60−69] has been developed at least since 2012 when Some et al.[60] reported the preparation of P-doped graphene, air-stable n-type field effect transistors. The system consisted of P-doped, double-layered graphene sheets. Subsequent reports by Li et al.[61] and Zhang et al.[62] also reported the preparation of P-doped graphene in 2013. This system has unique electronic and magnetic properties[39,40,53,66,67] for designing metal-free ORR catalysts,[61,62] Li ion batteries,[62] and NH_3 sensors.[63] It is important to notice that Susi et al.[64] were the first to obtain atomic resolution imaging and electron energy loss spectroscopy evidencing the presence of phosphorus atoms in the graphene lattice.

In 2009, I reported one of the first studies about sulfur-doped graphene and found that this material may have remarkable properties.[42,43,70] Three years later, Yang et al.[71] reported the preparation of sulfur-doped graphene as an efficient metal-free cathode catalyst for ORR reactions. Similarly, Yang et al.[72] also reported the preparation of S-doped graphene based on ultrathin graphene oxide for ORR reactions. Also, in 2012, Rao et al.[73] used liquid precursors to prepare S-doped graphene. The synthesis of the latter has been mastered during the last years, and many routes are available to obtain S-doped graphene, even large area sheets.[71−76]

Going down in the periodic table, I studied graphene doped with the 4p elements Ga, Ge, As, and Se.[77] These nanomaterials exhibited outstanding electronic and magnetic properties and high reactivity near the dopant site, which may render them valuable catalysts. In 2018, Tripathi et al.[78] implanted germanium in a graphene framework. The authors claimed that $^{74}Ge^+$ was the heaviest impurity implanted into monolayer graphene at that time. This atom can substitute a single carbon atom, bonding to three neighbors, or be 4-fold coordinated in a divacancy. In their 2012 article about S-doped graphene, Yang et al.[71] also claimed to have prepared Se-doped graphene by direct annealing of graphene oxide in the presence of diphenyl diselenide in argon. XPS studies confirmed the presence of Se atoms, and Se content did not change after sonication. Therefore, it was concluded that diphenyl diselenide was not adsorbed. However, further studies are necessary to have a more specific description of Se doping. In 2018, Meng et al.[79] prepared Se-doped graphene for high-efficiency triiodide reduction in dye-sensitized solar cells. SEM mappings revealed the presence of C, O, and Se. The distribution of Se was uniform, and it was concluded that Se atoms were incorporated into the graphene framework.

Turning our attention to the 3d metals, Toh et al.[80] prepared Mn-, Fe-, Co-, and Ni-doped graphene hybrids, which are helpful in electrocatalysis. Carnevali et al.[81] doped epitaxial graphene by direct incorporation of Ni adatoms. Scandium-doped graphene was also reported in 2019 by Wen et al.,[82] but nitrogen was necessary as a stabilizer. Again, as observed for Al and Si, the presence of Sc−N was confirmed by XPS. Robertson et al.[83] studied the dynamics of Fe atoms in graphene single and double vacancies, as can be appreciated in Figure 1, and as early as 2014, Zhao et al.[84] reported the synthesis of a free-standing, single-atom-thick Fe layer in a graphene pore. More recently, Mn-doped graphene[85] was prepared with a Mn concentration of 0.04 atom %. Magnesium was unambiguously located in a single vacancy, but the introduction in divacancies and other structures were observed also. Nevertheless, their structural identification is not clear.

Heavier elements like gold were implanted by Trentino et al.[86] using a two-step implantation process. The new doping method utilizes a two-step low-energy ion implantation technique that, according to the authors, "overcomes the limitation posed by momentum conservation on the mass of the implanted species." The gold atoms occupy double vacancy sites. Finally, Nb-doped graphene was prepared by Li et al.[87] The strategy employed to obtain Nb-self-doped graphene was to prepare it from 2D NbC, only by one step of incomplete chlorination. This proposal is similar to the procedure I suggested to prepare Si-doped graphene. The structure is shown in Figure 2. The partial annealing to the SiC layer may leave some Si atoms in a specific disposition of the dopants.[88] Finally, Sofer et al.[89] reported the preparation of U- and Th-doped graphene. However, XPS was not conclusive in the nature of the dopants since the energies of the U 4f peaks indicated the presence of the form UO_3, U_3O_8, or uranium carbide.

4. CODOPED OR DUAL-DOPED GRAPHENE

4.1. B and N Codoped Graphene. Boron and nitrogen are the most obvious choices to dope graphene because they bracket

https://doi.org/10.1021/acsomega.2c06010
ACS Omega 2022, 7, 45935−45961

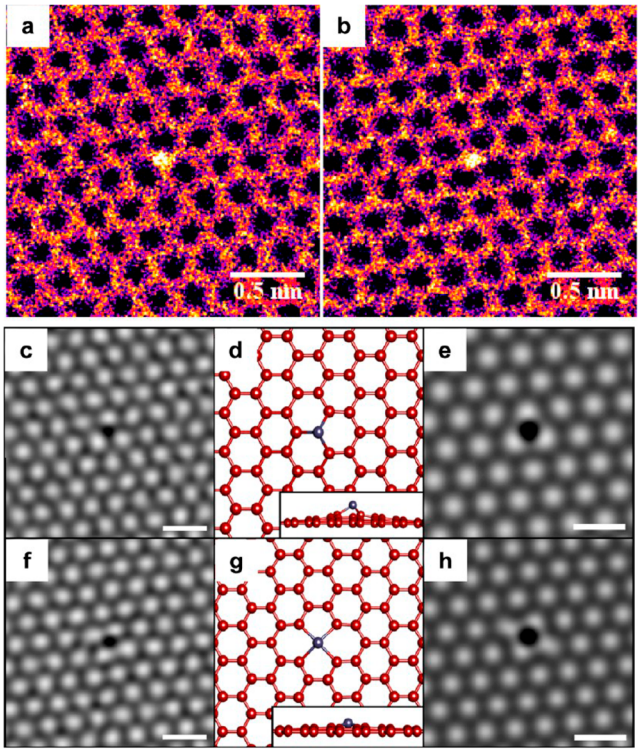

Figure 1. False color aberration-corrected TEM images of (a) an Fe substitutional defect in a graphene monovacancy (Fe@MV) and (b) an Fe interstitial defect occupying a divacancy (Fe@DV). (c) Smoothed aberration-corrected TEM image of the Fe@MV shown in (a). (d) DFT optimization of the Fe@MV structure (the inset shows a side view) and (e) a multislice TEM image simulation of the system. (f–h) Similar to (c)–(e) but for a DFT-optimized Fe@DV. Scale bars denote 0.5 nm. Reproduced from ref 83. Copyright 2013 American Chemical Society.

carbon in the periodic table. The fact that they have smaller and larger electronegativities than carbon makes them very appealing to develop metal-free catalysts, thanks to the charge imbalance induced by their presence. In 2013, Zheng et al.[90] reported the preparation of B and N codoped graphene with long-term stability and excellent activity for the ORR. The two-step method prevented the formation of catalytically inactive byproducts such as hexagonal boron nitride and induced a cooperative effect between the dopants. One year later, the solvothermal synthesis of B and N codoped graphene was achieved,[91] and various theoretical studies were published highlighting the unique electronic properties of this system.[92−98] As discussed in section 3, one of the main applications of doped graphene is as a catalyst for the ORR. B and N codoped graphene is not the exception, and multiple studies demonstrated that it could be an excellent catalyst for the ORR.[98−108] Another essential use of B and N codoped graphene is in lithium batteries[109−112] and sodium ion batteries.[113] Huang et al.[109] reported a high capacity of up to 909 mAh g^{-1} and an excellent discharge capacity after 125 cycles. Three-dimensional B and N codoped graphene has been employed to construct symmetric and asymmetric supercapacitor electrodes.[114−116] The work by Kang et al.[114] demonstrated that the specific capacitance of 283 F g^{-1} at 1 A g^{-1}, in alkaline aqueous electrolyte, is more remarkable than those corresponding to N or B monodoped graphene.

In the catalysis area, it has been demonstrated that B and N codoped graphene can be an excellent catalyst for the electrooxidation of formic acid[117] methanol[118] and the reduction of nitroarenes[119] and triiodide.[120] The development of graphene based sensors is another field in which B and N codoped graphene has excelled. It has been able to detect aflatoxin B1,[121] mercury(II),[122,123] fluorine ions,[123] hydrogen peroxide,[124] cymoxanil,[125] and NO_2,[126] to mention just a few examples of molecules that can be monitored using B and N codoped graphene.

B and N codoped graphene quantum dots have fascinating optical properties.[127−130] They can be used in imaging and photothermal therapies.[128] In a related area, B and N codoped graphene was used in dye-sensitized solar cells,[129,130] as a counter electrode for iodine reduction.[130] Finally, it has been shown that codoping with B and N enhances the electromagnetic interference shielding (EMI)[131−134] to −42 dB (99.99% of attenuation) at a critical thickness of 1.2 mm.[133]

4.2. O and N Codoped Graphene. I explained above that I considered an atom a dopant if embedded in the graphene framework replacing one or more carbon atoms. Nevertheless, I have included O and N codoped graphene in this review because plenty of works report preparations and applications of this system.[135−146] In 2014, Chen et al.[135] reported that N and O codoped carbon hydrogel could be used as substrate-free electrode for highly efficient oxygen evolution reaction.[135] The nitrogen atoms were introduced with ammonium hydroxide, but the oxygen atoms were residual oxygen impurities on graphene prepared by a chemical method. Oxygen was present in the forms carboxyl and epoxy, so it is questionable if oxygen is a dopant because COOH and COC groups can be present without replacing carbon atoms. I do not argue against the utility of these groups as catalytic centers for the oxygen evolution reaction, but they should be named functional groups instead of dopants, in my opinion. Again the discussion if oxygen can be considered a dopant emerges. Li et al.[138] assembled O and N

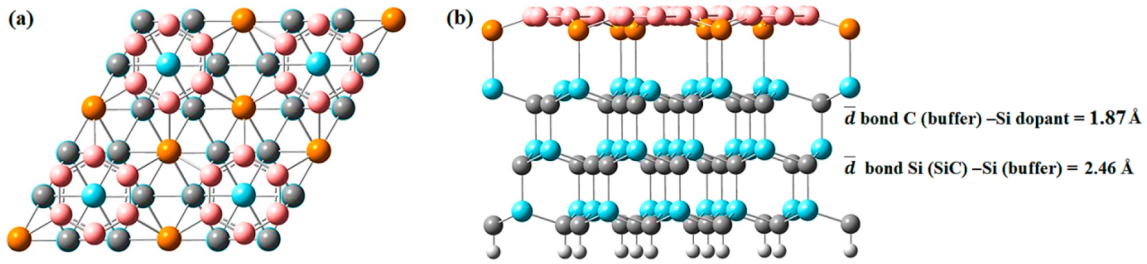

Figure 2. Top (a) and side (b) views of the optimized unit cell for 4 × 4 siligraphene on 6H-SiC(0001). Carbon, silicon, and hydrogen atoms in SiC are colored in gray, light blue, and white, respectively. Carbon and silicon atoms in the siligraphene layer are colored pink and orange, respectively.

https://doi.org/10.1021/acsomega.2c06010
ACS Omega 2022, 7, 45935−45961

Table 2. Relative Energies (eV) between the Five Configurations Studied of the Dopants and Heteroatom Bond Distances (Å) at the M06-L/6-31G* and VDW-DF/DZP Levels of Theory

	ortho M06-L	meta M06-L	para M06-L	para VDW-DF	same latt M06-L	diff latt M06-L	XY distance (Å)[a] M06-L
AlB	0.0	0.57	0.10	−0.20	0.76	0.80	2.16
AlN	0.0	1.82	1.90	1.70	2.19	2.18	1.81
AlO	0.0	3.97	3.69	3.48	4.55	4.65	1.97
SiB	0.47	0.22	0.0	−0.60	0.19	0.26	1.88
SiN	0.0	1.34	1.34	1.19	1.59	1.54	1.80
SiO	0.0	3.57	2.91	2.76	3.76	3.64	2.02
PB	0.0	0.35	0.04	−0.05	0.60	0.67	1.80
PN	0.0	1.01	0.70	0.61	1.09	1.00	1.78
PO	0.0	3.13	2.71	2.51	3.27	3.17	2.48
SB	0.0	0.86	0.82	0.67	1.25	1.34	1.82
SN	0.0	1.56	1.32	1.18	1.46	1.43	2.58
SO	0.0	5.20	5.64	5.28	5.17	5.41	2.59

[a]XY distance corresponds to the 2p and 3p dopants in an ortho arrangement (case a)).

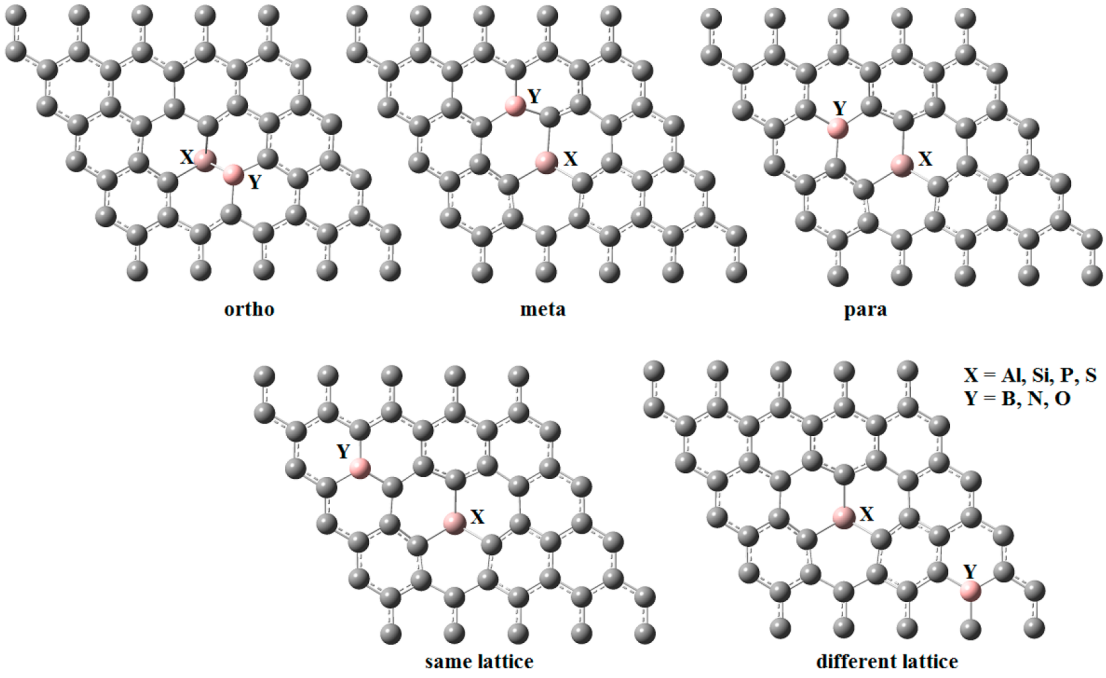

Figure 3. Substitution sites considered to study the structure of codoped graphene.

codoped graphene on hierarchical carbon networks for all-solid-state flexible supercapacitors. XPS studies revealed that 11% of N was pyridinic and 85% was pyrrolic. However, oxygen was located at the edges as hydroxyl groups. Therefore, in this case, the claim that oxygen is a dopant is at least questionable. In our opinion, the material is N-doped graphene functionalized with hydroxyl groups. Supercapacitor electrodes were constructed using N- and O-doped graphene.[136−139] Lithium[140−143] and potassium[143−146] ion batteries based on N and O codoped graphene are available. Excellent potassium storage was achieved. For example, a reversible capacity of 464.9 mAh g^{-1} at 0.05 A g^{-1} was reported by Ruan et al.[146]

4.3. S and N Codoped Graphene. Despite the fact that sulfur does not fit in the graphene plane and bulges out of the sheet,[70] the most studied codoped graphene system is sulfur and nitrogen codoped graphene. There are so many articles published about this system[147−360] that a review could be written. Including all the works dealing with this system would be an interminable task, so I apologize for the papers not being cited. In 2012, Liang et al.[147] reported the one-step synthesis of sulfur and nitrogen codoped mesoporous graphene for the ORR with a synergistically enhanced performance. The ORR activity was comparable to that of the best commercial Pt/C catalysts and better than the activity measured when only one of the dopants was present. The N and S elemental contents were 4.5 and 2.0 atom %, respectively. Nitrogen was present in the typically observed forms of pyridinic, pyrrolic, and graphitic, while sulfur was present in the thiophenic forms of C−S−C. These results are in partial agreement with our investigations on this system. By means of first principles calculations, I studied all codoped graphene systems with one 3p and one 2p element.[48,49,148] Our results revealed a notorious preference for the dopants to be located in specific positions. All XY codoped graphene systems (X = B, N, O; Y = Al, Si, P, S) preferred to replace contiguous C atoms (a CC bond) instead of being separated at large distances or in para/meta positions, as can be appreciated in Table 2; the structures are presented in Figure 3. There was only one exception to this empirical rule: Si

https://doi.org/10.1021/acsomega.2c06010
ACS Omega 2022, 7, 45935−45961

and B codoped graphene, for which there was a slight preference for the atoms to adopt a para arrangement. The case of S and N codoped graphene is very particular because the atoms replace a CC bond but the dopants are not bonded. In effect, the nitrogen atoms adopt a pyridinic disposition and the sulfur atom protrudes out of the sheet, as shown in Figure 4. Therefore,

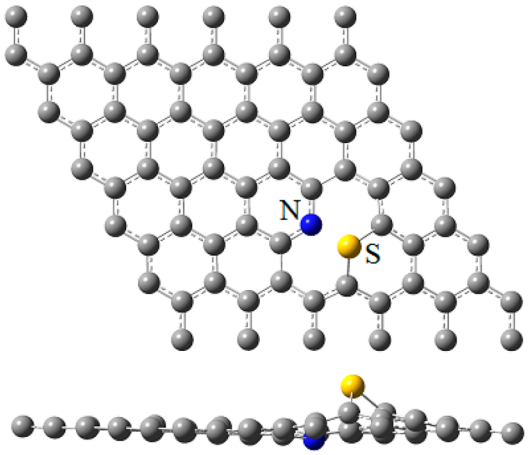

Figure 4. Optimized 6 × 6 unit cell for sulfur and nitrogen dual-doped graphene.

nitrogen prefers a C−N−C environment and sulfur prefers a C−S−C environment. This particular dopant disposition may explain this system's unusual properties. For example, adding O_2 to S and N codoped graphene is very exothermic, forming an SO_2 unit bonded to graphene.[148]

Many methods are capable of producing S and N codoped graphene. It is possible to start from graphene oxide produced via Hummers' method and use melamine and benzyl disulfide as N and S precursors. A different approach was proposed by Kicinski et al.,[155] who copolymerized S- and N-containing heterocyclic aldehydes, whereas Chen et al.[156] used methyl blue/montmorillonite composites. A green route to S and N codoped graphene is also available by using Chinese medical herbs, as proposed by Feng et al.[157] Along the same line, Wu et al.[158] reported that, assisted by supramolecular polymerization, petroleum coke can be converted into S and N codoped graphene. This approach is exciting because it starts from a byproduct of the oil refinery industry. In theory, creating a new synthetic route using a different heterocycle is possible. For example, Zhang et al.[159] self-polymerized polydopamide and then reacted the product with cysteine. These are six examples of the methods available to obtain S and N codoped graphene. More synthetic routes can be found in the references cited, but in our opinion, all of them offer advantages and disadvantages, such as the quality of the sheets prepared, their area, and the bonding nature of the dopants. The main problem with the synthetic procedures available is that there is no good structure−activity relationship.

The main application of the prepared S and N codoped graphene materials has been in perhaps the most critical reaction in the industry, the oxygen reduction reaction. Following the first work by Liang et al.[147] commented on above, more than 40 papers were published reporting the catalytic power of S and N codoped graphene for the ORR reaction.[154,158−201] Most of these works evidence a performance similar to or superior to those of commercial Pt/C catalysts and superior stability. Nevertheless, more work is needed because, to the best of our knowledge, S and N codoped graphene is not the most used catalyst for oxygen reduction/evolution reactions. For a more detailed review of carbon based metal-free ORR catalysts, I refer the reader to the review by Ma et al.[202]

Another vital reaction that the graphene community has intensively studied is the hydrogen evolution reaction (HER).[203−212] Jiang et al.[203] used an intelligent approach to synthesize S and N codoped graphene from a mixture of urea, glucose, and phosphoric acid. The high dopant content and porosity conferred a high catalytic activity in the HER reaction with an onset potential of 0.12 V and a Tafel slope of 79 meV/dec, values that are comparable with those of an average metallic catalyst. There have been some improvements in these values. For example, Guruprasad et al.[204] reduced the Tafel slope to 47 meV/dec However, to the best of our knowledge, graphene based catalysts have not replaced the ones previously utilized in the industry. In this line, the photocatalytic production of hydrogen from water splitting is crucial for humankind. S and N codoped graphene has been combined with TiO_2 to improve the activity under visible light significantly. S and N graphene based materials are generally used as light absorbers combined with TiO_2 or similar materials.[208,209]

The use of S and N codoped graphene as a catalyst is not limited to the ORR and HER reactions. It has been used with great success for catalytic phenol degradation,[212,213] nitrogen reduction,[214] methanol[213−217] and ethanol[218] electrooxidation, aerobic oxidation of alcohols[219] under visible light irradiation, and sonocatalytic decolorization of methylene blue.[220] Another area of utmost importance is organic catalysis. Some works reported using S and N codoped graphene for Sonogashira[221] and Heck couplings.[222] Although Pd nanoparticles were still necessary, the presence of the graphene material contributed to a more effective use of the expensive Pd catalyst.

There are several examples in which S and N codoped graphene has been employed in photocatalysis.[223,224] For example, it can degrade rhodamine B[223,224] and methyl orange.[225] In the former case, the activity is 3 and 10 times higher than those determined for N-doped graphene and P25 TiO_2, respectively.[223] Efficient photocatalytic H_2O_2 production was achieved since the codoped graphene induced a better light absorption and promoted a more significant charge migration.[226] Sulfur and nitrogen codoped graphene nanomaterials have broad visible absorption[223,224] and superb luminescence properties.[226−232] They can be used in bioimaging.[233,234] Also, they were reported to have a fluorescence quantum yield 9.3 times higher than that of undoped graphene. Thus, they are promising materials for developing light-emitting devices.[228]

The development of alkali metal ion batteries is another area that has been invaded by publications that use S and N codoped graphene.[235−269] In 2014, Ma et al.[153] produced S and N cocoped graphene using a chemical vapor deposition approach. The three-dimensional codoped graphene networks were utilized as anode materials for lithium ion batteries. The capacity was 3525 mAh/g at a current density of 50 mA/g, and the rate capability was as high as 870 mAh/g at 1000 mA/g, with with excellent cycling stability. Following Ma et al.'s[153] landmark investigation, several works continued this line of research.[235−261] In some cases, metal nanoparticles,[235,236] nanocables,[237] and nanospheres[238] are also combined with S and N doped graphene to improve performance. Although the numbers obtained are impressive, and are in agreement with our theoretical predictions,[13] to the best of my knowledge, there

https://doi.org/10.1021/acsomega.2c06010
ACS Omega 2022, 7, 45935−45961

Table 3. Sodium Adsorption Energies onto Codoped Graphene 5 × 5 and Circumcoronene

dopant	VDW-DF/DZP G5×5[a]	M06-2X/6-311G* circumcoronene[b]	PBE-D2/VASP G5×5	PBE-D2/6-311G* circumcoronene
AlB	−1.58	−1.81	−2.44	−2.10
AlN	−1.55	−1.98	−2.44	−2.05
AlO	−1.63	−1.64	−2.43	−1.99
SiB	**−2.13**	**−2.90**	**−2.72**	**−2.94**
SiN	−1.63	−2.11	−2.42	−2.09
SiO	−1.42	−1.34	−2.21	−1.62
PB	−1.47	−1.75	−2.36	−1.91
PN	−0.96	−1.15	−1.92	−1.37
PO	−1.71	−1.97	−2.51	−2.18
SB	−1.10	−1.96	−2.35	−2.03
SN	**−2.00**	**−3.35**	**−2.91**	**−2.92**
SO	−0.97	−1.30	−2.13	−1.49
G5×5	−0.67	−0.45	−1.08	−0.71

[a]Calculations were performed using periodic conditions and a 5 × 5 unit cell of graphene. [b]Calculations were performed using a graphene flake (circumcoronene).

Table 4. Potassium Adsorption Energies onto Codoped Graphene 5 × 5 and Circumcoronene

dopant	VDW-DF/DZP G5×5[a]	M06-2X/6-311G* circumcoronene[b]	PBE-D2/VASP G5×5	PBE-D2/6-311G* circumcoronene
AlB	−1.81	−2.22	−2.55	−2.33
AlN	−1.75	−2.35	−2.51	−2.27
AlO	−1.78	−1.95	−2.47	−2.18
SiB	**−2.42**	**−3.36**	**−3.06**	**−3.24**
SiN	−1.84	−2.47	−2.51	−2.32
SiO	−1.64	−1.75	−2.31	−1.88
PB	−1.81	−2.20	−2.51	−1.93
PN	−1.40	−1.57	−2.05	−1.65
PO	−1.95	−2.32	−2.58	−1.39
SB	−1.08	−2.36	−2.47	−2.31
SN	**−2.42**	**−3.64**	**−3.03**	**−3.05**
SO	−1.20	−1.69	−2.22	−1.73
G5×5	−1.1	−0.96	−1.40	−1.10

[a]Calculations were performed using periodic conditions and a 5 × 5 unit cell of graphene. [b]Calculations were performed using a graphene flake (circumcoronene).

is not a commercial lithium ion battery based on S and N codoped graphene. Therefore much work is needed in this area.

The excellent performance observed for lithium batteries prompted researchers to study if the effect was similar for heavier and cheaper alkali metals like Na and K. In effect, superb performances were observed for sodium[261−267] and potassium storage.[268,269] Recent theoretical calculations that I carried out support these results.[152] I demonstrated that, as observed for lithium,[13] S and N codoped graphene presents the strongest affinity toward Na and K adsorption.[152] The adsorption energies of Na and K are gathered in Tables 3 and 4, respectively, and the structure is giving in Figure 5. The adsorption energies for Na and K were dramatically increased by the presence of the S and N dopants, another system for which I observed comparable adsorption energies was Si and B codoped graphene. Therefore, at least for Na and K, there seems to be another alternative to dope graphene and improve alkali metal storage. Metal−air batteries,[270−277] in particular Zn−air ones,[270−276] were also constructed using S and N codoped graphene. Geng et al.[270] used S and N codoped graphene decorated with CoS nanoparticles as a cathode material for Zn−air batteries. The product could be charged and discharged for 50 cycles at 1.25 mA/cm^2, for 50 h with an almost constant discharge voltage of 1.23 V. In sharp contrast, the discharge voltage of the commercial Pt/C catalyst was reduced from 1.36 to 1.20 V. In

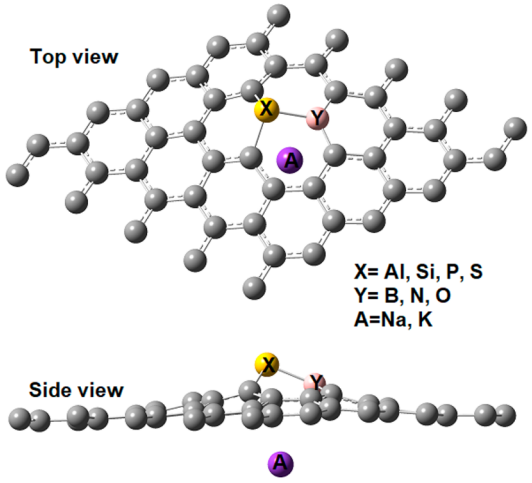

Figure 5. Optimized structure for codoped graphene with an ortho disposition of dopants and an alkali metal atom adsorbed below the 3p dopant.

general, the catalytic performances of the commercial catalyst and the S and N codoped graphene based one were similar, so it is a cheaper alternative. Ganesan et al.[271] also claimed that N and S codoped graphene/CoS_2 nanoparticles could be a suitable air

https://doi.org/10.1021/acsomega.2c06010
ACS Omega 2022, 7, 45935−45961

cathode for Zn−air batteries. Chen et al.[272] went one step further and did not use nanoparticles to construct a cathode for Zn−air batteries. Instead, they used S and N codoped graphene microwires and obtained a superior performance. For more details on this topic, I refer the reader to refs 270−277. Finally, vanadium redox flow batteries were built using S and N codoped graphene by Li et al.[278] and Daugherty et al.[279] An improvement of 85.37% at a current density of 80 mA/cm^2 was reported by Li et al.[278]

Symmetric and asymmetric supercapacitor electrodes were created using S and N codoped graphene.[280−305] As early as 2015, Xing et al.[281] prepared three-dimensional S and N codoped graphene hydrogels using thiocarbohydrazide as a reducing and doping agent. Thanks to the highly porous architecture and presence of dopants, the materials exhibited a high specific capacitance of 141.1 F/g in KOH electrolyte. Their specific capacitance could be maintained at 71.3% even with a discharging current density of 10 A/g. Also, excellent electrochemical stability and reversibility were obtained, with about 90% of retention after 4000 cycles. Even more interesting results were obtained by Tran et al.,[283] who prepared a S and N codoped hole defect graphene hydrogel. A maximum energy density of 14.8 Wh/kg and excellent cycle stability were reported. In general, the porous nature of the S and N based materials is crucial for the performance of the supercapacitor.[280−305] Comparing the performances of the electrodes prepared is not easy because different conditions are employed. Thus, I refer the reader to refs 280−305 gathered on this topic.

The quest for dye-sensitized solar cells with higher efficiency has also tested if the inclusion of S and N codoped graphene can be useful.[306−315] The advantages of codoping as compared with the monodoping when preparing dye-sensitized solar cells (DSSCs) were also confirmed by Luo et al.[306] A power conversion efficiency (PCE) of 4.23% was obtained for sulfur reduced graphene oxide, while for sulfur and nitrogen reduced graphene oxide the value increased to 4.73%. In 2015, Xu et al.[307] built bifacial DSSCs capable of utilizing incidental light from the rear and front sides that relied on transparent S and N codoped graphene as counter electrodes. A drastically enhanced power conversion efficiency was obtained for both front and rear illumination. Kannan et al.[311] reported a PCE as high as 7.42% when S and N codoped graphene was utilized as a counter electrode. The latter value is comparable to the one determined for the Pt counter electrodes, namely 7.42%. The high catalytic activity of the codoped graphene electrode was attributed to the difference in electronegativity between S and N as well as to the structural distortions caused by the presence of the sulfur atom in the graphene framework. Theoretical investigations have also proven the utility of the codoping of graphene in this area. Liu et al.[312] performed first principles calculations to show that the synergistic effect between the S and N dopants resulted in a much better charge transfer between the substrate and the adsorbed I_2 on the surface of S and N codoped graphene. Therefore, a much better efficiency would be obtained in DSSCs that employ codoped graphene.

S and N codoped graphene based sensors have been extensively studied in the literature.[316−347] S and N codoped graphene was used by Li et al.[316] as a support for CuO nanoparticles to promote electrocatalytic glucose oxidation. A low detection limit of 0.07 μM was reported by Li et al.[316] and a detection limit of 0.5 μM was reported by Tian et al.[318] using S and N codoped graphene prepared with a one-step and cost-effective microwave assisted solvothermal method. Masteri-Farahani et al.[319] developed a fluorescence based sensor to detect glucose. They combined boronic acid with the codoped graphene sheets to obtain a lower detection limit of 5.5 μM. The codoped graphene based new sensor is much cheaper because it reduces the use of the expensive boronic acid. In the biological area, S and N codoped graphene based sensors have been constructed for L-cysteine,[320] hydroquinone/catechol,[321] cyanide,[322] an immunosensor for cardiac troponin I,[323] okadaic acid,[324] an immunosensor for cardiac troponin,[325] ascorbic acid,[326,327] and dopamine,[327,328] to mention just a few examples. In the same vein, pesticides[329] and toxic pollutants[330] can be detected. The sensor array built by Zhu et al.[329] was able to discriminate among five pesticides: lactofen, fluoroxypyr-meptyl, bensulfuron-methyl, fomesafen, and diafenthiuron. In this case, there was a practical application of the sensor array as it was validated by discriminating pesticides in soil. In food samples, ethion[331] and nitrites[332] are easily monitored using the fluorescence properties of S and N codoped graphene quantum dots. Martins et al.[333] used glassy carbon electrodes modified with S and N codoped graphene quantum dots for monitoring multivitamins. The detection limits for vitamins B_2, B_6, and B_{12} were 0.30, 30.1, and 0.32 nmol/L. The sensor was effectively implemented in the quantification of vitamins in classic and fruit based energy drinks. Simpler molecules like water[334] and ammonia[335] can be sensed using S and N graphene quantum dots. Jlassi et al.[334] constructed a S and N graphene carbon dot based impedance sensor with good sensitivity for water and excellent response and recovery times of 15 s and 55 s, respectively. The detection of explosives is a very sensitive topic that needs constant updates. Mondal et al.[336] observed a remarkable increase in fluorescence quenching effect using a micromolar solution of 2,4,6-trinitrophenol (TNP). The detection limit was as low as 19.05 ppb. Zhang et al.[337] used an electrochemical sensing platform using S and N codoped graphene nanoribbons that showed a highly sensitive and selective response to trinitrotoluene (TNT) with a wide linear range from 0.0008 to 5.1 ppm and a detection limit as low as 0.1 ppb. Finally, S and N codoped graphene has been employed to detect a variety of metal and nonmetal atoms. For example, the fluorescence detection of Co(II) ions in water was reported by Boonta et al.,[338] while the successful detection of Hg^{2+} ions is well documented.[339−342] In general, the detection is related to fluorescence quenching after interacting with the metal ion. Gu et al.[340] demonstrated that the sensitivity of S and N graphene carbon dots was 4.23 times higher than that of N-doped counterparts. The sensor was sensitive enough to ensure that drinking water had less than 10 ppb Hg^{2+} ions. In addition to this, a report by Tian et al.[344] revealed that Hg(II) ultra-selectively separated from Pb(II) and Cu(II). A high removal ability above 99% was obtained. The list of elements that can be detected in quite long, but it includes Fe^{3+}, with a low detection limit of 0.07 μM,[342,343] Pb(II)[345] with a detection limit as low as 0.29 nM, iodide[341−346] with a detection limit of 4.23 nM, and Cu^{2+} and Ag^{+} with detection limits of 250 and 50 nM, respectively.[347] Interestingly, the sensor constructed by Zhang et al.[341] was an off−on sensor that had the chemiluminescence quenched by iodide and recovered by mercury ions.

We have listed a few areas in which S and N codoped graphene has made an impact, but I limit them to maintain a balance in this review. There are others such as CO_2 capture,[348] removal of organic dyes,[349−352] design of efficient electromagnetic wave absorbers,[353−356] piezocatalysis,[357,358] bioelectricity produc-

https://doi.org/10.1021/acsomega.2c06010
ACS Omega 2022, 7, 45935−45961

tion,[359] and synthesis of high performance polymer nanocomposites.[360]

4.4. P and N Codoped Graphene. It is not a surprise that another of the most studied cocoped graphene systems also contains nitrogen, but in this case it is chaperoned by a pnictogen: phosphorus.[361−420] In 2014, Zheng et al.[361] reported the synthesis of P and N codoped graphene and its use as nonmetal catalyst for the hydrogen evolution reaction. The performance was much better than those corresponding to monodoped graphene and comparable to some commercial catalysts. Two approaches were employed to synthesize this material. In the first approach, a single-step method, graphene oxide was annealed in the presence of melamine and triphenylphosphine, while in the second approach, which involved two steps, first P-doped graphene was obtained and the nitrogen was incorporated. K-edge NEXAFS and XPS studies indicated that nitrogen was present in pyridinic, graphitic, and pyrrolic forms whereas phosphorus was bonded to carbon or oxygen. The presence of P−N bonds was excluded. This result is in contrast to experimental studies that indicated the presence of AlN bonds in Al-doped graphene[47] and SiN bonds in Si-doped graphene.[51] Also it is in disagreement with our investigations which indicated that the P and N dopants prefer to form PN in P and N codoped graphene. In effect, the ortho disposition of the dopants is 1.01 and 0.70 eV more stable than the meta and para ones, respectively.[48,49] A few months later, Xue et al.[362] prepared P and N codoped graphene with air-stable n-type characteristics. Phosphorus played a critical role in achieving improved charge donation. The material was synthesized over a Cu surface and using phosphonitrilic chlorine trimer as a P and N source. A different approach to prepare P and N codoped graphene was proposed by Li et al.[363] The method was facile and cost-effective; they pyrolyzed a dried hydrogel composed of graphene oxide, polyaniline, and phytic acid. These are three examples of how P and N codoped graphene can be synthesized. Since there is not a standard method to obtain it, I refer the readers to the references included, as most of them report a unique method.[361−422] For example, Ananthanarayanan et al.[364] used adenosine triphosphate and Guo et al.[365] used hypophosphorous acid as a P source to dope graphene oxide.

In line with our discussion about S and N codoped graphene, the oxygen reduction reaction (ORR) and the oxygen evolution reaction (OER) were the subject of several investigations that tested the viability of using P and N codoped graphene as a catalyst.[363,365−373] Li et al.'s[363] study was one of the first to not only prepare the material but also to use P and N codoped graphene as a catalyst for ORR and OER reactions. The authors claimed that up to 2015 it was the best nonmetal bifunctional electrocatalyst reported for the latter reaction, with a potential gap of 0.71 V between the OER potential, at a current density of 10 mA/cm^2, and the ORR potential, at a current density of −3 mA/cm^2. A similar ORR and OER overpotential of 705 mV was reported by Chai et al.[366] using P and N codoped graphene prepared via a one-pot hydrothermal method utilizing graphene oxide, ammonium dihydrogen phosphate, and cyanamide as precursors. The P sites were very active and could be oxidized, becoming nonactive for catalysts. However, it was pointed out by Chai et al.[366] that if P is oxidized and bounded to an N codopant it stabilizes the graphitic N and increases the reactivity of the neighboring carbon atoms. For this reason the synthetic conditions were tuned to increase the number of P−N bonds, in line with our previous studies.[48,49] P and N codoped graphene can be synthesized using green chemistry. Cheng et al.[367] used low-cost inorganic fertilizers and graphene oxide as precursors to obtain the said nanomaterial. The material presented super electrocatalytic activity and methanol tolerance. In particular, the electrochemical stability was better than those of commercial Pt/C catalysts. Molina-García et al.[368] combined codoped graphene and perovskites to build a catalyst for the ORR reaction. Among the codoped graphenes tested, S/N, P/N, and B/N were employed. The lowest overpotential was obtained when perovskites were combined with P and N codoped graphene. Further experimental[369−372] and theoretical[373] studies also corroborated the excellent performance of P and N codoped graphene as a catalyst for the ORR.

As mentioned above, the hydrogen evolution reaction has also been studied using P and N codoped graphene. However, it has received less attention than the ORR. Zheng et al.[361] demonstrated that the HER activity of P and N codoped graphene is comparable to those of metal catalysts such as gold, molybdenum, and Mo/Ni alloy. However, it is less effective than nanostructured MoS_2/WS_2. It was speculated that, via nanostructure engineering, the graphene based catalysts have the potential to replace all the commercial ones for the HER. Some years later, Hung et al.[374] devised a procedure to dope graphene with P and N, paying particular attention to obtaining better crystallinity, conductivity, and elemental functionalities to obtain improved catalytic performance. The amount of P doping was as high as 6 atom %, and the electrode displayed excellent catalytic activity with an increase of 142% in sp^2 domain size and enormous lowering in overpotential and the Tafel slope, namely 78%. The efficiency of the catalyst was 25% better than that of the MoS_x one. An et al.[375] prepared a stable catalyst composed of a Co/Ru alloy and P and N codoped graphene. The catalyst exhibited high activity, a low overpotential of 52 mV at 10 mA/cm^2, and a Tafel slope of 38 mV/dec.

P and N codoped graphene has been used for methanol electrooxidation. Chen et al.[376] decorated the doped graphene sheets with Pd nanoparticles. The nanomaterial delivered a catalytic current density of 11.9 A/cm^2 in 1 M KOH with 1 M CH_3OH at −0.2 V after a test duration of 3600 s. The aerobic oxidation of alcohols was achieved using Co porphyrins supported on P and N codoped graphene.[377] The catalyst converted 92% of the sample and exhibited a high selectivity of 86%, better than most reported photocatalysts. Among other processes that P and N codoped graphene can catalyze, I can highlight the work by Xi et al.,[378] which reported the reduction of nitroarenes or the good performance of P and N codoped graphene as a cathode electrode catalyst in microbial fuel cells.[379]

In the biological field, P and N codoped graphene has been used for cellular imaging.[364,380,381] Ananthanarayanan et al.[364] used P and N codoped graphene quantum dots that exhibited high photostability, strong two-photon upconversion, and small molecular weight for real-time tracking of transferring in live cells. Gong et al.[380] also used the doped carbon dots for monitoring because of their exceptional fluorescent properties. The material was also utilized for doxorubicin delivery because the effectivity of the drug was much better when combined with the carbon material. Liu et al.[381] were able to use similar carbon dots for sensitive and selective detection of nitrite in live cells. Finally, Shumba and Nyokong[382] modified P and N codoped graphene with Co(II) phthalocyanine to detect H_2O_2; the sensitivity was 12 mA/M and the detection limit was 1.21 nM.

A topic that always is fueled by graphene doped with heteroatoms is that of rechargeable batteries. P and N codoped

https://doi.org/10.1021/acsomega.2c06010
ACS Omega 2022, 7, 45935−45961

graphene was successfully used in lithium,[383−390] sodium,[391−394] potassium,[395] and Zn−air batteries.[396−398] In 2015, Gu et al.[383] prepared P and N codoped graphene using graphene oxide, triphenylphosphine, and ammonia with polytetrafluoroethylene as a binder. They constructed a membrane which was used as blocking layer to conductively confine polysulfides in the cathodes of lithium−sulfur batteries. The performance of the new battery was remarkable and significantly better than the ones prepared using monodoped graphene. The initial capacity was 1158.3 mAh/g at a current density of 1 C. The cycling stability was reasonable, decaying 0.09% per cycle. Wu et al.[384] were able to suppress polysulfide dissolution by physical confinement and chemical interaction; the assembled Li−S batteries had an initial discharge capacity of 1446 mAh/g at a current density of 0.1 C. The capacity decay was extremely low: 0.034% per cycle. Other reports by Zhou et al.,[385] Zeng et al.,[386] and Zhang et al.[387] also utilized P and N codoped graphene to solve the shuttle effect of polysulfides and volume expansion of sulfur that seriously affect performance. A slightly different approach was chosen by Muhammad et al.,[388] who prepared P and N codoped graphene microspheres embedded with core−shell CoP@C and MoP@C nanoparticles. The interior carbon shell limited volume evolution and prevented nanoparticle aggregation. As a consequence, excellent lithium storage was achieved.

In an attempt to use sodium instead of lithium, Li et al.[391] constructed carbonaceous anodes for sodium batteries. P and N codoped graphene was obtained via low temperature phosphidation of NH_2 rich graphene precursor. A large reversible capacity of 330 mAh/g at 50 mA/g was measured. Studies by Wang et al.,[392] Qin et al.,[393] and Wu et al.[394] were also devoted to producing sodium battery anodes, with great performances. Potassium ion batteries were prepared by Gao et al.[395] using P and N codoped graphene aerogels with a specific capacity of 507 mAh/g at 100 mA/g. Zn−air batteries were the focus of several studies that used P and N codoped graphene as an efficient electrocatalyst.[396−398] The 3D P and N codoped holey graphene foam presented excellent activity, showing a half-wave potential of 0.865 V in alkaline electrolytes. The design of supercapacitors is another field that experienced important innovations thanks to the use of P and N codoped graphene.[399−413] Wen et al.[399] synthesized P and N codoped graphene monoliths by a facile hydrothermal method that used melamine phosphate as a single precursor. Excellent capacitive performance was obtained. Supercapacitors with an energy density of 8.2 Wh/kg were produced by Xia et al.[400] when P and N codoped graphene with a high surface area and hierarchical pore structure was utilized. It was prepared by prefunctionalization of graphene and subsequent one-step ammonia phosphate activation. A high specific capacitance of 219 F/g at 0.25 A/g was obtained. Hierarchical porous P and N codoped graphene was also utilized by Zhao et al.;[401] the specific capacitance obtained was 204.4 F/g at 0.2 A/g. In this case, the codoped graphene was produced using nitrogen-containing biomass derived compounds in conjunction with phosphoric acid treatment. The specific capacity retained 97% after 2000 cycles. For more examples about this application of P and N codoped graphene, I refer the readers to refs 399−419. In all of them, the advantages of codoping are demonstrated. Finally, it has been postulated that P and N codoped graphene can be used as a flame retardant and smoke suppressant,[414−416] CO oxidator,[417] O_2 adsorbent,[418] electronic transport material,[419] and oxidation retardant of reduced graphene oxide.[420]

4.5. Codoped Graphene with Other Main Group Elements. The possibilities to construct codoped graphene systems are almost unlimited as there are plenty of possibilities. In this section I mention some of the systems prepared or studied theoretically. P and B codoped graphene was prepared this year by carbonizing in an Ar atmosphere a cellulose/phosphoric acid supramolecular collosol. Then sodium tetraborate decahydrate was used to adjust the B content, as indicated by Meng et al.[421] The nanomaterial presented an outstanding catalytic performance for benzyl alcohol oxidation. As early as 2015, I studied theoretically all 3p/2p codoped graphene systems, finding that P and B codoped graphene was very particular because it was one the few examples for which the stability of the ortho and para dispositions of the dopants were almost equally stable. In fact the ortho configuration, i.e., P and B replacing a CC bond, was more stable by 0.04 eV at the M06-L/6-31G* level.[48] The system is nonmagnetic and a semiconductor with a band gap of 0.2 eV at a 2 atom % doping. In a following article, I showed that when a B dopant is added to P-doped graphene, the effective masses of holes and electrons decrease.

Some studies reported the synthesis of P and O codoped graphene. I discussed above if oxygen can be considered a dopant. In this section I recall that any P-doped graphene produced from graphene oxide will have some amount of residual oxygen, which may be comparable to the levels of doping attained for P-doped graphene.[60−69] Ma et al.[422] reported the preparation of P and O codoped graphene with exceptional properties as anode materials for potassium ion batteries. The authors prepared the codoped graphene by thermal annealing of graphene oxide with triphenylphosphine. The material had ultralong cycling stability and a capacity of 474 mAh/g at 50 mA/g.

In 2016, Yu et al.[423] utilized P and S codoped hierarchically porous graphene aerogels for enhancing supercapacitor performance. The material was prepared by heating graphene oxide prepared by the modified Hummers method, thioglycoic acid, and pythic acid. The doping level was 5.8 and 4.6 atom % for S and P, respectively. XPS revealed the presence of S−C and P−C bonds. The specific capacitance was 438 F/g at 19 mV/s, greater than the ones measured for the monodoped counterparts. Patel et al.[424] prepared P and S codoped graphitic carbons for aerobic oxidation reactions. Further studies indicated that P and S codoped graphene can be a good catalyst of the HER[425] and methanol electrooxidation[426] and improved capacitance.[427−429]

Sulfur and boron doped graphene was synthesized and combined with Au@Pt nanorods. It was utilized as a immunosensing platform for the electrochemical determination of aflatoxin.[430] The codoped graphene was prepared using a microwave-assisted hydrothermal approach. Boron trioxide and sodium sulfide were used as heteroatom sources. XPS indicated the presence of C−B and C−S bonds. Theoretical studies characterized SBe,[431] SiN,[432] NAl,[433] and SiP[434] codoped graphene, materials which presented outstanding electronic, NO_2 sensing, optical, and catalytic properties, respectively. I note that Al and N codoped graphene has not been synthesized, but when Al-doped graphene was reported, Al−N bonds were observed.[46,47] A facile synthesis for halogen (Cl, Br, and I) and nitrogen codoped graphene was reported by Liu et al.[435] The material was utilized as advanced anodes for lithium ion batteries. The Cl and N codoped system presented a specific capacitance of 1200 mAh/g at 0.1 A/g.

https://doi.org/10.1021/acsomega.2c06010
ACS Omega 2022, 7, 45935−45961

Among the theoretical investigations I can highlight my study about graphene with two 3p elements,[436] which revealed unexpected properties because the addition of a second dopant decreased the band gaps with respect to the monodoped systems. Ullah and co-workers[437−439] studied BeB, BeN,[440] and BeO codoped graphene, which exhibited outstanding properties for alkali adsorption thanks to the presence of Be which makes the graphene sheet electron deficient. I studied codoped graphene with one 4p element and one 2p element, which exhibited remarkable properties when a perfect sheet was place above the codoped one because of the formation of interlayer bonds, in particular when Ga and Ge dopants were present.[441] In the same line, Safaei Ardakani et al.[442] studied theoretically SeX codoped graphene (X = Ga, P, and S), which exhibited outstanding electronic properties. N and Cl dopants were successfully incorporated into the graphene framework as revealed by the different characterization techniques employed.

Finally, again with the help of nitrogen, Se and N codoped graphene was prepared. Chen et al.[443] synthesized codoped aerogels that showed a synergistically enhanced capacitive performance. The specific capacity was 302.9 F/g at 1 A/g. In my theoretical study about Se and N codoped graphene,[441] I found that this system has the larger gap among the 4p/2p codoped graphenes: 0.83 eV (spin up) and 0.84 eV (spin down) at the M06-L/6-31G* level for a 4 atom % level of doping. Excellent activity for iodine reduction reaction was calculated by Zhong et al.[444] for Se and N codoped graphene.

4.6. Transition Metal and Nitrogen Codoped Graphene. Along this review I have highlighted the key role played by nitrogen to synthesize codoped graphene systems. Although in section 2 I mentioned that Mn, Fe, Co, Ni, Ir, and Au metal dopants have been embedded in the graphene framework,[80−86] nitrogen has been intensively used to stabilize metals in the graphene sheet.[445−471] Among these systems Fe and N codoped graphene is one of the most studied ones,[445−453] probably because they can be used in single-atom catalysis. In 2015, Dong et al.[445] demonstrated that the latter system is a very effective catalyst for the ORR. These authors exfoliated graphite using cyclopentadienyl iron, and then upon pyrolysis and ammonia activation, the material was converted into Fe and N codoped graphene. The new catalyst exhibited excellent methanol tolerance, superior to that of commercial Pt/C. Other studies by Zitolo et al.,[446] Niu et al.,[447] and Jiang et al.[448] also supported the strong catalytic power of Fe and N codoped graphene. In particular the study by Zitolo et al.[446] revealed the existence of porphyrin-like FeN_4C_{12} moieties. Sibul el al.[449] found that Fe and N codoped graphene is a superior catalyst for anion exchange membranes rather than proton exchange membranes for fuel cell applications. A maximum power density of 243 mW/cm^2 was obtained. Continuing with the use of Fe and N codoped graphene in catalysis, Zhang et al.[450] employed density functional theory to show that by anchoring two Fe atoms with four nitrogen dopants it is possible to obtain an excellent catalyst for the oxygen reduction reaction. In a different area, Gao et al.[451] reported a fluorometric and colorimetric dual-mode sensor based on nitrogen and iron codoped graphene quantum dots for detection of Fe^{3+} ions in biological fluids and cellular imaging. Finally, there is evidence[452,453] indicating the usefulness of Fe and N codoped graphene in the development of lithium−sulfur batteries. Zhang et al. found that the codoped graphene can be used as an anchor material for sulfur in Li−S batteries. Li_2S and Li_2S_2 presented very low decomposition energies on its surface.

Cu and N codoped graphene has been produced by Ni et al.[454] by the thermal conversion of Cu(II) 2,2′-bipyridine in the confined space of lamellar montmorillonites. The product presented excellent results in terms of ORR catalytic activity and methanol tolerance in alkaline media. Mn and N codoped graphene has been the subject of several investigations.[455−460] Zhu et al.[455] employed density functional theory to show that this doped graphene is an excellent catalyst for the ORR, while Luo et al.[456] employed first principles calculations to postulate that it can be a low-cost catalyst for CO oxidation at room temperature. Finally, Lee et al.[457] prepared Co and N codoped graphene quantum dots used as bimodal resonance and fluorescence imaging nanoprobes.

In 2015, Li et al.[458] performed a landmark theoretical investigation which proved that Co and N codoped graphene is a superior catalyst for the ORR and OER. It had a high selectivity for the four-electron-reduction pathway. These hypotheses were confirmed by experimental investigations.[459−461] Han et al.[459] ultrasonicated g-C_3N_4, glucose, and $Co(CH_3COOH)_2{\cdot}4H_2O$, and after several processes Co and N codoped carbon sheets were obtained. As usual for codoped carbons, the material had excellent ORR catalytic activity. The overpotential between ORR and OER reactions was 0.80 V at 10 mA/cm^2. A similar behavior was observed by Liu et al.,[460] but in this case the Co and N codoped graphene was synthesized using a simple $Mg(OH)_2$ nanocasting method. In this case, the OER properties were similar to those corresponding to IrO_2. Finally, Du et al.[461] studied the use of Co and N codoped graphene as a single-atom catalyst for high sulfur content lithium−sulfur batteries, a result also supported by the work of Zhang et al.[462] It is important to note that the latter work studied not only Co and N codoped graphene as an anchor material in Li−S batteries but also the V, Cr, Mn, Fe, Co, Ni, and Cu counterparts. The Co−N−C coordination center served as a bifunctional electrocatalyst that facilitated the formation of Li_2S in discharge and its decomposition in the charge process. Finally, Ir and N codoped graphene which mimicked Ir porphyrins was synthesized by Xiao et al.,[463] and it exhibited ORR catalytic activity significantly higher than that of Ir nanoparticles. These properties were attributed to the moderate adsorption energies of the intermediates. The idea of embedding metal atoms on N-doped graphene was extended to include more and different metals. Dual-metal and N-doped graphene has been predicted by theoretical calculations to have outstanding HER activity[464] and catalytic effects for the CO_2 reduction reaction.[462]

Other combinations of metals were used to codope graphene include; for example, Fe and S codoped graphene quantum dots were synthesized by Kharangarh et al.[466] using a facile one-pot hydrothermal method. The material had excellent electrochemical properties and improved electrical conductivity. The specific capacitance was 476.2 F/g, about 3.3 times higher than that corresponding to the undoped material. Gu et al.[467] reported the preparation of Ni and Al codoped graphene by the reduction of graphene oxide. The product had an impressive hydrogen storage uptake of 5.7 wt %, at 473 K.

4.7. Triple-Atom and Higher Codoped Graphene. The obvious question that some scientists asked was that if two are good why not three or more dopants? I studied XBN tridoped graphene where X = Al, Si, P, or S.[468] As expected, the XNB motif was preferred because nitrogen stabilizes most dopants. The exception was sulfur, which preferred an SBN motif. In line with my previous findings for two dopants, the theoretical calculations indicated that in general the dopants considered

https://doi.org/10.1021/acsomega.2c06010
ACS Omega 2022, 7, 45935−45961

preferred to be bonded instead of separated. The tridoped sheets presented interesting electronic properties and high reactivity. For AlNB, PNB, and SNB the carbon atoms are more reactive than in their AlN, PN, and SN codoped counterparts. However, for SiNB the reactivity is lower than that of SiN dual-doped graphene. As a consequence I recommended that, in order to increase reactivity, Al, P, and S should be combined with BN motifs. There is experimental evidence available indicating that the use of three dopants is beneficial. Razmjooei et al.[469] prepared P, S, and N triple-doped graphene finding that its ORR activity is 2 times higher than that of S and N codoped graphene and 5 times higher than that of single P-doped graphene. Three dopants were also used by Wang et al.[470] to capture the harmful bisphenol A, but in this case the dopants utilized were P, S, and N. The same combination of dopants was selected by Wang et al.[471] to design a electrocatalyst of the ORR in alkaline medium. The material presented superior properties which indicated that it is a promising cathode catalyst for alkaline fuel cells. The good performance of P, S, and N triple-doped graphene for the ORR was also confirmed by the investigations of Dou et al.[472] Last year, Wang et al.[473] also prepared P, S, and N codoped graphene and showed that it is an excellent metal-free bifunctional catalyst for superior electrocatalytic oxygen reaction in rechargeable Zn−air batteries. The dopants were introduced by an interesting modified ball-milling process. Zheng et al.[474] also incorporated P, S, and N codoped graphene as cathodes for Zn−air batteries, but in this case the triple-doped graphene was derived from onium salts. Finally, Xu et al.[475] reported that P, S, and N tridoped graphene quantum dots are a very interesting ion fluorescence probe. The material was prepared from inexpensive coal, and fluorescence was quenched by Pb^{2+}.

Some reports are focused on N, F, and S tridoped graphene[476−479] and N, P, and S tridoped graphene.[480] However, as I mentioned in the preceding sections, it is highly questionable whether fluorine is a dopant or not. Nevertheless, these materials were useful in catalysis,[476,477,480] solar cells,[478] and photoluminescence.[479]

B, N, and P tridoped graphene has been synthesized at least in two reports that observed excellent catalytic properties for the ORR.[481,482] Lin et al.[481] synthesized the material using boron phosphate and a B/P source and ammonia as the N-dopant agent. First graphene oxide was combined with boron phosphate to introduce the B and P dopants. After the B and P codoped graphene aerogel was obtained, it was activated with NH_3 atmosphere to obtain the final tridoped graphene. P, N, and O tridoped graphene was reported by Zhao et al.[483] and was proposed as a supercapacitor electrode and a metal-free catalyst for the oxygen reduction reaction. The specific capacitance was 426 F/g. Again the question of whether oxygen is a dopant is open because it is hard to evaluate if it is replacing a carbon atom or it is a functional group.

The high stabilization of metal dopants induced by graphene elicited several investigations of tridoped graphene containing two different metals and nitrogen. Hu et al.[484] performed theoretical calculations which revealed that Fe, Co, and N tridoped graphene can be a superior catalyst of the ORR and OER. An extremely low overpotential of 0.22 V for both reactions was obtained. He and Santiago[485] combined a variety of metal dimers on N-doped graphene, finding ultrahigh efficiency for the nitrogen reduction reaction. The landmark experimental and theoretical investigation by Zhou et al.[486] proved that FeNi-N6 sites, where each metal is coordinated to four nitrogen atoms, dominate the catalytic activity of noble metal free catalysts. Excellent methane activation was indicated by the theoretical calculations performed by Wu et al.[487] for tridoped graphene with two 3d metals and nitrogen.

Fe, S, and N tridoped graphene was obtained by Qiao et al.[488] and Feng et al.[489] In both works, it was fond that this tridoped graphene is an excellent catalyst of the ORR. Feng et al.[489] obtained this material by using melamine and 2-aminotriazole. The addition of melamine increased the number of nitrogen atoms with pyridinic structure, and as a consequence the amount of FeN_x was augmented.

Finally, I mention the study by Molina-García el al.[490] published in 2018 that achieved the inclusion of four dopants in the graphene sheet: boron, nitrogen, phosphorus, and sulfur. The level of doping was determined via XPS as 6.4, 6.1, 2.6, and 0.5% for B, N, P, and S, respectively. The presence of P−N, P−C, B−C, and S−C bonds was confirmed among many other types. There was improved performance of the quaternary-doped graphene as indicated by the effective number of electron transferred: 3.2.

5. CONCLUSIONS AND FUTURE PROSPECTS

In this review, I have presented a thorough analysis of the multiple atom doped graphene systems that have been synthesized and studied theoretically. I first raised the question of when a foreign atom can be considered a dopant. Although I have discussed works that claim to have doped graphene with fluorine, I believe that this atom cannot be considered a dopant but is a functional group. The case of oxygen is more complicated because it may possibly replace a carbon atom in graphene's framework. However, if oxygen is considered a dopant in all the chemical forms that it can adopt, most of the single-atom graphene systems that have been prepared from graphene oxide are likely to be considered as codoped graphene systems. The amount of oxygen present may be similar to that achieved for the introduced dopant. Also, the effect of this residual oxygen on the properties studied should be clarified. Will it be the same if oxygen is not present?

Regarding the codoped graphene systems synthesized, the list includes (but is not limited to) B/N, N/O, N/F, S/N, P/N, P/B, P/O, S/P, S/B, Si/N, Cl/N, Se/N, TM/N (where TM is a metal), Fe/S, and Al/Ni. By far, the most studied system is S and N codoped graphene, followed by P/N, B/N, and TM/N codoped graphene. From this list of codoped systems, it is crystal clear that nitrogen dominates the list not only in the number of systems but also in the list of articles published because it is present in the four most studied codoped graphene systems. Therefore, the question emerges: are we codoping graphene or doping N-doped graphene? The strong electron-withdrawing properties of nitrogen and its ability to form multiple bonds are crucial for introducing other heteroatoms. Also, nitrogen can be present in various forms—pyridinic, graphitic, and pyrrolic—that can adapt to the needs of the dopant. For example, in B/N doped graphene, it may prefer to be in graphitic form to pair boron. However, for sulfur it can adopt a pyridinic structure, allowing sulfur to be present in thiophenic form CSC (see Figure 4). In the case of transition metals, they can be trapped in an N4 environment, as in porphyrins, anchoring the metal to graphene's surface and avoiding the undesired metal clustering. Therefore, one of the field's critical challenges is synthesizing new codoped graphene systems that do not include nitrogen. Finally, the question of what the effect is of the residual oxygen in the codoped graphene systems prepared remains open.

https://doi.org/10.1021/acsomega.2c06010
ACS Omega 2022, 7, 45935−45961

Related to the latter point, it is impossible not to mention the article by Martin Pumera's research group[11] asking if any "crap" that we put in graphene will enhance its catalytic activity. I believe this challenging paper has not received enough attention, and more studies are needed to give a final answer. In my opinion, one of the significant problems in the field is that the large number of methods available to synthesize codoped graphene makes it almost impossible to have a clear structure−property relationship. It is crucial to devise more promising approaches to synthesize codoped graphene systems with a specific disposition of the dopants. This may be attained, for example, by using adequate substrates as I proposed for siligraphene,[88] or with the aid of specific molecular precursors as in the work by Nguyen et al.[491] that reported the bottom-up synthesis of sulfur-doped graphene nanoribbons.

In this review, I have commented on how the multielemental doped graphene has been utilized in catalysis to develop new energy storage systems, sensing, protection against microwave radiation, piezoelectronics, and solar cells. Even though most of the works report outstanding properties, to the best of my knowledge, there is no widespread use of these nanomaterials in the industry. Maybe it is a bit soon because graphene was synthesized only 18 years ago and the time that doping has been investigated is even shorter. However, to achieve more maturity, this field needs an improved relationship with real-life applications so that society can realize how important graphene is. To that end, in my opinion, theory can be coupled with experiment to improve the synthesis protocols improving the structure−property relationship.

I expect that this review will contribute to introducing more researchers to this fascinating field and enlarge the list of codoped graphene systems that have been synthesized.

AUTHOR INFORMATION

Corresponding Author

Pablo A. Denis − *Computational Nanotechnology, DETEMA, Facultad de Química, UDELAR, 11800 Montevideo, Uruguay;* orcid.org/0000-0003-3739-5061; Email: pablod@fq.edu.uy

Complete contact information is available at: https://pubs.acs.org/10.1021/acsomega.2c06010

Notes

The author declares no competing financial interest.

ACKNOWLEDGMENTS

The author thanks PEDECIBA-Quimica, CSCI, and ANII for financial support.

REFERENCES

(1) Novoselov, K. S.; Geim, A. K.; Morozov, S. V.; Jiang, D.; Zhang, Y.; Grigorieva; Dubonos, S. V.; Firsov, A. A. Electric field effect in atomically thin carbon films. *Science* **2004**, *306*, 666−669.

(2) Novoselov, K. S.; Geim, A. K.; Morozov, S. V.; Jiang, D.; Katsnelson, M. I.; Grigorieva, I.; Dubonos, S. V.; Firsov, A. A. Two-dimensional gas of massless Dirac fermions in graphene. *Nature* **2005**, *438*, 197−200.

(3) Georgakilas, V.; Otyepka, M.; Bourlinos, A. B.; Chandra, V.; Kim, N.; Kemp, K. C.; Hobza, P.; Zboril, R.; Kim, K. S. Functionalization of graphene: covalent and non-covalent approaches, derivatives and applications. *Chem. Rev.* **2012**, *112* (11), 6156−6214.

(4) Denis, P. A. Covalently Functionalized Graphene. *Carbon Nanomaterials Sourcebook*; CRC Press: 2016; pp 105−122.

(5) Wang, X.; Sun, G.; Routh, P.; Kim, D. H.; Huang, W.; Chen, P. Heteroatom-doped graphene materials: syntheses, properties and applications. *Chem. Soc. Rev.* **2014**, *43*, 7067−7098.

(6) Terrones, H.; Lv, R.; Terrones, M.; Dresselhaus, M. S. The role of defects and doping in 2D graphene sheets and 1D nanoribbons. *Rep. Prog. Phys.* **2012**, *75*, No. 062501.

(7) Wang, Y.; Yu, L.; Zhu, W.; Zhou, X.; Chen, Y.; Peng, W. Promotion of the performance of nitrogen-doped graphene by secondary heteroatoms doping in energy transformation and storage. *Ionics* **2019**, *25*, 3499−3522.

(8) Lee, S. J.; Theerthagiri, J.; Nithyadharseni, P.; Arunachalam, P.; Balaji, D.; Madan Kumar, A.; Madhavan, J.; Mittal, V.; Choi, M. Y. Heteroatom-doped graphene-based materials for sustainable energy applications: A review. *Renewable Sustainable Energy Rev.* **2021**, *143*, 110849.

(9) Duan, J.; Chen, S.; Jaroniec, M.; Qiao, S. Z. Heteroatom-doped graphene-based materials for energy-relevant electrocatalytic processes. *ACS Catal.* **2015**, *5* (9), 5207−5234.

(10) Ullah, S.; Shi, Q.; Zhou, J.; Yang, X.; Ta, H. Q.; Hasan, M.; Ahmad, N. M.; Fu, L.; Bachmatiuk, A.; Rummeli, M. H. Advances and trends in chemically doped graphene. *Adv. Mater. Interfaces* **2020**, *7*, 2000999.

(11) Wang, L.; Sofer, Z.; Pumera, M. Will any crap we put into graphene increase its electrocatalytic effect? *ACS Nano* **2020**, *14* (1), 21−25.

(12) Kretschmer, S.; Ghaderzadeh, S.; Facsko, S.; Krasheninnikov, A. V. Threshold Ion Energies for Creating Defects in 2D Materials from First-Principles Calculations: Chemical Interactions Are Important. *J. Phys. Chem. Lett.* **2022**, *13* (2), 514−519.

(13) Denis, P. A. Lithium adsorption on heteroatom mono and dual doped graphene. *Chem. Phys. Lett.* **2017**, *672*, 70−79.

(14) Vineesh, T. V.; Nazrulla, M. A.; Krishnamoorthy, S.; Narayanan, T. N.; Alwarappan, S. Synergistic effects of dopants on the spin density of catalytic active centres of N-doped fluorinated graphene for oxygen reduction reaction. *Appl. Mater. Today* **2015**, *1*, 74−79.

(15) Jiang, S.; Sun, Y.; Dai, H.; Hu, J.; Ni, P.; Wang, Y.; Li, Z.; Li, Z. Nitrogen and fluorine dual-doped mesoporous graphene: a high-performance metal-free ORR electrocatalyst with a super-low HO_2^- yield. *Nanoscale* **2015**, *7*, 10584−10589.

(16) Liu, Y.; Feng, Q.; Xu, Q.; Li, M.; Tang, N.; Du, Y. Synthesis and photoluminescence of F and N co-doped reduced graphene oxide. *Carbon* **2013**, *61*, 436−440.

(17) Yue, X.; Huang, S.; Cai, J.; Jin, Y.; Shen, P. K. Heteroatoms dual doped porous graphene nanosheets as efficient bifunctional metal-free electrocatalysts for overall water-splitting. *J. Mater. Chem. A* **2017**, *5*, 7784−7790.

(18) Yue, X.; Huang, S.; Jin, Y.; Shen, P. K. Nitrogen and fluorine dual-doped porous graphene-nanosheets as efficient metal-free electrocatalysts for hydrogen-evolution in acidic media. *Catal. Sci. Technol.* **2017**, *7*, 2228−2235.

(19) Huang, S.; Li, Y.; Feng, Y.; An, H.; Long, P.; Qin, C.; Feng, W. Nitrogen and fluorine co-doped graphene as a high-performance anode material for lithium-ion batteries. *J. Mater. Chem. A* **2015**, *3*, 23095−23105.

(20) An, H.; Li, Y.; Gao, Y.; Cao, C.; Han, J.; Feng, Y.; Feng, W. Free-standing fluorine and nitrogen co-doped graphene paper as a high-performance electrode for flexible sodium-ion batteries. *Carbon* **2017**, *116*, 338−346.

(21) Wang, C.; Chen, D.; Yang, Y.; Tang, S.; Li, X.; Xie, F.; Wang, G.; Guo, Q. Synthesis of multi-color fluorine and nitrogen co-doped graphene quantum dots for use in tetracycline detection, colorful solid fluorescent ink, and film. *J. Colloid Interface Sci.* **2021**, *602*, 689−698.

(22) Wu, A.; Wei, G.; Yang, F.; Xia, G.; Yan, X.; Shen, S.; Zhu, F.; Ke, C.; Zhang, J. Nitrogen and iodine dual-doped 3D porous graphene as a bi-functional cathode catalyst for Li-O_2 batteries. *Electrochim. Acta* **2019**, *318*, 354−361.

(23) Zhan, Y.; Huang, J.; Lin, Z.; Yu, X.; Zeng, D.; Zhang, X.; Xie, F.; Zhang, W.; Chen, J.; Meng, H. Iodine/nitrogen co-doped graphene as

metal free catalyst for oxygen reduction reaction. *Carbon* **2015**, *95*, 930−939.
(24) Park, O.-K.; Kim, H. J.; Hwang, J. Y.; Lee, D. S.; Koo, J.; Lee, H.; Yu, J.-S.; Ku, B.-C.; Lee, J. K. Synthesis and mechanistic study of in situ halogen/nitrogen dual-doping in graphene tailored by stepwise pyrolysis of ionic liquids. *Nanotechnology* **2015**, *26*, 115601.
(25) Wang, L.; Sofer, Z.; Zboril, R.; Cepe, K.; Pumera, M. Phosphorus and Halogen Co-Doped Graphene Materials and their Electrochemistry. *Chem.—Eur. J.* **2016**, *22*, 15444.
(26) Panchakarla, L. S.; Subrahmanyam, K. S.; Saha, S. K.; Govindaraj, A.; Krishnamurthy, H. R.; Waghmare, U. V.; Rao, C. N. R. Synthesis, Structure, and Properties of Boron- and Nitrogen-Doped Graphene. *Adv. Mater.* **2009**, *21*, 4726−4730.
(27) Wang, L.; Sofer, Z.; Simek, P.; Tomandl, I.; Pumera, M. Boron-Doped Graphene: Scalable and Tunable p-Type Carrier Concentration Doping. *J. Phys. Chem. C* **2013**, *117*, 23251−23257.
(28) Laref, A.; Ahmed, A.; Binomran, S.; Luo, S. J. First-principle analysis of the electronic and optical properties of boron and nitrogen doped carbon mono-layer graphenes. *Carbon* **2015**, *81*, 179−192.
(29) Poh, H. L.; Šimek, P.; Sofer, Z.; Tomandl, I.; Pumera, M. Boron and nitrogen doping of graphene via thermal exfoliation of graphite oxide in a BF_3 or NH_3 atmosphere: contrasting properties. *J. Mater. Chem. A* **2013**, *1*, 13146−13153.
(30) Wang, L.; Sofer, Z.; Luxa, J.; Pumera, M. Nitrogen doped graphene: influence of precursors and conditions of the synthesis. *J. Mater. Chem. C* **2014**, *2*, 2887−2893.
(31) Megawati, M.; Chua, C. K.; Sofer, Z.; Klímová, K.; Pumera, M. Nitrogen-doped graphene: effect of graphite oxide precursors and nitrogen content on the electrochemical sensing properties. *Phys. Chem. Chem. Phys.* **2017**, *19*, 15914−15923.
(32) Lv, R.; Li, Q.; Botello-Mendez, A. R.; Hayashi, T.; Wang, B.; Berkdemir, A.; Hao, Q.; Elias, A. L.; Cruz-Silva, E.; Gutierrez, H. R.; Kim, Y. A.; Muramatsu, H.; Zhu, J.; Endo, M.; Terrones, H.; Charlier, J.-C.; Pan, M.; Terrones, M. Nitrogen-doped graphene: beyond single substitution and enhanced molecular sensing. *Sci. Rep.* **2012**, *2*, 586.
(33) Yuan, Z.; Li, J.; Yang, M.; Fang, Z.; Jian, J.; Yu, D.; Chen, X.; Dai, L. Ultrathin black phosphorus-on-nitrogen doped graphene for efficient overall water splitting: dual modulation roles of directional interfacial charge transfer. *J. Am. Chem. Soc.* **2019**, *141* (12), 4972−4979.
(34) Ullah, S.; Denis, P. A.; Sato, F. Coupled cluster investigation of the interaction of beryllium, magnesium, and calcium with pyridine: Implications for the adsorption on nitrogen-doped graphene. *Comput.Theor. Chem.* **2019**, *1150*, 57−62.
(35) Vesel, A.; Zaplotnik, R.; Primc, G.; Mozetič, M. A Review of Strategies for the Synthesis of N-Doped Graphene-Like Materials. *Nanomaterials* **2020**, *10*, 2286.
(36) Ullah, S.; Hussain, A.; Syed, W.; Saqlain, M. A.; Ahmad, I.; Leenaerts, O.; Karim, A. Band-gap tuning of graphene by Be doping and Be, B co-doping: a DFT study. *RSC Adv.* **2015**, *5*, 55762−55773.
(37) Ullah, S.; Denis, P. A.; Sato, F. Beryllium doped graphene as an efficient anode material for lithium-ion batteries with significantly huge capacity: A DFT study. *Appl. Mater. Today* **2017**, *9*, 333−340.
(38) Ao, Z. M.; Yang, J.; Li, S.; Jiang, Q. Enhancement of CO detection in Al doped graphene. *Chem. Phys. Lett.* **2008**, *461*, 276−279.
(39) Ao, Z. M.; Li, S.; Jiang, Q. Thermal stability of interaction between the CO molecules and the Al doped graphene. *Phys. Chem. Chem. Phys.* **2009**, *11*, 1683−1687.
(40) Fukushima, A.; Sawairi, A.; Doi, K.; Senami, M.; Chen, L.; Cheng, H.; Tachibana, A. Role of an Aluminum Atom on Graphene for Hydrogen Adsorption. *J. Phys. Soc. Jpn.* **2011**, *80*, No. 074705.
(41) Tayyab, M.; Hussain, A.; Adil, W.; Nabi, S.; Asif, Q. Band-gap engineering of graphene by Al doping and adsorption of Be and Br on impurity: A computational study. *Comput. Cond. Matter* **2020**, *23*, No. e00463.
(42) Denis, P. A. Band gap opening of monolayer and bilayer graphene doped with aluminium, silicon, phosphorus, and sulfur. *Chem. Phys. Lett.* **2010**, *492*, 251−257.
(43) Denis, P. A. When noncovalent interactions are stronger than covalent bonds: Bilayer graphene doped with second row atoms, aluminum, silicon, phosphorus and sulfur. *Chem. Phys. Lett.* **2011**, *508*, 95−101.
(44) Denis, P. A. Tuning the electronic properties of doped bilayer graphene with small structural changes. *Comput. Theor. Chem.* **2011**, *974*, 21−25.
(45) Su, C.; Tripathi, M.; Yan, Q. B.; Wang, Z.; Zhang, Z.; Hofer, C.; Wang, H.; Basile, L.; Su, G.; Dong, M.; Meyer, J. C.; Kotakoski, J.; Kong, J.; Idrobo, J. C.; Susi, T.; Li, J. Engineering single-atom dynamics with electron irradiation. *Sci. Adv.* **2019**, *5*, eaav2252.
(46) Ullah, S.; Liu, Y.; Hasan, M.; Zeng, W.; Shi, Q.; Yang, X.; Fu, L.; Ta, H. Q.; Lian, X.; Sun, J.; Yang, R.; Liu, L.; Rümmeli, M. H. Direct synthesis of large-area Al-doped graphene by chemical vapor deposition: Advancing the substitutionally doped graphene family. *Nano. Res.* **2022**, *15*, 1310−1318.
(47) Zagler, G.; Stecher, M.; Trentino, A.; Kraft, F.; Su, C.; Postl, A.; Längle, M.; Pesenhofer, C.; Mangler, C.; Åhlgren, E. H.; Markevich, A.; Zettl, A.; Kotakoski, J.; Susi, T.; Mustonen, K. Beam-driven dynamics of aluminium dopants in graphene. *2D Materials* **2022**, *9*, No. 035009.
(48) Denis, P. A.; Pereyra Huelmo, C. Structural characterization and chemical reactivity of dual doped graphene. *Carbon* **2015**, *87*, 106−115.
(49) Denis, P. A.; Pereyra Huelmo, C.; Martins, A. S. Band Gap Opening in Dual-Doped Monolayer Graphene. *J. Phys. Chem. C* **2016**, *120*, 7103−7112.
(50) Zhou, W.; Kapetanakis, M. D.; Prange, M. P.; Pantelides, S. T.; Pennycook, S. J.; Idrobo, J.-C. Direct Determination of the Chemical Bonding of Individual Impurities in Graphene. *Phys. Rev. Lett.* **2012**, *109*, 206803.
(51) Ramasse, Q. M.; Seabourne, C. R.; Kepaptsoglou, D.-M.; Zan, R.; Bangert, U.; Scott, A. J. Probing the Bonding and Electronic Structure of Single Atom Dopants in Graphene with Electron Energy Loss Spectroscopy. *Nano Lett.* **2013**, *13*, 4989−4995.
(52) Majeti, V. K.; Roy, A.; Gupta, K. K.; Dey, S. Effect of silicon dopant on mechanical properties of monolayer graphene. *IOP Conf. Ser.: Mater. Sci. Eng.* **2020**, *872*, No. 012188.
(53) Denis, P. A.; Pereyra Huelmo, C.; Iribarne, F. On the band gaps and effective masses of mono and dual doped monolayer graphene. *Comput. Mater. Sci.* **2017**, *137*, 20−29.
(54) Rafique, M.; Shuai, Y.; Hussain, N. First-principles study on silicon atom doped monolayer graphene. *Phys. E: Low-Dimens. Syst. Nanostructures* **2018**, *95*, 94−101.
(55) Houmad, M.; Zaari, H.; Benyoussef, A.; El Kenz, A.; Ez-Zahraouy, H. Optical conductivity enhancement and band gap opening with silicon doped graphene. *Carbon* **2015**, *94*, 1021−1027.
(56) Denis, P. A. Heteroatom promoted cycloadditions for graphene. *ChemistrySelect* **2016**, *1*, 5497−5500.
(57) Denis, P. A. Organic chemistry of graphene: the Diels−Alder reaction. *Chem.—Eur. J.* **2013**, *19*, 15719−15725.
(58) Denis, P. A. Diels-Alder reactions onto fluorinated and hydrogenated graphene. *Chem. Phys. Lett.* **2017**, *684*, 79−85.
(59) Denis, P. A.; Pereyra Huelmo, C.; Iribarne, F. Cycloaddition reactions on epitaxial graphene. *New J. Chem.* **2019**, *43*, 11251−11257.
(60) Some, S.; Kim, J.; Lee, K.; Kulkarni, A.; Yoon, Y.; Lee, S.; Kim, T.; Lee, H. Highly Air-Stable Phosphorus-Doped n-Type Graphene Field-Effect Transistors. *Adv. Mater.* **2012**, *24*, 5481−5486.
(61) Li, R.; Wei, Z.; Gou, X.; Xu, W. Phosphorus-doped graphene nanosheets as efficient metal-free oxygen reduction electrocatalysts. *RSC Adv.* **2013**, *3*, 9978−9984.
(62) Zhang, C.; Mahmood, N.; Yin, H.; Liu, F.; Hou, Y. Synthesis of Phosphorus-Doped Graphene and its Multifunctional Applications for Oxygen Reduction Reaction and Lithium Ion Batteries. *Adv. Mater.* **2013**, *25*, 4932−4937.
(63) Niu, F.; Tao, L. M.; Deng, Y. C.; Wang, Q. H.; Song, W.-G. Phosphorus doped graphene nanosheets for room temperature NH_3 sensing. *New J. Chem.* **2014**, *38*, 2269−2272.
(64) Susi, T.; Hardcastle, T. P.; Hofsäss, H.; Mittelberger, A.; Pennycook, T. J.; Mangler, C.; Drummond-Brydson, R.; Scott, A. J.; Meyer, J. C.; Kotakoski, J. Single-atom spectroscopy of phosphorus dopants implanted into graphene. *2D Mater.* **2017**, *4*, No. 021013.

https://doi.org/10.1021/acsomega.2c06010
ACS Omega 2022, 7, 45935−45961

(65) Gonzalez Larrude, D.; Garcia-Basabe, Y.; Freire, F. L., Jr.; Rocco, M. L. M. Electronic structure and ultrafast charge transfer dynamics of phosphorous doped graphene layers on a copper substrate: a combined spectroscopic study. *RSC Adv.* **2015**, *5*, 74189−74197.
(66) Denis, P. A. Concentration dependence of the band gaps of phosphorus and sulfur doped graphene. *Comput. Mater. Sci.* **2013**, *67*, 203−206.
(67) Dai, J.; Yuan, J. Modulating the electronic and magnetic structures of P-doped graphene by molecule doping. *J. Phys.: Condens. Matter* **2010**, *22*, 225501.
(68) Gueorguiev, G. K.; Furlan, A.; Czigany, Z.; Stafstrom, S.; Hultman, L. Intercalation of P atoms in Fullerene-like CPx. *Chem. Phys. Lett.* **2011**, *501*, 400−403.
(69) Poh, H. L.; Sofer, Z.; Novacek, M.; Pumera, M. Concurrent Phosphorus Doping and Reduction of Graphene Oxide. *Chem.—Eur. J.* **2014**, *20*, 4284−4291.
(70) Denis, P. A.; Faccio, R.; Mombru, A. W. Is It Possible to Dope Single-Walled Carbon Nanotubes and Graphene with Sulfur? *ChemPhysChem* **2009**, *10*, 715−722.
(71) Yang, Z.; Yao, Z.; Li, G.; Fang, G.; Nie, H.; Liu, Z.; Zhou, X.; Chen, X.; Huang, S. Sulfur-doped graphene as an efficient metal-free cathode catalyst for oxygen reduction. *ACS Nano* **2012**, *6* (1), 205−211.
(72) Yang, S.; Zhi, L.; Tang, K.; Feng, X.; Maier, J.; Müllen, K. Efficient Synthesis of Heteroatom (N or S)-Doped Graphene Based on Ultrathin Graphene Oxide-Porous Silica Sheets for Oxygen Reduction Reactions. *Adv. Funct. Mater.* **2012**, *22*, 3634−3640.
(73) Gao, H.; Liu, Z.; Song, L.; Guo, W.; Gao, W.; Ci, L.; Rao, A.; Quan, W.; Vajtai, R.; Ajayan, P. M Synthesis of S-doped graphene by liquid precursor. *Nanotechnology* **2012**, *23*, 275605.
(74) Zhang, J.; Li, J.; Wang, Z.; Wang, X.; Feng, W.; Zheng, W.; Cao, W.; Hu, P. Low-Temperature Growth of Large-Area Heteroatom-Doped Graphene Film. *Chem. Mater.* **2014**, *26*, 2460−2466.
(75) Wang, Z.; Li, P.; Chen, Y.; He, J.; Zhang, W.; Schmidt, O. G.; Li, Y. Pure thiophene−sulfur doped reduced graphene oxide: synthesis, structure, and electrical properties. *Nanoscale* **2014**, *6*, 7281−7287.
(76) Poh, H. L.; Šimek, P.; Sofer, Z.; Pumera, M. Sulfur-Doped Graphene via Thermal Exfoliation of Graphite Oxide in H_2S, SO_2, or CS_2 Gas. *ACS Nano* **2013**, *7*, 5262−5272.
(77) Denis, P. A. Chemical Reactivity and Band-Gap Opening of Graphene Doped with Gallium, Germanium, Arsenic, and Selenium Atoms. *ChemPhysChem* **2014**, *15*, 3994−4000.
(78) Tripathi, M.; Markevich, A.; Böttger, R.; Facsko, S.; Besley, E.; Kotakoski, J.; Susi, T. Implanting Germanium into Graphene. *ACS Nano* **2018**, *12* (5), 4641−4647.
(79) Meng, X.; Yu, C.; Song, X.; Iocozzia, J.; Hong, J.; Rager, M.; Jin, H.; Wang, S.; Huang, L.; Qiu, J.; Lin, Z. Scrutinizing Defects and Defect Density of Selenium-Doped Graphene for High-Efficiency Triiodide Reduction in Dye-Sensitized Solar Cells. *Angew. Chem., Int. Ed.* **2018**, *57*, 4682.
(80) Toh, R. J.; Poh, H. L.; Sofer, Z.; Pumera, M. Transition Metal (Mn, Fe, Co, Ni)-Doped Graphene Hybrids for Electrocatalysis. *Chem.—Asian J.* **2013**, *8*, 1295−1300.
(81) Carnevali, V.; Patera, L. L.; Prandini, G.; Jugovac, M.; Modesti, S.; Comelli, G.; Peressi, M.; Africh, C. Doping of epitaxial graphene by direct incorporation of nickel adatoms. *Nanoscale* **2019**, *11*, 10358−10364.
(82) Wen, X.; Duan, Z.; Bai, L.; Guan, J. Atomic scandium and nitrogen-codoped graphene for oxygen reduction reaction. *J. Power Sources* **2019**, *431*, 265−273.
(83) Robertson, A. W.; Montanari, B.; He, K.; Kim, J.; Allen, C. S.; Wu, Y. A.; Olivier, J.; Neethling, J.; Harrison, N.; Kirkland, A. I.; Warner, J. H. Dynamics of Single Fe Atoms in Graphene Vacancies. *Nano Lett.* **2013**, *13*, 1468−1475.
(84) Zhao, J.; Deng, Q.; Bachmatiuk, A.; Sandeep, G.; Popov, A.; Eckert, J.; Rümmeli, M. H. Free-standing single-atom-thick iron membranes suspended in graphene pores. *Science* **2014**, *343*, 1228−1232.
(85) Lin, P.-C.; Villarreal, R.; Achilli, S.; Bana, H.; Nair, M. N.; Tejeda, A.; Verguts, K.; De Gendt, S.; Auge, M.; Hofsäss, H.; De Feyter, S.; Di Santo, G.; Petaccia, L.; Brems, S.; Fratesi, G.; Pereira, L. M. C. Doping Graphene with Substitutional Mn. *ACS Nano* **2021**, *15* (3), 5449−5458.
(86) Trentino, A.; Mizohata, K.; Zagler, G.; Längle, M.; Mustonen, K.; Susi, T.; Kotakoski, J.; Åhlgren, E. H. Two-step implantation of gold into graphene. *2D Mater.* **2022**, *9*, No. 025011.
(87) Li, W.; Amiinu, I. S.; Zhang, B.; Zhang, C.; Zhang, Z.; Zhu, J.; Liu, J.; Pu, Z.; Kou, Z.; Mu, S. Distorted niobium-self-doped graphene in-situ grown from 2D niobium carbide for catalyzing oxygen reduction. *Carbon* **2018**, *139*, 1144−1151.
(88) Pereyra Huelmo, C.; Denis, P. A. Silicon Carbide Induced Doping of Graphene: A New Potential Synthetic Route for SiC_3 Siligraphene. *J. Phys. Chem. C* **2019**, *123*, 30341−30350.
(89) Sofer, Z.; Jankovsky, O.; Simek, P.; Klimova, K.; Mackova, A.; Pumera, M. Uranium and Thorium-Doped Graphene for Efficient Oxygen and Hydrogen Peroxide Reduction. *ACS Nano* **2014**, *8*, 7106−7114.
(90) Zheng, Y.; Ge, L.; Jaroniec, M.; Qiao, S. Z.; Jiao, Y. Two-step boron and nitrogen doping in graphene for enhanced synergistic catalysis. *Angew. Chem., Int. Ed.* **2013**, *125*, 3192−3198.
(91) Jung, S.-M.; Lee, E. K.; Choi, M.; Shin, D.; Jeon, I.-Y.; Seo, J.-M.; Jeong, H. Y.; Park, N.; Oh, J. H.; Baek, J.-B. Direct Solvothermal Synthesis of B/N-Doped Graphene. *Angew. Chem., Int. Ed.* **2014**, *53*, 2398−2401.
(92) Rani, P.; Jindal, V. K. Stability and electronic properties of isomers of B/N co-doped graphene. *Appl. Nanosci.* **2014**, *4*, 989−996.
(93) Rani, P.; Dubey, G. S.; Jindal, V. K. DFT study of optical properties of pure and doped graphene. *Physica E: Low-Dimensional Systems and Nanostructures* **2014**, *62*, 28−35.
(94) Wang, B. Y.; Wang, H.; Chen, L. Y.; Hsueh, H. C.; Li, X.; Guo, J.; Luo, Y.; Chiou, J. W.; Wang, W. H.; Wang, P. H.; Chen, K. H.; Chen, Y. C.; Chen, L. C.; Chen, C. H.; Wang, J.; Pong, W. F. Nonlinear bandgap opening behavior of BN co-doped graphene. *Carbon* **2016**, *107*, 857−864.
(95) Nath, P.; Sanyal, D.; Jana, D. Semi-metallic to semiconducting transition in graphene nanosheet with site specific co-doping of boron and nitrogen. *Phys. E: Low-Dimens. Syst. Nanostructures* **2014**, *56*, 64−68.
(96) Nascimento, R.; Martins, J. R.; Batista, R. J. C.; Chacham, H. Band gaps of BN-doped graphene: fluctuations, trends, and bounds. *J. Phys. Chem. C* **2015**, *119* (9), 5055−5061.
(97) Omidvar, A. Electronic structure tuning and band gap opening of nitrogen and boron doped holey graphene flake: the role of single/dual doping. *Mater. Chem. Phys.* **2017**, *202*, 258−265.
(98) Novodchuk, I.; Kayaharman, M.; Ibrahim, K.; Al-Tuairqi, S.; Irannejad, M.; Abdel-Rahman, E.; Sanderson, J.; Bajcsy, M.; Yavuz, M. B/N co-doped graphene oxide gel with extremely-high mobility and ION/IOFF for large-area field effect transistors. *Carbon* **2020**, *158*, 624−630.
(99) Zhu, J.; He, C.; Li, Y.; Kang, S.; Shen, P. K. One-step synthesis of boron and nitrogen-dual-self-doped graphene sheets as non-metal catalysts for oxygen reduction reaction. *J. Mater. Chem. A* **2013**, *1*, 14700−14705.
(100) Xu, C.; Su, Y.; Liu, D.; He, X. Three-dimensional N, B-doped graphene aerogel as a synergistically enhanced metal-free catalyst for the oxygen reduction reaction. *Phys. Chem. Chem. Phys.* **2015**, *17*, 25440−25448.
(101) Chen, W.; Xu, L.; Tian, Y.; Li, H.; Wang, K. Boron and nitrogen co-doped graphene aerogels: facile preparation, tunable doping contents and bifunctional oxygen electrocatalysis. *Carbon* **2018**, *137*, 458−466.
(102) Zhang, M.; Tao, H.; Liu, Y.; Yan, C.; Hong, S.; Masa, J.; Robertson, A. W.; Liu, S.; Qiu, J.; Sun, Z. Ultrasound-assisted nitrogen and boron codoping of graphene oxide for efficient oxygen reduction reaction. *ACS Sustainable Chem. Eng.* **2019**, *7*, 3434−3442.
(103) Yuan, R.; Xu, Y.; Wang, Y.; You, F.; Chen, W.; Ding, C.; Jiang, D.; Wang, K. One-pot hydrothermal preparation of B and N co-doped

https://doi.org/10.1021/acsomega.2c06010
ACS Omega 2022, 7, 45935−45961

graphene aerogels loaded with cobalt oxides for the synergistic enhancement of oxygen reduction. *J. Electroanal. Chem.* **2020**, *877*, 114555.
(104) Zhu, J.; He, G.; Tian, Z.; Liang, L.; Shen, P. K. Facile synthesis of boron and nitrogen-dual-doped graphene sheets anchored platinum nanoparticles for oxygen reduction reaction. *Electrochim. Acta* **2016**, *194*, 276−282.
(105) Mazánek, V.; Matějková, S.; Sedmidubský, D.; Pumera, M.; Sofer, Z. One-Step Synthesis of B/N Co-doped Graphene as Highly Efficient Electrocatalyst for the Oxygen Reduction Reaction: Synergistic Effect of Impurities. *Chem.—Eur. J.* **2018**, *24*, 928.
(106) Tai, J.; Hu, J.; Chen, Z.; Lu, H. Two-step synthesis of boron and nitrogen co-doped graphene as a synergistically enhanced catalyst for the oxygen reduction reaction. *RSC Adv.* **2014**, *4*, 61437−61443.
(107) Kattel, S.; Atanassov, P.; Kiefer, B. Density functional theory study of the oxygen reduction reaction mechanism in a BN co-doped graphene electrocatalyst. *J. Mater. Chem. A* **2014**, *2*, 10273−10279.
(108) Han, J.; Zhang, Y.; Niu, F.; Chen, T.; Liu, J.; Xu, Y. Low-cost and highly efficient metal-free electrocatalysts for oxygen reduction reaction: environment-friendly three-dimensional B, N co-doped graphene aerogels. *Electrocatalysis* **2019**, *10*, 56−62.
(109) Huang, S.; Zhang, L.; Zhu, J.; Shen, P. K.; Jiang, S. P. Crumpled nitrogen-and boron-dual-self-doped graphene sheets as an extraordinary active anode material for lithium ion batteries. *J. Mater. Chem. A* **2016**, *4*, 14155−14162.
(110) Li, F.; Su, Y.; Zhao, J. Shuttle inhibition by chemical adsorption of lithium polysulfides in B and N co-doped graphene for Li−S batteries. *Phys. Chem. Chem. Phys.* **2016**, *18*, 25241−25248.
(111) Xiao, F.; Lin, Z.; Zhang, J.; Lei, Y.; Meng, Y.; Chen, X.; Zhao, S.; Hong, B.; Wang, J.; Li, D.; Xu, J. A novel approach to facile synthesis of boron and nitrogen co-doped graphene and its application in lithium oxygen batteries. *Energy Storage Mater.* **2021**, *41*, 61−68.
(112) Jiang, H. R.; Zhao, T. S.; Shi, L.; Tan, P.; An, L. First-Principles Study of Nitrogen-, Boron-Doped Graphene and Co-Doped Graphene as the Potential Catalysts in Nonaqueous Li−O_2 Batteries. *J. Phys. Chem. C* **2016**, *120* (12), 6612−6618.
(113) Wang, M.; Yang, Y.; Yang, Z.; Gu, L.; Chen, Q.; Yu, Y. Sodium-ion batteries: improving the rate capability of 3D interconnected carbon nanofibers thin film by boron, nitrogen dual-doping. *Adv. Sci.* **2017**, *4*, 1600468.
(114) Kang, Y.; Wang, B.; Yan, Y.; Rana, H. H.; Lee, J. Y.; Kim, J. H.; Park, H. S. Three-dimensionally macroporous nitrogen and boron co-doped graphene aerogels derived from polyaspartamide for supercapacitor electrodes. *Mater. Today Commun.* **2020**, *25*, 101495.
(115) Wu, Z. S.; Winter, A.; Chen, L.; Sun, Y.; Turchanin, A.; Feng, X.; Müllen, K. Three-dimensional nitrogen and boron co-doped graphene for high-performance all-solid-state supercapacitors. *Adv. Mater.* **2012**, *24*, 5130−5135.
(116) Tabassum, H.; Mahmood, A.; Wang, Q.; Xia, W.; Liang, Z.; Qiu, B.; Zhao, R.; Zou, R. Hierarchical cobalt hydroxide and B/N Co-doped graphene nanohybrids derived from metal-organic frameworks for high energy density asymmetric supercapacitors. *Sci. Rep.* **2017**, *7*, 43084.
(117) Chen, D.; Pei, S.; He, Z.; Shao, H.; Wang, J.; Wang, K.; Wang, Y.; Jin, Y. High active PdSn binary alloyed catalysts supported on B and N codoped graphene for formic acid electro-oxidation. *Catalysts* **2020**, *10*, 751.
(118) Sun, Y.; Du, C.; Han, G.; Qu, Y.; Du, L.; Wang, Y.; Chen, G.; Gao, Y.; Yin, G. Boron, nitrogen co-doped graphene: a superior electrocatalyst support and enhancing mechanism for methanol electrooxidation. *Electrochim. Acta* **2016**, *212*, 313−321.
(119) Yang, F.; Cao, Y.; Chen, Z.; He, X.; Hou, L.; Li, Y. Large-scale preparation of B/N co-doped graphene-like carbon as an efficient metal-free catalyst for the reduction of nitroarenes. *New J. Chem.* **2018**, *42*, 2718−2725.
(120) Yu, C.; Fang, H.; Liu, Z.; Hu, H.; Meng, X.; Qiu, J. Chemically grafting graphene oxide to B, N co-doped graphene via ionic liquid and their superior performance for triiodide reduction. *Nano Energy* **2016**, *25*, 184−192.
(121) Feng, S.; Meng, J.; Guo, J.; Chen, X.; Zhang, G. B, N dual-doped Graphene/Au@ Pt Nanomaterials as Sensor for Determination of Aflatoxin B1. *Int. J. Electrochem. Sci.* **2020**, *15*, 7722−7732.
(122) Liu, Z.; Mo, Z.; Niu, X.; Yang, X.; Jiang, Y.; Zhao, P.; Liu, N.; Guo, R. Highly sensitive fluorescence sensor for mercury (II) based on boron- and nitrogen-co-doped graphene quantum dots. *J. Colloid Interface Sci.* **2020**, *566*, 357−368.
(123) Yang, P.; Su, J.; Guo, R.; Yao, F.; Yuan, C. B, N-Co-doped graphene quantum dots as fluorescence sensor for detection of Hg^{2+} and F^- ions. *Anal. Methods* **2019**, *11*, 1879−1883.
(124) Yang, G. H.; Zhou, Y. H.; Wu, J. J.; Cao, J. T.; Li, L. L.; Liu, H. Y.; Zhu, J. J. Microwave-assisted synthesis of nitrogen and boron co-doped graphene and its application for enhanced electrochemical detection of hydrogen peroxide. *RSC Adv.* **2013**, *3*, 22597−22604.
(125) Varodi, C.; Pogăcean, F.; Coros, M.; Magerusan, L.; Stefan-van Staden, R. I.; Pruneanu, S. Hydrothermal Synthesis of Nitrogen, Boron Co-Doped Graphene with Enhanced Electro-Catalytic Activity for Cymoxanil Detection. *Sensors* **2021**, *21*, 6630.
(126) Esrafili, M. D. Boron and nitrogen co-doped graphene nanosheets for NO and NO_2 gas sensing. *Phys. Lett. A* **2019**, *383*, 1607−1604.
(127) Budak, E.; Ünlü, C. Boron regulated dual emission in B, N doped graphene quantum dots. *Opt. Mater.* **2021**, *111*, 110577.
(128) Wang, H.; Mu, Q.; Wang, K.; Revia, R. A.; Yen, C.; Gu, X.; Tian, B.; Liu, J.; Zhang, M. Nitrogen and boron dual-doped graphene quantum dots for near-infrared second window imaging and photothermal therapy. *Appl. Mater. Today* **2019**, *14*, 108−107.
(129) Ngidi, N. P. D.; Muchuweni, E.; Nyamori, V. O. Dual heteroatom-doped reduced graphene oxide and its application in dye-sensitized solar cells. *Opt. Mater.* **2021**, *122*, 111689.
(130) Lin, K. Y.; Nguyen, M. T.; Waki, K.; Jiang, J. C. Boron and nitrogen co-doped graphene used as counter electrode for iodine reduction in dye-sensitized solar cells. *J. Phys. Chem. C* **2018**, *122* (46), 26385−26392.
(131) Wang, S.; Feng, J.; Meng, Q.; Cao, B.; Tian, G. Study on boron and nitrogen co-doped graphene xerogel for high-performance electrosorption application. *J. Solid State Electrochem.* **2019**, *23*, 2377−2390.
(132) Sun, Z.; Yan, Z.; Yue, K.; Li, A.; Qian, L. Novel high-performance electromagnetic absorber based on Nitrogen/Boron co-doped reduced graphene oxide. *Compos. B. Eng.* **2020**, *196*, 108132.
(133) Umrao, S.; Gupta, T. K.; Kumar, S.; Singh, V. K.; Sultania, M. K.; Jung, J. H.; Oh, I.-K.; Srivastava, A. Microwave-assisted synthesis of boron and nitrogen co-doped reduced graphene oxide for the protection of electromagnetic radiation in Ku-band. *ACS Appl. Mater. Interfaces* **2015**, *7* (35), 19831−19842.
(134) Zhu, X.; Yan, F.; Li, C.; Qi, L.; Yuan, H.; Liu, Y.; Zhu, C.; Chen, Y. Nitrogen and boron co-doped carbon nanotubes embedded with nickel nanoparticles as highly efficient electromagnetic wave absorbing material. *Chin. Phys. Lett.* **2021**, *38*, No. 015201.
(135) Chen, S.; Duan, J.; Jaroniec, M.; Qiao, S. Z. Nitrogen and Oxygen Dual-Doped Carbon Hydrogel Film as a Substrate-Free Electrode for Highly Efficient Oxygen Evolution Reaction. *Adv. Mater.* **2014**, *26*, 2925−2930.
(136) Qin, T.; Wan, Z.; Wang, Z.; Wen, Y.; Liu, M.; Peng, S.; et al. 3D flexible O/N Co-doped graphene foams for supercapacitor electrodes with high volumetric and areal capacitances. *J. Power Sources* **2016**, *336*, 455−464.
(137) Li, Z.; Mi, H.; Bai, Z.; Ji, C.; Sun, L.; Gao, S.; Qiu, J. Sustainable biowaste strategy to fabricate dual-doped carbon frameworks with remarkable performance for flexible solid-state supercapacitors. *J. Power Sources* **2019**, *418*, 112−121.
(138) Li, Z.; Li, Y.; Wang, L.; Cao, L.; Liu, X.; Chen, Z.; Pan, D.; Wu, M. Assembling nitrogen and oxygen co-doped graphene quantum dots onto hierarchical carbon networks for all-solid-state flexible supercapacitors. *Electrochim. Acta* **2017**, *235*, 561−569.
(139) Li, Z.; Cao, L.; Qin, P.; Liu, X.; Chen, Z.; Wang, L.; Pan, D.; Wu, M. Nitrogen and oxygen co-doped graphene quantum dots with high

https://doi.org/10.1021/acsomega.2c06010
ACS Omega 2022, 7, 45935−45961

capacitance performance for micro-supercapacitors. *Carbon* **2018**, *139*, 67−75.
(140) Mi, K.; Chen, S.; Xi, B.; Kai, S.; Jiang, Y.; Feng, J.; Qian, Y.; Xiong, S. Sole chemical confinement of polysulfides on nonporous nitrogen/oxygen dual-doped carbon at the kilogram scale for lithium−sulfur batteries. *Adv. Funct. Mater.* **2017**, *27*, 1604265.
(141) Shi, M.; Zhang, S.; Jiang, Y.; Jiang, Z.; Zhang, L.; Chang, J.; Wei, T.; Fan, Z. Sandwiching sulfur into the dents between N, O Co-doped graphene layered blocks with strong physicochemical confinements for stable and high-rate Li−S batteries. *Nano-Micro Lett.* **2020**, *12*, 146.
(142) Peng, Y.; Zhang, Y.; Huang, J.; Wang, Y.; Li, H.; Hwang, B. J.; Zhao, J. Nitrogen and oxygen dual-doped hollow carbon nanospheres derived from catechol/polyamine as sulfur hosts for advanced lithium sulfur batteries. *Carbon* **2017**, *124*, 23−33.
(143) Sun, Y.; Zhu, D.; Liang, Z.; Zhao, Y.; Tian, W.; Ren, X.; Wang, J.; Li, X.; Gao, Y.; Wen, W.; Huang, Y.; Li, X.; Tai, R. Facile renewable synthesis of nitrogen/oxygen co-doped graphene-like carbon nanocages as general lithium-ion and potassium-ion batteries anode. *Carbon* **2020**, *167*, 685−695.
(144) Zhu, Y.; Wang, M.; Zhang, Y.; Wang, R.; Zhang, Y.; Wang, C. Nitrogen/oxygen dual-doped hierarchically porous carbon/graphene composite as high-performance anode for potassium storage. *Electrochim. Acta* **2021**, *377*, 138093.
(145) Yang, J.; Ju, Z.; Jiang, Y.; Xing, Z.; Xi, B.; Feng, J.; Xiong, S. Enhanced capacity and rate capability of nitrogen/oxygen dual-doped hard carbon in capacitive potassium-ion storage. *Adv. Mater.* **2018**, *30*, 1700104.
(146) Ruan, J.; Zhao, Y.; Luo, S.; Yuan, T.; Yang, J.; Sun, D.; Zheng, S. Fast and stable potassium-ion storage achieved by in situ molecular self-assembling N/O dual-doped carbon network. *Energy Storage Mater.* **2019**, *23*, 46−54.
(147) Liang, J.; Jiao, Y.; Jaroniec, M.; Qiao, S. Z. Sulfur and Nitrogen Dual-Doped Mesoporous Graphene Electrocatalyst for Oxygen Reduction with Synergistically Enhanced Performance. *Angew. Chem., Int. Ed.* **2012**, *51*, 11496−11500.
(148) Denis, P. A.; Huelmo, C. P.; Iribarne, F. Theoretical characterization of sulfur and nitrogen dual-doped graphene. *Comp. Theor Chem.* **2014**, *1049*, 13−19.
(149) Paraknowitsch, J. P.; Wienert, B.; Zhang, Y.; Thomas, A. Intrinsically Sulfur- and Nitrogen-Co-doped Carbons from Thiazolium Salts. *Chem.—Eur. J.* **2012**, *18*, 15416−15423.
(150) Su, Y.; Zhang, Y.; Zhuang, X.; Li, S.; Wu, D.; Zhang, F.; Feng, X. Low-temperature synthesis of nitrogen/sulfur co-doped three-dimensional graphene frameworks as efficient metal-free electrocatalyst for oxygen reduction reaction. *Carbon* **2013**, *62*, 296−301.
(151) Denis, P. A.; Iribarne, F. The effect of the dopant nature on the reactivity, interlayer bonding and electronic properties of dual doped bilayer graphene. *Phys. Chem. Chem. Phys.* **2016**, *18*, 24693−24703.
(152) Ullah, S.; Denis, P. A.; Sato, F. Unusual Enhancement of the Adsorption Energies of Sodium and Potassium in Sulfur−Nitrogen and Silicon−Boron Codoped Graphene. *ACS Omega* **2018**, *3*, 15821−15828.
(153) Ma, X.; Ning, G.; Sun, Y.; Pu, Y.; Gao, J. High capacity Li storage in sulfur and nitrogen dual-doped graphene networks. *Carbon* **2014**, *79*, 310−320.
(154) You, J. M.; Ahmed, M. S.; Han, H. S.; Choe, J.; Ustundag, Z.; Jeon, S. New approach of nitrogen and sulfur-doped graphene synthesis using dipyrrolemethane and their electrocatalytic activity for oxygen reduction in alkaline media. *J. Power Sources* **2015**, *275*, 73−79.
(155) Kicinski, W.; Norek, M.; Dziura, A.; Polanski, M. Copolycondensation of heterocyclic aldehydes: A general approach to sulfur and nitrogen dually-doped carbon gels. *Microporous Mesoporous Mater.* **2016**, *225*, 198−209.
(156) Chen, Q.; Liu, H.; Zhu, R.; Wang, X.; Wang, S.; Zhu, J.; He, H. Facile synthesis of nitrogen and sulfur co-doped graphene-like carbon materials using methyl blue/montmorillonite composites. *Microporous Mesoporous Mater.* **2016**, *225*, 137−143.
(157) Feng, B.; Xie, J.; Dong, C.; Zhang, S.; Cao, G.; Zhao, X. From graphite oxide to nitrogen and sulfur co-doped few-layered graphene by a green reduction route via Chinese medicinal herbs. *RSC Adv.* **2014**, *4*, 17902−17907.
(158) Wu, M.; Liu, Y.; Zhu, Y.; Lin, J.; Liu, J.; Hu, H.; Wang, Y.; Zhao, Q.; Lv, R.; Qiu, J. Supramolecular polymerization-assisted synthesis of nitrogen and sulfur dual-doped porous graphene networks from petroleum coke as efficient metal-free electrocatalysts for the oxygen reduction reaction. *J. Mater. Chem. A* **2017**, *5*, 11331−11339.
(159) Zhang, H.; Liu, X.; He, G.; Zhang, X.; Bao, S.; Hu, W. Bioinspired synthesis of nitrogen/sulfur co-doped graphene as an efficient electrocatalyst for oxygen reduction reaction. *J. Power Sources* **2015**, *279*, 252−258.
(160) Carraro, F.; Cattelan, M.; Favaro, M.; Calvillo, L. Aerosol Synthesis of N and NS Doped and Crumpled Graphene Nanostructures. *Nanomaterials* **2018**, *8*, 406.
(161) Li, J.; Zhang, Y.; Zhang, X.; Huang, J.; Han, J.; Zhang, Z.; Han, X.; Xu, P.; Song, B. S, N Dual-Doped Graphene-like Carbon Nanosheets as Efficient Oxygen Reduction Reaction Electrocatalysts. *ACS Appl. Mater. Interfaces* **2017**, *9*, 398−405.
(162) Zhang, Y.; Li, P.; Yin, X.; Yan, Y.; Zhan, K.; Yang, J.; Zhao, B. Cobalt sulfide supported on nitrogen and sulfur dual-doped reduced graphene oxide for highly active oxygen reduction reaction. *RSC Adv.* **2017**, *7*, 50246−50253.
(163) Akhter, T.; Islam, M. M.; Faisal, S. N.; Haque, E.; Minett, A. I.; Liu, H. K.; Konstantinov, K.; Dou, S. X. Self-assembled N/S codoped flexible graphene paper for high performance energy storage and oxygen reduction reaction. *ACS Appl. Mater. Interfaces* **2016**, *8* (3), 2078−2087.
(164) Zhao, J.; Liu, Y.; Quan, X.; Chen, S.; Zhao, H.; Yu, H. Nitrogen and sulfur co-doped graphene/carbon nanotube as metal-free electrocatalyst for oxygen evolution reaction: the enhanced performance by sulfur doping. *Electrochim. Acta* **2016**, *204*, 169−175.
(165) Zhang, X.; Wen, X.; Pan, C.; Xiang, X.; Hao, C.; Meng, Q.; Tian, Z. Q.; Shen, P. K.; Jiang, S. P. N species tuning strategy in N, S co-doped graphene nanosheets for electrocatalytic activity and selectivity of oxygen redox reactions. *Chem. Eng. J.* **2022**, *431*, 133216.
(166) Wu, M.; Wang, J.; Wu, Z.; Xin, H. L.; Wang, D. Synergistic enhancement of nitrogen and sulfur co-doped graphene with carbon nanosphere insertion for the electrocatalytic oxygen reduction reaction. *J. Mater. Chem. A* **2015**, *3*, 7727−7731.
(167) Higgins, D. C.; Hoque, M. A.; Hassan, F.; Choi, J. Y.; Kim, B.; Chen, Z. Oxygen reduction on graphene−carbon nanotube composites doped sequentially with nitrogen and sulfur. *ACS Catal.* **2014**, *4* (8), 2734−2740.
(168) Pan, F.; Duan, Y.; Zhang, X.; Zhang, J. A facile synthesis of nitrogen/sulfur co-doped graphene for the oxygen reduction reaction. *ChemCatChem* **2016**, *8*, 163−170.
(169) Xu, J.; Dong, G.; Jin, C.; Huang, M.; Guan, L. Sulfur and nitrogen co-doped, few-layered graphene oxide as a highly efficient electrocatalyst for the oxygen-reduction reaction. *ChemSusChem* **2013**, *6*, 493−499.
(170) Zhao, Z.; Xia, Z. Design principles for dual-element-doped carbon nanomaterials as efficient bifunctional catalysts for oxygen reduction and evolution reactions. *ACS Catal.* **2016**, *6*, 1553−1558.
(171) Wu, D.; Wang, T.; Wang, L.; Jia, D. Hydrothermal synthesis of nitrogen, sulfur co-doped graphene and its high performance in supercapacitor and oxygen reduction reaction. *Microporous Mesoporous Mater.* **2019**, *290*, 109556.
(172) Wu, M.; Dou, Z.; Chang, J.; Cui, L. Nitrogen and sulfur co-doped graphene aerogels as an efficient metal-free catalyst for oxygen reduction reaction in an alkaline solution. *RSC Adv.* **2016**, *6*, 22781−22790.
(173) He, G.; Qiao, M.; Li, W.; Lu, Y.; Zhao, T.; Zou, R.; Li, B.; Darr, S. J.A.; Hu, J.; Titirici, M. M.; Parkin, I. P. N-Co-doped graphene-nickel cobalt sulfide aerogel: improved energy storage and electrocatalytic performance. *Adv. Sci.* **2017**, *4*, 1600214.
(174) Abedi, H.; Mehrpooya, M. Synthesis of three-metal layered double hydroxide and dual doped graphene oxide composite as a novel electrocatalyst for oxygen reduction reaction. *J. Alloys Compd.* **2021**, *875*, 160047.

https://doi.org/10.1021/acsomega.2c06010
ACS Omega 2022, 7, 45935−45961

(175) Ma, R.; Xia, B. Y.; Zhou, Y.; Li, P.; Chen, Y.; Liu, Q.; Wang, J. Ionic liquid-assisted synthesis of dual-doped graphene as efficient electrocatalysts for oxygen reduction. *Carbon* **2016**, *102*, 58−65.
(176) Zhang, W.; Zhang, Y.; Li, Y.; Yang, S.; Zhang, L.-H.; Yu, F. Enhanced oxygen reduction performance of nitrogen and sulfur Co-doped graphene oxide by immobilized ionic liquid. *Chem. Eng. J.* **2021**, *236*, 116544.
(177) Cui, Z.; Wang, S.; Zhang, Y.; Cao, M. A simple and green pathway toward nitrogen and sulfur dual doped hierarchically porous carbons from ionic liquids for oxygen reduction. *J. Power Sources* **2014**, *259*, 138−144.
(178) Moosapour Siahkalroudi, Z.; Aghabarari, B.; Vaezi, M.; Rodríguez-Castellón, E.; Martínez-Huerta, M. V. Effect of secondary heteroatom (S, P) in N-doped reduced graphene oxide catalysts to oxygen reduction reaction. *Mol. Catal.* **2021**, *502*, 111372.
(179) Tang, Y.; Jing, F.; Xu, Z.; Zhang, F.; Mai, Y.; Wu, D. Highly Crumpled Hybrids of Nitrogen/Sulfur Dual-Doped Graphene and Co_9S_8 Nanoplates as Efficient Bifunctional Oxygen Electrocatalysts. *ACS Appl. Mater. Interfaces* **2017**, *9* (14), 12340−12347.
(180) Peng, W.; Jin, J.; Yang, S.; Shen, Z.; Wang, H.; Zhang, J.; Li, G. Hollow Co_9S_8 spheres-derived polyhedrons uniformly anchored on N, S-doped graphene for efficient oxygen electrocatalysts. *Compos. Commun.* **2021**, *23*, 100587.
(181) Ma, X. X.; Su, Y.; He, X. Q. Fe_9S_{10}-decorated N, S co-doped graphene as a new and efficient electrocatalyst for oxygen reduction and oxygen evolution reactions. *Catal. Sci. Technol.* **2017**, *7*, 1181−1192.
(182) Zhang, M.; Hong, W.; Xue, R.; Li, L.; Huang, G.; Xu, X.; Gao, J.; Yan, J. Nitrogen/sulfur dual-doped reduced graphene oxide supported $CuFeS_2$ as an efficient electrocatalyst for the oxygen reduction reaction. *New J. Chem.* **2018**, *42*, 2081−2088.
(183) Wang, X.; Wang, J.; Wang, D.; Dou, S.; Ma, Z.; Wu, J.; Tao, L.; Shen, A.; Ouyang, C.; Liu, Q.; Wang, S. One-pot synthesis of nitrogen and sulfur co-doped graphene as efficient metal-free electrocatalysts for the oxygen reduction reaction. *Chem. Commun.* **2014**, *50*, 4839−4842.
(184) Chae, G. S.; Youn, D. H.; Lee, J. S. Nanostructured iron sulfide/N, S dual-doped carbon nanotube-graphene composites as efficient electrocatalysts for oxygen reduction reaction. *Materials* **2021**, *14*, 2146.
(185) Sibul, R.; Kibena-Põldsepp, E.; Mäeorg, U.; Merisalu, M.; Kikas, A.; Kisand, V.; Treshchalov, A.; Sammelselg, V.; Tammeveski, K. Sulphur and nitrogen co-doped graphene-based electrocatalysts for oxygen reduction reaction in alkaline medium. *Electrochem. Commun.* **2019**, *109*, 106603.
(186) Ye, X.; Hu, L.; Liu, M.; Wang, G.; Yu, F. Improved oxygen reduction performance of a N, S co-doped graphene-like carbon prepared by a simple carbon bath method. *New Carbon Mater.* **2020**, *35*, 531−539.
(187) Rivera-Gavidia, L. M.; Luis-Sunga, M.; Bousa, M.; Vales, V.; Kalbac, M.; Arevalo, M. C.; Pastor, E.; Garcia, G. S-and N-doped graphene-based catalysts for the oxygen evolution reaction. *Electrochim. Acta* **2020**, *340*, 135975.
(188) Fan, T.; Zhang, G.; Jian, L.; Murtaza, I.; Meng, H.; Liu, Y.; Min, Y. Facile synthesis of defect-rich nitrogen and sulfur Co-doped graphene quantum dots as metal-free electrocatalyst for the oxygen reduction reaction. *J. Alloys Compd.* **2019**, *792*, 844−850.
(189) Mousavi, S. A.; Mehrpooya, M. Fabrication of copper centered metal organic framework and nitrogen, sulfur dual doped graphene oxide composite as a novel electrocatalyst for oxygen reduction. *Energy* **2021**, *214*, 119053.
(190) Chabu, J. M.; Wang, L.; Tang, F. Y.; Zeng, K.; Sheng, J.; Walle, M. D.; Deng, L.; Liu, Y. N. Synthesis of Three-Dimensional Nitrogen and Sulfur Dual-Doped Graphene Aerogels as an Efficient Metal-Free Electrocatalyst for the Oxygen Reduction Reaction. *ChemElectroChem.* **2017**, *4*, 1885−1890.
(191) Li, Y.; Yang, J.; Huang, J.; Zhou, Y.; Xu, K.; Zhao, N.; Cheng, X. Soft template-assisted method for synthesis of nitrogen and sulfur co-doped three-dimensional reduced graphene oxide as an efficient metal free catalyst for oxygen. *Carbon* **2017**, *122*, 237−246.
(192) Lei, Z.; Feng, W.; Feng, C.; Zhou, W.; Wei, C.; Wang, X. Nitrified coke wastewater sludge flocs: an attractive precursor for N, S dual-doped graphene-like carbon with ultrahigh capacitance and oxygen reduction performance. *J. Mater. Chem. A* **2017**, *5*, 2012−2020.
(193) Zhao, C.; Li, J.; Chen, Y.; Chen, J. Nitrogen and sulfur dual-doped graphene as an efficient metal-free electrocatalyst for the oxygen reduction reaction in microbial fuel cells. *New J. Chem.* **2019**, *43*, 9389−9395.
(194) Bag, S.; Mondal, B.; Das, A. K.; Raj, C. R. Nitrogen and sulfur dual-doped reduced graphene oxide: synergistic effect of dopants towards oxygen reduction reaction. *Electrochim. Acta* **2015**, *163*, 16−23.
(195) Amiinu, I. S.; Zhang, J.; Kou, Z.; Liu, X.; Asare, O. K.; Zhou, H.; Cheng, K.; Zhang, H.; Mai, L.; Pan, M.; Mu, S. Self-organized 3D porous graphene dual-doped with biomass-sponsored nitrogen and sulfur for oxygen reduction and evolution. *ACS Appl. Mater. Interfaces* **2016**, *8* (43), 29408−29418.
(196) He, D.; Zhao, W.; Li, P.; Sun, S.; Tan, Q.; Han, K.; Liu, L.; Liu, L.; Qu, X. Bifunctional biomass-derived N, S dual-doped ladder-like porous carbon for supercapacitor and oxygen reduction reaction. *J. Alloys Compd.* **2019**, *773*, 11−20.
(197) Zhang, J.; Wang, J.; Wu, Z.; Wang, S.; Wu, Y.; Liu, X. Heteroatom (nitrogen/sulfur)-doped graphene as an efficient electrocatalyst for oxygen reduction and evolution reactions. *Catalysts* **2018**, *8*, 475.
(198) Song, J.; Liu, T. F.; Ali, S.; Li, B.; Su, D. S. The synergy effect and reaction pathway in the oxygen reduction reaction on the sulfur and nitrogen dual doped graphene catalyst. *Chem. Phys. Lett.* **2017**, *677*, 65−69.
(199) Ma, X. X.; He, X. Q. Achieving superior performance for oxygen electrode catalyst by the assistance of NaCl to construct cobalt sulfide on nitrogen and sulfur dual-doped graphene. *Int. J. of Hydrog. Energy* **2018**, *43*, 13256−13265.
(200) Mathumba, P.; Fernandes, D. M.; Matos, R.; Iwuoha, E. I.; Freire, C. Metal Oxide (Co_3O_4 and Mn_3O_4) Impregnation into S, N-doped Graphene for Oxygen Reduction Reaction (ORR). *Materials* **2020**, *13*, 1562.
(201) Zhong, J.; Wu, T.; Wu, Q.; Du, S.; Chen, D.; Chen, B.; Chang, M.; Luo, X.; Liu, Y. N-and S-co-doped graphene sheet-encapsulated Co_9S_8 nanomaterials as excellent electrocatalysts for the oxygen evolution reaction. *J. Power Sources* **2019**, *417*, 90−98.
(202) Ma, R.; Lin, G.; Zhou, Y.; Liu, Q.; Zhang, T.; Shan, G.; Yang, M.; Wang, J. A review of oxygen reduction mechanisms for metal-free carbon-based electrocatalysts. *npj Comput. Mater.* **2019**, *5*, 78.
(203) Jiang, H.; Zhu, Y.; Su, Y.; Yao, Y.; Liu, Y.; Yang, X.; Li, C. Highly dual-doped multilayer nanoporous graphene: efficient metal-free electrocatalysts for the hydrogen evolution reaction. *J. Mater. Chem. A* **2015**, *3*, 12642−12645.
(204) Guruprasad, K.; Maiyalagan, T.; Shanmugam, S. Phosphorus Doped MoS_2 Nanosheet Promoted with Nitrogen, Sulfur Dual Doped Reduced Graphene Oxide as an Effective Electrocatalyst for Hydrogen Evolution. *ACS Appl. Energy Mater.* **2019**, *2* (9), 6184−6194.
(205) Cheng, T.-Y.; Chou, F.-P.; Huang, S.-C.; Chang, C.-Y.; Wu, T.-K. Electroluminescence and photocatalytic hydrogen evolution of S, N co-doped graphene oxide quantum dots. *J. Mater. Chem. A* **2022**, *10*, 3650−3658.
(206) Kumaran, Y.; Maiyalagan, T.; Yi, S. C. An efficient $CoMoS_2$ nanosheets on nitrogen, sulfur dual doped reduced graphene oxide as an electrocatalyst for the hydrogen evolution reaction. *Int. J.Energy Res.* **2021**, *45*, 17397−17407.
(207) Li, M.; Zhou, H.; Yang, W.; Chen, L.; Huang, Z.; Zhang, N.; Fu, C.; Kuang, Y. Co_9S_8 nanoparticles embedded in a N, S co-doped graphene-unzipped carbon nanotube composite as a high performance electrocatalyst for the hydrogen evolution reaction. *J. Mater. Chem. A* **2017**, *5*, 1014−1021.
(208) Li, X.; Duan, X.; Han, C.; Fan, X.; Li, Y.; Zhang, F.; Zhang, G.; Peng, W.; Wang, S. Chemical activation of nitrogen and sulfur co-doped graphene as defect-rich carbocatalyst for electrochemical water splitting. *Carbon* **2019**, *148*, 540−549.
(209) Xie, H.; Hou, C.; Wang, H.; Zhang, Q.; Li, Y. S, N co-doped graphene quantum dot/TiO_2 composites for efficient photocatalytic hydrogen generation. *Nanoscale Res. Lett.* **2017**, *12*, 400.

https://doi.org/10.1021/acsomega.2c06010
ACS Omega 2022, 7, 45935−45961

(210) Bayat, A.; Saievar-Iranizad, E. Vertically aligned rutile TiO_2 nanorods sensitized with sulfur and nitrogen co-doped graphene quantum dots for water splitting: an energy level study. *J. Alloys Compd.* **2018**, *755*, 192−198.
(211) Suryawanshi, U. P.; Ghorpade, U. V.; Lee, D. M.; He, M.; Shin, S. W.; Kumar, P. V.; Jang, J. S.; Jung, H. R.; Suryawanshi, M. P.; Kim, J. H. Colloidal Ni_2P Nanocrystals Encapsulated in Heteroatom-Doped Graphene Nanosheets: A Synergy of 0D@2D Heterostructure Toward Overall Water Splitting. *Chem. Mater.* **2021**, *33* (1), 234−245.
(212) Guo, X.; Duan, X.; Ji, J.; Fan, X.; Li, Y.; Zhang, F.; Zhang, G.; Zhu, Y. A.; Peng, W.; Wang, S. Synthesis of nitrogen and sulfur doped graphene on graphite foam for electro-catalytic phenol degradation and water splitting. *J. Colloid Interface Sci.* **2021**, *583*, 139−148.
(213) Wang, Q.; Li, L.; Luo, L.; Yang, Y.; Yang, Z.; Li, H.; Zhou, Y. Activation of persulfate with dual-doped reduced graphene oxide for degradation of alkylphenols. *Chem. Eng. J.* **2019**, *376*, 120891.
(214) Tian, Y.; Xu, D.; Chu, K.; Wei, Z.; Liu, W. Metal-free N, S co-doped graphene for efficient and durable nitrogen reduction reaction. *J. Mater. Sci.* **2019**, *54*, 9088−9097.
(215) Zhang, X.; Zhu, J.; Tiwary, C. S.; Ma, Z.; Huang, H.; Zhang, J.; Lu, Z.; Huang, W.; Wu, Y. Palladium Nanoparticles Supported on Nitrogen and Sulfur Dual-Doped Graphene as Highly Active Electrocatalysts for Formic Acid and Methanol Oxidation. *ACS Appl. Mater. Interfaces* **2016**, *8*, 10858−10865.
(216) An, M.; Du, L.; Du, C.; Sun, Y.; Wang, Y.; Yin, G.; Gao, Y. Pt nanoparticles supported by sulfur and phosphorus co-doped graphene as highly active catalyst for acidic methanol electrooxidation. *Electrochim. Acta* **2018**, *285*, 202−213.
(217) Zhang, K.; Chen, X.; Wang, L.; Zhang, D.; Xue, Z.; Zhou, X.; Lu, X. PtPd nanoparticles supported on sulfonated nitrogen sulfur co-doped graphene for methanol electro-oxidation. *Int. J. Hydrog. Energy* **2018**, *43*, 15931−15940.
(218) Zhang, J. X.; Yang, X. L.; Shao, H. F.; Tseng, C. C.; Wang, D. S.; Tian, S. S.; Hu, W. J.; Jing, C.; Tian, J. N.; Zhao, Y. C. Microwave-assisted Synthesis of Pd Oxide-rich Pd Particles on Nitrogen/Sulfur Co-Doped Graphene with Remarkably Enhanced Ethanol Electro-oxidation. *Fuel Cells* **2017**, *17*, 115−122.
(219) Mahyari, M.; Bide, Y.; Gavgani, J. N. Iron (III) porphyrin supported on S and N co-doped graphene quantum dot as an efficient photocatalyst for aerobic oxidation of alcohols under visible light irradiation. *Appl. Catal. A: Gen.* **2016**, *517*, 100−109.
(220) Sajjadi, S.; Khataee, A.; Soltani, R. D. C.; Hasanzadeh, A. N, S co-doped graphene quantum dot−decorated Fe_3O_4 nanostructures: Preparation, characterization and catalytic activity. *J. Phys. Chem. Solids* **2019**, *127*, 140−150.
(221) Rohani, S.; Ziarani, G. M.; Ziarati, A.; Badiei, A. Designer 3D CoAl-layered double hydroxide@N,S doped graphene hollow architecture decorated with Pd nanoparticles for Sonogashira couplings. *Appl. Surf. Sci.* **2019**, *496*, 143599.
(222) Rohani, S.; Ziarani, G. M.; Badiei, A.; Ziarati, A. Mesoporous hierarchically hollow flower-like CoAl-LDH@ N, S-doped Graphene@ Pd nanoarchitectures for heck couplings. *Catal. Lett.* **2019**, *149*, 2984−2993.
(223) Qu, D.; Zheng, M.; Du, P.; Zhou, Y.; Zhang, L.; Li, D.; Tan, H.; Zhao, Z.; Xie, Z.; Sun, Z. Highly luminescent S, N co-doped graphene quantum dots with broad visible absorption bands for visible light photocatalysts. *Nanoscale* **2013**, *5*, 12272−12277.
(224) Cai, A.; Wang, Q.; Chang, Y.; Wang, X. Graphitic carbon nitride decorated with S, N co-doped graphene quantum dots for enhanced visible-light-driven photocatalysis. *J. Alloys Compd.* **2017**, *692*, 183−189.
(225) Tian, H.; Shen, K.; Hu, X.; Qiao, L.; Zheng, W. N, S co-doped graphene quantum dots-graphene-TiO_2 nanotubes composite with enhanced photocatalytic activity. *J. Alloys Compd.* **2017**, *691*, 369−377.
(226) Zheng, L.; Su, H.; Zhang, J.; Walekar, L. S.; Molamahmood, H. V.; Zhou, B.; Long, M.; Hu, Y. H. Highly selective photocatalytic production of H_2O_2 on sulfur and nitrogen co-doped graphene quantum dots tuned TiO_2. *Appl. Catal. B: Environ.* **2018**, *239*, 475−484.
(227) Luo, Y.; Li, M.; Sun, L.; Xu, Y.; Hu, G.; Tang, T.; Wen, J.; Li, X. Tuning the photoluminescence of graphene quantum dots by co-doping of nitrogen and sulfur. *J. Nanoparticle Res.* **2017**, *19*, 363.
(228) Zhang, R.; Adsetts, J.R.; Nie, Y.; Sun, X.; Ding, Z. Electrochemiluminescence of nitrogen-and sulfur-doped graphene quantum dots. *Carbon* **2018**, *129*, 45−53.
(229) Wang, X. F.; Wang, G. G.; Li, J. B.; Liu, Z.; Zhao, W. F.; Han, J.-C. Towards high-powered remote WLED based on flexible white-luminescent polymer composite films containing S, N co-doped graphene quantum dots. *Chem. Eng. J.* **2018**, *336*, 406−415.
(230) Zhang, B. X.; Gao, H.; Li, X. L. Synthesis and optical properties of nitrogen and sulfur co-doped graphene quantum dots. *New J. Chem.* **2014**, *38*, 4615−4621.
(231) Li, J.; Yang, S.; Wang, G.; Huang, T.; Guo, Q.; Liu, Z.; He, P.; Zheng, X.; Wang, Y.; Xu, A.; Zhao, M.; Zhu, W.; Chen, D.; Ding, G. Seed-Initiated Synthesis and Tunable Doping Graphene for High-Performance Photodetectors. *Adv. Optical Mater.* **2019**, *7*, 1901388.
(232) Adaikalam, K.; Ramesh, S.; Santhoshkumar, P.; Kim, H. S.; Park, H. C.; Kim, H. S. MnO_2/Co_3O_4 with N and S co-doped graphene oxide bimetallic nanocomposite for hybrid supercapacitor and photosensor applications. *Int. J. Energy Res.* **2022**, *46*, 4494−4505.
(233) Schroer, Z. S.; Wu, Y.; Xing, Y.; Wu, X.; Liu, X.; Wang, Xu; Pino, O. G.; Zhou, C.; Combs, C.; Pu, Q.; Wu, M.; Zhao, J. X.; Chen, J. Nitrogen−sulfur-doped graphene quantum dots with metal ion-resistance for bioimaging. *ACS Appl. Nano Mater.* **2019**, *2* (11), 6858−6865.
(234) Qu, D.; Sun, Z.; Zheng, M.; Li, J.; Zhang, Y.; Zhang, G.; Zhao, H.; Liu, X.; Xie, Z. Three Colors Emission from S,N Co-doped Graphene Quantum Dots for Visible Light H_2 Production and Bioimaging. *Adv. Opt. Mater.* **2015**, *3*, 360−367.
(235) Chen, H.; Ma, X.; Shen, P. K. In-situ encapsulating FeS/Fe_3C nanoparticles into nitrogen-sulfur dual-doped graphene networks for high-rate and ultra-stable lithium storage. *J. Alloys Compd.* **2019**, *779*, 193−201.
(236) Li, G.; He, B.; Zhou, M.; Wang, G.; Zhou, N.; Xu, W.; Hou, Z. Solvothermal Synthesis of Mesoporous Manganese Sulfide Nanoparticles Supported on Nitrogen and Sulfur Co-doped Graphene with Superior Lithium Storage Performance. *ChemElectroChem.* **2017**, *4*, 81−89.
(237) Gao, X.; Wang, B.; Zhang, Y.; Liu, H.; Liu, H.; Wu, H.; Dou, S. Graphene-scroll-sheathed α-MnS coaxial nanocables embedded in N, S Co-doped graphene foam as 3D hierarchically ordered electrodes for enhanced lithium storage. *Energy Storage Mater.* **2019**, *16*, 46−55.
(238) Wang, M.; Huang, Y.; Chen, X.; Wang, K.; Wu, H.; Zhang, N.; Fu, H. Synthesis of nitrogen and sulfur co-doped graphene supported hollow $ZnFe_2O_4$ nanosphere composites for application in lithium-ion batteries. *J. Alloys. Compd.* **2017**, *691*, 407−415.
(239) Guo, P.; Xiao, F.; Liu, Q.; Liu, H.; Guo, Y.; Gong, J. R.; Wang, S.; Liu, Y. One-Pot Microbial Method to Synthesize Dual-Doped Graphene and Its Use as High-Performance Electrocatalyst. *Sci. Rep* **2013**, *3*, 3499.
(240) Idrees, M.; Batool, S.; Kong, J.; Zhuang, Q.; Liu, H.; Shao, Q.; Lu, N.; Feng, Y.; Wujcik, E. K.; Gao, Q.; Ding, T.; Wei, R.; Guo, Z. Polyborosilazane derived ceramics Nitrogen sulfur dual doped graphene nanocomposite anode for enhanced lithium ion batteries. *Electrochim. Acta* **2019**, *296*, 925−937.
(241) Song, X.; Ma, X.; Ning, G.; Gao, D.; Yu, Z.; Xiao, Z. The orientation construction of S and N dual-doped discoid-like graphene with high-rate electrode property. *Appl. Surf. Sci.* **2018**, *442*, 467−475.
(242) Kotal, M.; Kim, J.; Kim, K. J.; Oh, I. K. Sulfur and nitrogen co-doped graphene electrodes for high-performance ionic artificial muscles. *Adv. Mater.* **2016**, *28*, 1610−1615.
(243) Huo, J.; Ren, Y.; Xue, Y.; Liu, Y.; Guo, S. Sulfur/nitrogen dual-doped three-dimensional reduced graphene oxide modified with mesoporous TiO2 nanoparticles for promising lithium-ion battery anodes. *J. Alloys Compd.* **2021**, *868*, 159183.
(244) Kim, J.-H.; Kannan, A. G.; Woo, H.-S.; Jin, D.-G.; Kim, W.; Ryu, K.; Kim, D.-W. A bi-functional metal-free catalyst composed of dual-

https://doi.org/10.1021/acsomega.2c06010
ACS Omega 2022, 7, 45935−45961

doped graphene and mesoporous carbon for rechargeable lithium−oxygen batteries. *J. Mater. Chem. A* **2015**, *3*, 18456−18465.
(245) Jang, S.; Kim, J.; Na, E.; Song, M.; Choi, J.; Song, K. H.; Baeck, S. H.; Shim, S. E. Facile synthesis of mesoporous and highly nitrogen/sulfur dual-doped graphene and its ultrahigh discharge capacity in non-aqueous lithium oxygen batteries. *Carbon Lett.* **2019**, *29*, 297−305.
(246) Zeng, X.; You, C.; Leng, L.; Dang, D.; Qiao, X.; Li, X.; Li, Y.; Liao, S.; Adzic, R. R. Ruthenium nanoparticles mounted on multielement co-doped graphene: an ultra-high-efficiency cathode catalyst for Li−O_2 batteries. *J. Mater. Chem. A* **2015**, *3*, 11224−11231.
(247) Chen, D.; Yang, R.; Chen, L.; Zou, Y.; Ren, B.; Li, L.; Li, S.; Yan, Y.; Xu, Y. One-pot fabrication of nitrogen and sulfur dual-doped graphene/sulfur cathode via microwave assisted method for long cycle-life lithium-sulfur batteries. *J. Alloys Compd.* **2018**, *746*, 116−124.
(248) Li, X.; Yu, Y.; Tang, Z.; Yang, Y.; Li, Y.; Cao, J.; Chen, L. N,S-doped graphene derived from graphene oxide and thiourea-form-aldehyde resin for high stability lithium−sulfur batteries. *Phys. Chem. Chem. Phys.* **2022**, *24*, 2879−2886.
(249) Ci, H.; Wang, M.; Sun, Z.; Wei, C.; Cai, J.; Lu, C.; Cui, G.; Liu, Z.; Sun, J. Direct insight into sulfiphilicity-lithiophilicity design of bifunctional heteroatom-doped graphene mediator toward durable Li-S batteries. *J. Energy Chem.* **2022**, *66*, 474−482.
(250) Pang, Q.; Tang, J.; Huang, H.; Liang, X.; Hart, C.; Tam, K. C.; Nazar, L. F. A nitrogen and sulfur dual-doped carbon derived from Polyrhodanine@Cellulose for advanced lithium−sulfur batteries. *Adv. Mater.* **2015**, *27*, 6021−6028.
(251) Balach, J.; Singh, H. K.; Gomoll, S.; Jaumann, T.; Klose, M.; Oswald, S.; Richter, M.; Eckert, J.; Giebeler, L. Synergistically enhanced polysulfide chemisorption using a flexible hybrid separator with N and S dual-doped mesoporous carbon coating for advanced lithium−sulfur. *ACS Appl. Mater. Interfaces* **2016**, *8* (23), 14586−14595.
(252) Li, N.; Gan, F.; Wang, P.; Chen, K.; Chen, S.; He, X. In situ synthesis of 3D sulfur-doped graphene/sulfur as a cathode material for lithium-sulfur batteries. *J. Alloys Compd.* **2018**, *754*, 64−71.
(253) Zhou, Y.; Zeng, Y.; Xu, D.; Li, P.; Wang, H.-G.; Li, X.; Li, Y.; Wang, Y. Nitrogen and sulfur dual-doped graphene sheets as anode materials with superior cycling stability for lithium-ion batteries. *Electrochim. Acta* **2015**, *184*, 24−31.
(254) Shan, H.; Li, X.; Cui, Y.; Xiong, D.; Yan, B.; Li, D.; Lushington, A.; Sun, X. Sulfur/nitrogen dual-doped porous graphene aerogels enhancing anode performance of lithium ion batteries. *Electrochim. Acta* **2016**, *205*, 188−197.
(255) Feng, Q.; Li, T.; Sui, Y.; Xiao, B.; Wang, T.; Sun, Z.; Qi, J.; Wei, F.; Meng, Q.; Ren, Y.; Xue, X. Facile synthesis and first-principles study of nitrogen and sulfur dual-doped porous graphene aerogels/natural graphite as anode materials for Li-ion batteries. *J. Alloys Compd.* **2021**, *884*, 160923.
(256) Wang, C.; Zhang, X.; Qian, Y.; Wu, H.; Kan, E. First-principles study on S and N doping graphene/SnS_2 heterostructure for lithium-ion battery. *Chem. Phys. Lett.* **2021**, *769*, 138391.
(257) Zhu, J.; Tu, W.; Pan, H.; Zhang, H.; Liu, B.; Cheng, Y.; Deng, Z.; Zhang, H. Self-Templating Synthesis of Hollow Co_3O_4 Nanoparticles Embedded in N,S-Dual-Doped Reduced Graphene Oxide for Lithium Ion Batteries. *ACS Nano* **2020**, *14* (5), 5780−5787.
(258) Yang, Z.; Qian, K.; Lv, J.; Yan, W.; Liu, J.; Ai, J.; Zhang, Y.; Guo, T.; Zhou, Z.; Xu, S.; Guo, Z. Encapsulation of Fe_3O_4 Nanoparticles into N, S co-Doped Graphene Sheets with Greatly Enhanced Electrochemical Performance. *Sci. Rep.* **2016**, *6*, 27957.
(259) Cai, D.; Wang, C.; Shi, C.; Tan, N. Facile synthesis of N and S co-doped graphene sheets as anode materials for high-performance lithium-ion batteries. *J. Alloys Compd.* **2018**, *731*, 235−242.
(260) Li, R.; Li, J.; Qi, K.; Ge, X.; Zhang, Q.; Zhang, B. One-step synthesis of 3D sulfur/nitrogen dual-doped graphene supported nano silicon as anode for Li-ion batteries. *Appl. Surf. Sci.* **2018**, *433*, 367−373.
(261) Miao, X.; Sun, D.; Zhou, X.; Lei, Z. Designed formation of nitrogen and sulfur dual-doped hierarchically porous carbon for long-life lithium and sodium ion batteries. *Chem. Eng. J.* **2019**, *364*, 208−216.
(262) Wang, H.; Jiang, C.; Yuan, C.; Wu, Q.; Li, Q.; Duan, Q. Complexing agent engineered strategy for anchoring SnO_2 nanoparticles on sulfur/nitrogen co-doped graphene for superior lithium and sodium ion storage. *Chem. Eng. J.* **2018**, *332*, 237−244.
(263) Liu, X.; Hao, Y.; Shu, J.; Sari, H. M. K.; Lin, L.; Kou, H.; Li, J.; Liu, W.; Yan, B.; Li, D.; Zhang, J.; Li, X. Li, Nitrogen/sulfur dual-doping of reduced graphene oxide harvesting hollow $ZnSnS_3$ nano-microcubes with superior sodium storage. *Nano Energy* **2019**, *57*, 414−423.
(264) Jiang, Y.; Wu, Y.; Chen, Y.; Qi, Z.; Shi, J.; Gu, L.; Yu, Y. Design Nitrogen (N) and Sulfur (S) Co-Doped 3D Graphene Network Architectures for High-Performance Sodium Storage. *Small* **2018**, *14*, 1703471.
(265) Bag, S.; Roy, A.; Mitra, S. Sulfur, Nitrogen Dual Doped Reduced Graphene Oxide Supported Two-Dimensional Sb_2S_3 Nanostructures for the Anode Material of Sodium-Ion Battery. *ChemistrySelect* **2019**, *4*, 6679−6686.
(266) Xu, X.; Zeng, H.; Han, D.; Qiao, K.; Xing, W.; Rood, M. J.; Yan, Z. Nitrogen and sulfur co-doped graphene nanosheets to improve anode materials for sodium-ion batteries. *ACS Appl. Mater. Interfaces* **2018**, *10*, 37172−37180.
(267) Liang, X.; Ou, X.; Zheng, F.; Pan, Q.; Xiong, X.; Hu, R.; Yang, C.; Liu, M. Surface Modification of $Na_3V_2(PO_4)_3$ by Nitrogen and Sulfur Dual-Doped Carbon Layer with Advanced Sodium Storage Property. *ACS Appl. Mater. Interfaces* **2017**, *9* (15), 13151−13162.
(268) Lu, C.; Sun, Z.; Yu, L.; Lian, X.; Yi, Y.; Li, J.; Liu, Z.; Dou, S.; Sun, J. Enhanced kinetics harvested in heteroatom dual-doped graphitic hollow architectures toward high rate printable potassium-ion batteries. *Adv. Energy Mater.* **2020**, *10*, 2001161.
(269) Yang, W.; Zhou, J.; Wang, S.; Wang, Z.; Lv, F.; Zhang, W.; Zhang, W.; Sun, Q.; Guo, S. A three-dimensional carbon framework constructed by N/S co-doped graphene nanosheets with expanded interlayer spacing facilitates potassium ion storage. *ACS Energy Lett.* **2020**, *5* (5), 1653−1661.
(270) Geng, D.; Ding, N. N.; Hor, T. S. A.; Chien, S. W.; Liu, Z.; Zong, Y. Cobalt sulfide nanoparticles impregnated nitrogen and sulfur co-doped graphene as bifunctional catalyst for rechargeable Zn−air batteries. *RSC Adv.* **2015**, *5*, 7280−7284.
(271) Ganesan, P.; Ramakrishnan, P.; Prabu, M.; Shanmugam, S. Nitrogen and sulfur Co-doped graphene supported cobalt sulfide nanoparticles as an efficient air cathode for zinc-air battery. *Electrochim. Acta* **2015**, *183*, 63−69.
(272) Chen, S.; Duan, J.; Zheng, Y.; Chen, X.; Du, X. W.; Jaroniec, M.; Qiao, S.-Z. Ionic liquid-assisted synthesis of N/S-double doped graphene microwires for oxygen evolution and Zn−air batteries. *Energy Storage Mater.* **2015**, *1*, 17−24.
(273) Zhang, J.; Zhou, H.; Zhu, J.; Hu, P.; Hang, C.; Yang, J.; Peng, T.; Mu, S.; Huang, Y. Facile synthesis of defect-rich and S/N co-doped graphene-like carbon nanosheets as an efficient electrocatalyst for primary and all-solid-state Zn−air batteries. *ACS Appl. Mater. Interfaces* **2017**, *9* (29), 24545−24554.
(274) Chen, Y.; Wang, H.; Liu, F.; Gai, H.; Ji, S.; Linkov, V.; Wang, R. Hydrophobic 3D Fe/N/S doped graphene network as oxygen electrocatalyst to achieve unique performance of zinc-air battery. *Chem. Eng. J.* **2018**, *353*, 472−480.
(275) Shao, Q.; Liu, J.; Wu, Q.; Li, Q.; Wang, H.; Li, Y.; Duan, Q. In situ coupling strategy for anchoring monodisperse Co_9S_8 nanoparticles on S and N dual-doped graphene as a bifunctional electrocatalyst for rechargeable Zn−Air Battery. *Nano-Micro Lett.* **2019**, *11*, 4.
(276) Lai, C.; Gong, M.; Zhou, Y.; Fang, J.; Huang, L.; et al. Sulphur modulated Ni_3FeN supported on N/S co-doped graphene boosts rechargeable/flexible Zn-air battery performance. *Appl. Catal., B* **2020**, *274*, 119086.
(277) Zhao, Z.; Xia, Z. Interactions between Dopants in Dual-Doped Graphene Nanoribbons as Metal-Free Bifunctional Catalysts for Fuel Cell and Metal-Air Batteries. *MRS Advances* **2016**, *1*, 421−425.
(278) Li, Q.; Bai, A.; Xue, Z.; Zheng, Y.; Sun, H. Nitrogen and sulfur co-doped graphene composite electrode with high electrocatalytic activity for vanadium redox flow battery application. *Electrochim. Acta* **2020**, *362*, 137223.
(279) Daugherty, M. C.; Gu, S.; Aaron, D. S.; Mallick, B. C.; Gandomi, Y. A.; Hsieh, C. T. Decorating sulfur and nitrogen co-doped graphene

https://doi.org/10.1021/acsomega.2c06010
ACS Omega 2022, 7, 45935−45961

quantum dots on graphite felt as high-performance electrodes for vanadium redox flow batteries. *J. Power Sources* **2020**, *477*, 228709.
(280) Li, Z.; He, W.; Wang, X.; Wang, X.; Song, M.; Zhao, J. N/S dual-doped graphene with high defect density for enhanced supercapacitor properties. *Int. J. Hydrog. Energy* **2020**, *45*, 112−122.
(281) Xing, L. B.; Hou, S. F.; Zhang, J. L.; Zhou, J.; Li, Z.; Si, W.; Zhuo, S. A facile preparation of three dimensional N, S co-doped graphene hydrogels with thiocarbohydrazide for electrode materials in supercapacitor. *Mater. Lett.* **2015**, *147*, 97−100.
(282) Chen, W.; Shi, J.; Zhu, T.; Wang, Q.; Qiao, J.; Zhang, J. Preparation of nitrogen and sulfur dual-doped mesoporous carbon for supercapacitor electrodes with long cycle stability. *Electrochim. Acta* **2015**, *177*, 327−334.
(283) Tran, N. Q.; Kang, B. K.; Woo, M. H.; Yoon, D. H. Enrichment of Pyrrolic Nitrogen by Hole Defects in Nitrogen and Sulfur Co-Doped Graphene Hydrogel for Flexible Supercapacitors. *ChemSusChem* **2016**, *9*, 2261−2268.
(284) Wang, T.; Wang, L. X.; Wu, D. L.; Xia, W.; Jia, D. Z. Interaction between nitrogen and sulfur in co-doped graphene and synergetic effect in supercapacitor. *Sci. Rep.* **2015**, *5*, 9591.
(285) Poompiew, N.; Pattananuwat, P.; Potiyaraj, P. In situ hydrothermal synthesis of nickel cobalt sulfide nanoparticles embedded on nitrogen and sulfur dual doped graphene for a high performance supercapacitor electrode. *RSC Adv.* **2021**, *11*, 25057−25067.
(286) Ma, X. Q.; Shan, Y. Q.; Wang, M. Y.; Alothman, Z. A.; Xu, Z.-X; Duan, P. G.; Zhou, J.; Luque, R. Mechanochemical Preparation of N,S-Doped Graphene Oxide Using $(NH_4)_2SO_4$ for Supercapacitor Applications. *ACS Sustainable Chem. Eng.* **2020**, *8* (51), 18810−18815.
(287) Lu, Z.; Xu, X.; Chen, Y.; Wang, X.; Sun, L.; Zhuo, K. Nitrogen and sulfur co-doped graphene aerogel with hierarchically porous structure for high-performance supercapacitors. *Green Energy Environ.* **2020**, *5*, 69−75.
(288) Zhang, L.; Chen, H.; Lu, X.; Wang, Y.; Tan, L.; Sui, D.; Qi, W. Fabrication of N, S co-doped graphene aerogel for high-performance supercapacitors: π-conjugated planar molecules as efficient dopants and pillared agents. *Appl. Surf. Sci.* **2020**, *529*, 147022.
(289) Gopalsamy, K.; Balamurugan, J.; Thanh, T. D.; Kim, N. H.; Lee, J. H. Fabrication of nitrogen and sulfur co-doped graphene nanoribbons with porous architecture for high-performance supercapacitors. *Chem. Eng. J.* **2017**, *312*, 180−190.
(290) Tian, P.; Zang, J.; Jia, S.; Zhang, Y.; Gao, H.; Zhou, S.; Wang, W.; Xu, H.; Wang, Y. Preparation of S/N co-doped graphene through a self-generated high gas pressure for high rate supercapacitor. *Appl. Surf. Sci.* **2018**, *456*, 781−788.
(291) Domga; Oladoyinbo, F.; Noumi, G. B.; Tchatchueng, J. B.; Sieliechi, M. S.; Sathish, M.; Pattanayak, D. P.; Karnan, M. A simple, economical one-pot microwave assisted synthesis of nitrogen and sulfur co-doped graphene for high energy supercapacitors. *Electrochim. Acta* **2020**, *341*, 135999.
(292) Liu, J.; Chen, X.; Zhu, Y.; Chen, R.; Yuan, W. $NiCo_2S_4$/nitrogen and sulfur dual-doped three-dimensional holey-reduced graphene oxide composite architectures as high-rate battery-type cathode materials for hybrid supercapacitors. *Vacuum* **2021**, *190*, 110302.
(293) Kan, Y.; Ma, X.; Ning, G.; Li, Y.; Zhou, Y. S, N Dual-Doped Graphene Fibers: A High-Performance Electrode Material for Supercapacitors. *ChemElectroChem.* **2017**, *4*, 2677−2682.
(294) Zhang, D.; Lei, L.; Shang, Y.; Wang, K.; Wang, Y. The composite capacitive behaviors of the N and S dual doped ordered mesoporous carbon with ultrahigh doping level. *Appl. Surf. Sci.* **2016**, *360*, 807−815.
(295) Li, Z.; Wang, X.; Xu, M.; Yin, Z.; Tan, X.; Zhao, J. Facile Synthesis and Outstanding Supercapacitor Performance of Ternary Nanocomposite of Silver Particles Decorated N/S Dual-Doped Graphene and MoS_2 Microspheres Stabilized by Graphene. *J. Electrochem. Soc.* **2022**, *169*, No. 020525.
(296) Li, Z.; Wang, X.; Yin, Z.; Zhao, J.; Song, M.; Wu, Z.; Li, H.; Wang, X. Ag nanoparticles decorated N/S dual-doped graphene nanohybrids for high-performance asymmetric supercapacitors. *Carbon* **2020**, *161*, 726−735.
(297) Li, Z.; Zhao, J.; Yin, Z.; Wang, X.; Wu, Z.; Liu, D.; Zhu, M.; Wang, X. Novel Robust Nanohybrids of Pompon-like MoS_2 and N/S Dual-Doped Graphene for High-Performance Asymmetric Supercapacitors. *Energy Fuels* **2021**, *35* (3), 2692−2703.
(298) Jia, S.; Wei, J.; Meng, X.; Shao, Z. Facile and friendly preparation of N/S Co-doped graphene-like carbon nanosheets with hierarchical pore by molten salt for all-solid-state supercapacitor. *Electrochim. Acta* **2020**, *331*, 135338.
(299) Wu, X.; Ding, B.; Zhang, C.; Li, B.; Fan, Z. Self-activation of nitrogen and sulfur dual-doping hierarchical porous carbons for asymmetric supercapacitors with high energy densities. *Carbon* **2019**, *153*, 225−233.
(300) Ma, L.; Liu, J.; Lv, S.; Zhou, Q.; Shen, X.; Mo, S.; Tong, H. Scalable one-step synthesis of N, S co-doped graphene-enhanced hierarchical porous carbon foam for high-performance solid-state supercapacitors. *J. Mater. Chem. A* **2019**, *7*, 7591−7603.
(301) Wang, W.; Zhang, W.; Wang, G.; Li, C. Electrophoresis-microwave synthesis of S, N-doped graphene foam for high-performance supercapacitors. *J. Mater. Chem. A* **2021**, *9*, 15766−15775.
(302) Cheng, L.; Hu, Y.; Qiao, D.; Zhu, Y.; Wang, H.; Jiao, Z. One-step radiolytic synthesis of heteroatom (N and S) co-doped graphene for supercapacitors. *Electrochim. Acta* **2018**, *259*, 587−597.
(303) Wang, Y.; Zhang, M.; Pan, D.; Li, Y.; Ma, T.; Xie, J. Nitrogen/sulfur co-doped graphene networks uniformly coupled N-Fe_2O_3 nanoparticles achieving enhanced supercapacitor performance. *Electrochim. Acta* **2018**, *266*, 242−253.
(304) Chen, L.; Li, X.; Ma, C.; Wang, M.; Zhou, J. Interaction and quantum capacitance of nitrogen/sulfur co-doped graphene: a theoretical calculation. *J. Phys. Chem. C* **2017**, *121* (34), 18344−18350.
(305) Kannan, A. G.; Samuthirapandian, A.; Kim, D. W. Electric double layer capacitors employing nitrogen and sulfur co-doped, hierarchically porous graphene electrodes with synergistically enhanced performance. *J. Power Sources* **2017**, *337*, 65−72.
(306) Luo, Q.; Hao, F.; Wang, S.; Shen, H.; Zhao, L.; Li, J.; Gratzel, M.; Lin, H. Highly efficient metal-free sulfur-doped and nitrogen and sulfur dual-doped reduced graphene oxide counter electrodes for dye-sensitized solar cells. *J. Phys. Chem. C* **2014**, *118* (30), 17010−17018.
(307) Xu, X.; Yang, W.; Li, Y.; Tu, Z.; Wu, S.; Ma, X.; Yang, F.; Zhang, L.; Chen, S.; Wang, A.; Liu, H.; Richard, P. Heteroatom-doped graphene-like carbon films prepared by chemical vapour deposition for bifacial dye-sensitized solar cells. *Chem. Eng. J.* **2015**, *267*, 289−296.
(308) Raji Karunagaran, J.; Janakiraman, M.; Jonna, N.; Natesan, B.; Nallamuthu, P. A PDDA functionalized nitrogen and sulphur doped graphene composite as the counter electrode for dye-sensitized solar cells. *New J. Chem.* **2018**, *42*, 10184−10190.
(309) Wang, G.; Dong, W.; Ma, P.; Yan, C.; Zhang, W.; Liu, J. Interconnected nitrogen and sulfur co-doped graphene-like porous carbon nanosheets with high electrocatalytic activity as counter electrodes for dye-sensitized and Electrochim. *Acta* **2018**, *290*, 273−281.
(310) Di, Y.; Xiao, Z.; Yan, X.; Ru, G.; Chen, B.; Feng, J. Nitrogen and sulfur dual-doped chitin-derived carbon/graphene composites as effective metal-free electrocatalysts for dye sensitized solar cells. *Appl. Surf. Sci.* **2018**, *441*, 807−815.
(311) Kannan, A. G.; Zhao, J.; Jo, S. G.; Kang, Y. S.; Kim, D. W. Nitrogen and sulfur co-doped graphene counter electrodes with synergistically enhanced performance for dye-sensitized solar cells. *J. Mater. Chem. A* **2014**, *2*, 12232−12239.
(312) Liu, Y.; Wang, Y.; Zheng, X.; Wang, Y. Synergistic effect of nitrogen and sulfur co-doped graphene as efficient metal-free counter electrode for dye-sensitized solar cells: a first-principle study. *Comput. Mater. Sci.* **2017**, *136*, 44−51.
(313) Chen, H.; Luo, Q.; Liu, T.; Tai, M.; Lin, J.; Murugadoss, V.; Lin, H.; Wang, J.; Guo, Z.; Wang, N. Boosting multiple interfaces by co-doped graphene quantum dots for high efficiency and durability perovskite solar cells. *ACS Appl. Mater. Interfaces* **2020**, *12* (12), 13941−13949.
(314) Zhao, T.; Yang, D.; Xu, T.; Zhang, M.; Zhang, S.; Qin, L.; Yu, Z.-Z. Cold-Resistant Nitrogen/Sulfur Dual-Doped Graphene Fiber

https://doi.org/10.1021/acsomega.2c06010
ACS Omega 2022, 7, 45935−45961

Supercapacitors with Solar−Thermal Energy Conversion Effect. *Chem.—Eur. J.* **2021**, *27*, 3473−3482.
(315) Majumder, T.; Dhar, S.; Debnath, K.; Mondal, S. P. Role of S, N co-doped graphene quantum dots as a green photosensitizer with Ag-doped ZnO nanorods for improved electrochemical solar energy conversion. *Mater. Res. Bull.* **2017**, *93*, 214−222.
(316) Li, M.; Guo, Q.; Xie, J.; Li, Y.; Feng, Y. CuO nanoparticles supported on nitrogen and sulfur co-doped graphene nanocomposites for non-enzymatic glucose sensing. *J. Nanoparticle Res.* **2017**, *19*, 11.
(317) Chen, G.; Liu, Y.; Liu, Y.; Tian, Y.; Zhang, X. Nitrogen and sulfur dual-doped graphene for glucose biosensor application. *J. Electroanal. Chem.* **2015**, *738*, 100−107.
(318) Tian, Y.; Ma, Y.; Liu, H.; Zhang, X.; Peng, W. One-step and rapid synthesis of nitrogen and sulfur co-doped graphene for hydrogen peroxide and glucose sensing. *J. Electroanal. Chem.* **2015**, *742*, 8−14.
(319) Masteri-Farahani, M.; Ghorbani, F.; Mosleh, N. Boric acid modified S and N co-doped graphene quantum dots as simple and inexpensive turn-on fluorescent nanosensor for quantification of glucose. *Spectrochim. Acta A Mol. Biomol. Spectrosc.* **2021**, *245*, 118892.
(320) Varodi, C.; Pogăcean, F.; Cioriţă, A.; Pană, O.; Leoştean, C.; Cozar, B.; Radu, T.; Coros, M.; Stefan-van-Staden, R. L.; Pruneanu, S. M. Nitrogen and sulfur co-doped graphene as efficient electrode material for l-cysteine detection. *Chemosensors* **2021**, *9*, 146.
(321) Qi, Y.; Cao, Y.; Meng, X.; Cao, J.; Li, X.; Hao, Q.; Lei, W.; Li, Q.; Li, J.; Si, W. Facile synthesis of 3D sulfur/nitrogen co-doped graphene derived from graphene oxide hydrogel and the simultaneous determination of hydroquinone and catechol. *Sens. Actuators B: Chem.* **2019**, *279*, 170−176.
(322) Chen, C.; Zhao, D.; Hu, T.; Sun, J.; Yang, X. Highly fluorescent nitrogen and sulfur co-doped graphene quantum dots for an inner filter effect-based cyanide sensor. *Sens. Actuators B: Chem.* **2017**, *241*, 779−788.
(323) Lv, H.; Zhang, X.; Li, Y.; Ren, Y.; Zhang, C.; Wang, P.; Xu, Z.; Li, X.; Chen, Z.; Dong, Y. An electrochemical sandwich immunosensor for cardiac troponin I by using nitrogen/sulfur co-doped graphene oxide modified with Au@Ag nanocubes as amplifiers. *Microchim. Acta* **2019**, *186*, 416.
(324) Peng, J.; Zhao, Z.; Zheng, M.; Su, B.; Chen, X.; Chen, X. Electrochemical synthesis of phosphorus and sulfur co-doped graphene quantum dots as efficient electrochemiluminescent immunomarkers for monitoring okadaic acid. *Sens. Actuators B: Chem.* **2020**, *304*, 127383.
(325) Liu, Z.; Xiao, J.; Wu, X.; Lin, L.; Weng, S.; Chen, M.; Cai, X.; Lin, X. Switch-on fluorescent strategy based on N and S co-doped graphene quantum dots (NS/GQDs) for monitoring pyrophosphate ions in synovial fluid of arthritis patients. *Sens. Actuators B: Chem.* **2016**, *229*, 217−224.
(326) Safardoust-Hojaghan, H.; Amiri, O.; Hassanpour, M.; Panahi-Kalamuei, M.; Moayedi, H.; Salavati-Niasari, M. S, N co-doped graphene quantum dots-induced ascorbic acid fluorescent sensor: Design, characterization and performance. *Food Chem.* **2019**, *295*, 530−536.
(327) Yasmin, S.; Ahmed, M. S.; Jeon, S. Determination of dopamine by dual doped graphene-Fe_2O_3 in presence of ascorbic acid. *J. Electrochem. Soc.* **2015**, *162*, B363.
(328) Zhang, K.; Chen, X.; Li, Z.; Wang, Y.; Sun, S.; Guo, T.; Zhang, D.; Xue, Z.; Zhou, X.; Lu, X.; Wang, L. Au-Pt bimetallic nanoparticles decorated on sulfonated nitrogen sulfur co-doped graphene for simultaneous determination of dopamine and uric acid. *Talanta* **2018**, *178*, 315−323.
(329) Zhu, Y.; Wu, J.; Han, L.; Wang, X.; Li, W.; Guo, H.; Wei, H. Nanozyme sensor arrays based on heteroatom-doped graphene for detecting pesticides. *Anal. Chem.* **2020**, *92*, 7444−7452.
(330) Zhu, W.; Gao, J.; Song, H.; Lin, X.; Zhang, S. Nature of the synergistic effect of N and S Co-Doped graphene for the enhanced simultaneous determination of toxic pollutants. *ACS Appl. Mater. Interfaces* **2019**, *11* (47), 44545−44555.
(331) Nemati, F.; Hosseini, M.; Zare-Dorabei, R.; Ganjali, M. R. Sensitive recognition of ethion in food samples using turn-on fluorescence N and S co-doped graphene quantum dots. *Anal. Methods* **2018**, *10*, 1760−1766.
(332) Wang, W.; Xu, S.; Li, N.; Huang, Z.; Su, B.; Chen, X. Sulfur and phosphorus co-doped graphene quantum dots for fluorescent monitoring of nitrite in pickles. *Spectrochim. Acta A Mol. Biomol. Spectrosc.* **2019**, *221*, 117211.
(333) Martins, E. C.; Santana, E. R.; Spinelli, A. Nitrogen and sulfur co-doped graphene quantum dot-modified electrode for monitoring of multivitamins in energy drinks. *Talanta* **2023**, *252*, 123836.
(334) Jlassi, K.; Mallick, S.; Eribi, A.; Chehimi, M. M.; Ahmad, Z.; Touati, F.; Krupa, I. Facile preparation of NS co-doped graphene quantum dots (GQDs) from graphite waste for efficient humidity sensing. *Sens. Actuators B: Chem.* **2021**, *328*, 129058.
(335) Gavgani, J. N.; Hasani, A.; Nouri, M.; Mahyari, M.; Salehi, A. Highly sensitive and flexible ammonia sensor based on S and N co-doped graphene quantum dots/polyaniline hybrid at room temperature. *Sens. Actuators B* **2016**, *229*, 239−248.
(336) Mondal, T. K.; Dinda, D.; Saha, S. K. Nitrogen, sulphur co-doped graphene quantum dot: An excellent sensor for nitroexplosives. *Sens. Actuators B: Chem.* **2018**, *257*, 586−596.
(337) Zhang, R.; Zhang, C.; Zheng, F.; Li, X.; Sun, C. L.; Chen, W. Nitrogen and sulfur co-doped graphene nanoribbons: a novel metal-free catalyst for high performance electrochemical detection of 2, 4, 6-trinitrotoluene (TNT). *Carbon* **2018**, *126*, 328−337.
(338) Boonta, W.; Talodthaisong, C.; Sattayaporn, S.; Chaicham, C.; Chaicham, A.; Sahasithiwat, S.; Kangkaew, L.; Kulchat, S. The synthesis of nitrogen and sulfur co-doped graphene quantum dots for fluorescence detection of cobalt (II) ions in water. *Mater. Chem. Front.* **2020**, *4*, 507−516.
(339) Qu, C.; Zhang, D.; Yang, R.; Hu, J.; Qu, L. Nitrogen and sulfur co-doped graphene quantum dots for the highly sensitive and selective detection of mercury ion in living cells. *Spectrochim. Acta A Mol. Biomol. Spectrosc.* **2019**, *206*, 588−596.
(340) Gu, S.; Hsieh, C. T.; Tsai, Y. Y.; Gandomi, Y. A.; Yeom, S.; Kihm, K. D.; Fu, C. C.; Juang, R. S. Sulfur and nitrogen co-doped graphene quantum dots as a fluorescent quenching probe for highly sensitive detection toward mercury ions. *ACS Appl. Nano Mater.* **2019**, *2*, 790−798.
(341) Zhang, J.; Li, Y.; Han, S. Simultaneous detection of iodide and mercuric ions by nitrogen-sulfur co-doped graphene quantum dots based on flow injection "turn off-on" chemiluminescence analysis system. *Microchem. J.* **2019**, *147*, 1141−1146.
(342) Yang, Y.; Zou, T.; Wang, Z.; Xing, X.; Peng, S.; Zhao, R.; Zhang, X.; Wang, Y. The Fluorescent Quenching Mechanism of N and S Co-Doped Graphene Quantum Dots with Fe^{3+} and Hg^{2+} Ions and Their Application as a Novel Fluorescent. *Nanomaterials* **2019**, *9*, 738.
(343) Xu, H.; Zhou, S.; Xiao, L.; Yuan, Q.; Gan, W. Time-efficient syntheses of nitrogen and sulfur co-doped graphene quantum dots with tunable luminescence and their sensing applications. *RSC Adv.* **2016**, *6*, 36554−36560.
(344) Tian, H.; Guo, J.; Pang, Z.; Hu, M.; He, J. A sulfur, nitrogen dual-doped porous graphene nanohybrid for ultraselective Hg (ii) separation over Pb (ii) and Cu (ii). *Nanoscale* **2020**, *12*, 16543−16555.
(345) Wang, M.; Sun, Y.; Yang, M. CdS QDs amplified electrochemiluminescence of N, S co-doped graphene quantum dots and its application for Pb (II) determination. *Chem. Lett.* **2018**, *47*, 44−47.
(346) Liu, B.; Ren, X.; Chen, L.; Ma, X.; Chen, Q.; Sun, Q.; Zhang, L.; Si, P.; Ci, L. High efficient adsorption and storage of iodine on S, N co-doped graphene aerogel. *J. Hazard. Mater.* **2019**, *373*, 705−715.
(347) Shen, C.; Ge, S.; Pang, Y.; Xi, F.; Liu, J.; Dong, X.; Chen, P. Facile and scalable preparation of highly luminescent N, S co-doped graphene quantum dots and their application for parallel detection of multiple metal ions. *J. Mater. Chem. B* **2017**, *5*, 6593−6600.
(348) Li, J.; Hou, M.; Chen, Y.; Cen, W.; Chu, Y.; Yin, S. Enhanced CO_2 capture on graphene via N, S dual-doping. *Appl. Surf. Sci.* **2017**, *399*, 420−425.
(349) Kong, Q.; Wei, C.; Preis, S.; Hu, Y.; Wang, F. Facile preparation of nitrogen and sulfur co-doped graphene-based aerogel for

https://doi.org/10.1021/acsomega.2c06010
ACS Omega 2022, 7, 45935−45961

simultaneous removal of Cd^{2+} and organic dyes. *Environ. Sci. Pollut. Res.* **2018**, *25*, 21164−21175.
(350) Sun, P.; Liu, H.; Feng, M.; Guo, L.; Zhai, Z.; Fang, Y.; Zhang, X.; Sharma, V. K. Nitrogen-sulfur co-doped industrial graphene as an efficient peroxymonosulfate activator: Singlet oxygen-dominated catalytic degradation of organic contaminants. *Appl. Catal. B Envorin.* **2019**, *251*, 335−345.
(351) Brindha, A.; Sivakumar, T. Visible active N, S co-doped TiO2/graphene photocatalysts for the degradation of hazardous dyes. *J. Photochem. Photobiol., A* **2017**, *340*, 146−156.
(352) Ren, X.; Feng, J.; Si, P.; Zhang, L.; Lou, J.; Ci, L. Enhanced heterogeneous activation of peroxydisulfate by S, N co-doped graphene via controlling S, N functionalization for the catalytic decolorization of dyes in water. *Chemosphere* **2018**, *210*, 120−128.
(353) Quan, L.; Qin, F. X.; Lu, H. T.; Estevez, D.; Wang, Y. F.; et al. Sequencing dual dopants for an electromagnetic tunable graphene. *Chem. Eng. J.* **2021**, *413*, 127421.
(354) Zhang, N.; Chen, W.; Chen, P.; Wang, Y. Insight of S, N co-doped graphene aerogel (double reduction)/cobalt (II)-substituted α-Keggin-type polyoxometalate nanocomposites with synergistically enhanced impedance matching and energy conservation performance. *Compos. B. Eng.* **2020**, *191*, 107962.
(355) Sun, Z.; Yan, Z.; Li, A.; Yue, K.; Zhao, L.; Qian, L. Dual heteroatoms co-doping strategy of graphene-based dielectric loss electromagnetic absorbent. *Appl. Surf. Sci.* **2021**, *564*, 150380.
(356) Kumar, R.; Macedo, W. C., Jr; Singh, R. K.; Tiwari, V. S.; Constantino, C. J. L.; Matsuda, A.; Moshkalev, S. A. Nitrogen−sulfur co-doped reduced graphene oxide-nickel oxide nanoparticle composites for electromagnetic interference shielding. *ACS Appl. Nano Mater.* **2019**, *2* (7), 4626−4636.
(357) Farahmand Habibi, M.; Arvand, M.; Schröder, U.; Sohrabnezhad, S. Self-assembled cauliflower-like pyrite-S, N co-doped graphene quantum dots as free-standing anode with high conductivity and biocompatibility for bioelectricity production. *Fuel* **2021**, *286*, 119291.
(358) Pan, M.; Liu, S.; Pan, B.; Chew, J. W. Directionally tailoring the macroscopic polarization of piezocatalysis for hollow zinc sulfide on dual-doped graphene. *Nano Energy* **2021**, *88*, 106312.
(359) Pan, M.; Liu, S.; Chew, J. W. Unlocking the high redox activity of MoS_2 on dual-doped graphene as a superior piezocatalyst. *Nano Energy* **2020**, *68*, 104366.
(360) Wang, J.; Ma, C.; Mu, X.; Zhou, X.; He, L.; Xiao, Y.; Song, L.; Hu, Y. Designing 3D ternary-structure based on SnO_2 nanoparticles anchored hollow polypyrrole microspheres interconnected with N, S co-doped graphene towards high-performance polymer composite. *Chem. Eng. J.* **2020**, *402*, 126221.
(361) Zheng, Y.; Jiao, Y.; Li, L. H.; Xing, T.; Chen, Y.; Jaroniec, M.; Qiao, S. Z. Toward Design of Synergistically Active Carbon-Based Catalysts for Electrocatalytic Hydrogen Evolution. *ACS Nano* **2014**, *8*, 5290−5296.
(362) Xue, Y.; Wu, B.; Liu, H.; Tan, J.; Hu, W.; Liu, Y. Direct synthesis of phosphorus and nitrogen co-doped monolayer graphene with air-stable n-type characteristics. *Phys. Chem. Chem. Phys.* **2014**, *16*, 20392−20397.
(363) Li, R.; Wei, Z.; Gou, X. Nitrogen and Phosphorus Dual-Doped Graphene/Carbon Nanosheets as Bifunctional Electrocatalysts for Oxygen Reduction and Evolution. *ACS Catal.* **2015**, *5*, 4133−4142.
(364) Ananthanarayanan, A.; Wang, Y.; Routh, P.; Sk, M. A.; Than, A.; Lin, M.; Zhang, J.; Chen, J.; Sun, H.; Chen, P. Nitrogen and phosphorus co-doped graphene quantum dots: synthesis from adenosine triphosphate, optical properties, and cellular imaging. *Nanoscale* **2015**, *7*, 8159−8165.
(365) Guo, W.; Ma, X.; Zhang, X.; Zhang, Y.; Yu, D.; He, X. Spinel $CoMn_2O_4$ nanoparticles supported on a nitrogen and phosphorus dual doped graphene aerogel as efficient electrocatalysts for the oxygen reduction reaction. *RSC Adv.* **2016**, *6*, 96436−96444.
(366) Chai, G.-L.; Qiu, K.; Qiao, M.; Titirici, M.-M.; Shang, C.; Guo, Z. Active sites engineering leads to exceptional ORR and OER bifunctionality in P, N Co-doped graphene frameworks. *Energy Environ. Sci.* **2017**, *10*, 1186−1195.
(367) Cheng, C.; Li, Y.; Maouche, C.; Li, B.; Zhou, Y.; Wang, S.; Cheng, X.; Yang, J. Green synthesis of N, P-co doped porous reduced graphene oxide as an active metal-free electrocatalyst toward oxygen reduction reaction. *J. Electroanal. Chem.* **2021**, *883*, 115058.
(368) Molina-García, M. A.; Rees, N. V. Dual-doped graphene/perovskite bifunctional catalysts and the oxygen reduction reaction. *Electrochem. Commun.* **2017**, *84*, 65−70.
(369) Liao, Y.; Chen, H.; Ou, C.; Bao, L.; Li, R.; Liu, H. N, P co-doped graphene enriched Phosphorus as a highly efficient oxygen reduction catalyst. *J. Electroanal. Chem.* **2022**, *921*, 116560.
(370) Wang, J.; Wu, Z. X.; Han, L. L.; Liu, Y. Y.; Guo, J. P.; Xin, H. L.; Wang, D. L. Rational design of three-dimensional nitrogen and phosphorus co-doped graphene nanoribbons/CNTs composite for the oxygen reduction. *Chin. Chem. Lett.* **2016**, *27*, 597−601.
(371) Qiao, X.; Liao, S.; You, C.; Chen, R. Phosphorus and nitrogen dual doped and simultaneously reduced graphene oxide with high surface area as efficient metal-free electrocatalyst for oxygen reduction. *Catalysts* **2015**, *5*, 981−991.
(372) Han, C.; Chen, Z. The mechanism study of oxygen reduction reaction (ORR) on non-equivalent P, N co-doped graphene. *Appl. Surf. Sci.* **2020**, *511*, 145382.
(373) Liang, Z.; Liu, C.; Chen, M.; Qi, X.; Pramod Kumar, U.; Peera, S. G.; Liu, J.; He, J.; Liang, T. Oxygen reduction reaction mechanism on P, N co-doped graphene: a density functional theory study. *New J. Chem.* **2019**, *43*, 19308−19317.
(374) Hung, Y. H.; Dutta, D.; Tseng, C. J.; Chang, J. K.; Bhattacharyya, A. J.; Su, C. Y. Manipulation of heteroatom substitution on nitrogen and phosphorus co-doped graphene as a high active catalyst for hydrogen evolution reaction. *J. Phys. Chem. C* **2019**, *123* (36), 22202−22211.
(375) An, L.; Zhang, W.; Ma, W.; Wang, S.; Ma, L.; Liu, Q.; Guo, J.; Zhang, X. Ultrafine cobalt−ruthenium alloy on nitrogen and phosphorus co-doped graphene for electrocatalytic water splitting. *J. Taiwan Inst. Chem. Eng.* **2019**, *104*, 75−81.
(376) Chen, D.; He, Z.; Pei, S.-E.; Huang, L.-A.; Shao, H.; Jin, Y.; Wang, J. Pd nanoparticles supported on N and P dual-doped graphene as an excellent composite catalyst for methanol electro-oxidation. *J. Alloys Compd.* **2019**, *785*, 781−788.
(377) Mahyari, M.; Gavgani, J. N. Cobalt porphyrin supported on N and P co-doped graphene quantum dots/graphene as an efficient photocatalyst for aerobic oxidation of alcohols under visible-light irradiation. *Res. Chem. Intermed.* **2018**, *44*, 3641−3657.
(378) Xi, J.; Wang, Q.; Liu, J.; Huan, L.; He, Z.; Qiu, Y.; Zhang, J.; Tang, C.; Xiao, J.; Wang, S. N, P-dual-doped multilayer graphene as an efficient carbocatalyst for nitroarene reduction: a mechanistic study of metal-free catalysis. *J. Catal.* **2018**, *359*, 233−241.
(379) Liang, B.; Li, K.; Liu, Y.; Kang, X. Nitrogen and phosphorus dual-doped carbon derived from chitosan: An excellent cathode catalyst in microbial fuel cell. *Chem. Eng. J.* **2019**, *358*, 1002−1011.
(380) Gong, X.; Zhang, Q.; Gao, Y.; Shuang, S.; Choi, M. M. F.; Dong, C. Phosphorus and nitrogen dual-doped hollow carbon dot as a nanocarrier for doxorubicin delivery and biological imaging. *ACS Appl. Mater. Interfaces* **2016**, *8* (18), 11288−11297.
(381) Liu, R.; Zhao, J.; Huang, Z.; Zhang, L.; Zou, M.; Shi, B.; Zhao, S. Nitrogen and phosphorus co-doped graphene quantum dots as a nanosensor for highly sensitive and selective imaging detection of nitrite in live cell. *Sens. Actuators B Chem.* **2017**, *240*, 604−612.
(382) Shumba, M.; Nyokong, T. Development of nanocomposites of phosphorus-nitrogen co-doped graphene oxide nanosheets and nano-sized cobalt phthalocyanines for electrocatalysis. *Electrochim. Acta* **2016**, *213*, 529−539.
(383) Gu, X.; Tong, C.-J.; Lai, C.; Qiu, J.; Huang, X.; Yang, W.; Wen, B.; Liu, L.-M.; Hou, Y.; Zhang, S. A porous nitrogen and phosphorous dual doped graphene blocking layer for high performance Li−S batteries. *J. Mater. Chem. A* **2015**, *3*, 16670−16678.
(384) Wu, H.; Xia, L.; Ren, J.; Zheng, Q.; Xu, C.; Lin, D. A high-efficiency N/P co-doped graphene/CNT@ porous carbon hybrid

https://doi.org/10.1021/acsomega.2c06010
ACS Omega 2022, 7, 45935−45961

matrix as a cathode host for high performance lithium−sulfur batteries. *J. Mater. Chem. A* **2017**, *5*, 20458−20472.
(385) Zhou, X.; Liao, Q.; Bai, T.; Yang, J. Rational design of graphene@ nitrogen and phosphorous dual-doped porous carbon sandwich-type layer for advanced lithium−sulfur batteries. *J. Mater. Sci.* **2017**, *52*, 7719−7732.
(386) Zeng, P.; Huang, L.; Zhang, X.; Zhang, R.; Wu, L.; Chen, Y. Long-life and high-areal-capacity lithium-sulfur batteries realized by a honeycomb-like N, P dual-doped carbon modified separator. *Chem. Eng. J.* **2018**, *349*, 327−337.
(387) Zhang, M.; Wang, L.; Wang, B.; Zhang, B.; Sun, X.; Wang, D.; kong, Z.; Xu, L. Phosphorus-modified Fe_4N@ N, P co-doped graphene as an efficient sulfur host for high-performance lithium−sulfur batteries. *J. Mater. Chem. A* **2021**, *9*, 6538−6546.
(388) Muhammad, I.; Jabeen, M.; Wang, P.; He, Y. S.; Liao, X. Z.; Ma, Z. F. Spray-dried assembly of 3D N, P-Co-doped graphene microspheres embedded with core−shell CoP/MoP@C nanoparticles for enhanced lithium-ion storage. *Dalton Trans.* **2021**, *50*, 4555−4566.
(389) Wang, K.; Li, Z. Synthesis of nitrogen and phosphorus dual-doped graphene oxide as high-performance anode material for lithium-ion batteries. *J. Nanosci. Nanotechnol.* **2020**, *20*, 7673−7679.
(390) Ma, X.; Ning, G.; Xu, C.; Gao, J.; Qi, C. Phosphorus and Nitrogen Dual-Doped Few-Layered Porous Graphene: A High-Performance Anode Material for Lithium-Ion Batteries. *ACS Appl. Mater. Interfaces* **2014**, *6*, 14415−14422.
(391) Li, C.; Fu, Q.; Zhao, K.; Wang, Y.; Tang, H.; Li, H.; Jiang, H.; Chen, L. Nitrogen and phosphorous dual-doped graphene aerogel with rapid capacitive response for sodium-ion batteries. *Carbon* **2018**, *139*, 1117−1125.
(392) Wang, Y.; Fu, Q.; Li, C.; Li, H.; Tang, H. Nitrogen and Phosphorus Dual-Doped Graphene Aerogel Confined Monodisperse Iron Phosphide Nanodots as an Ultrafast and Long-Term Cycling Anode Material for Sodium-Ion Batteries. *ACS Sustainable Chem. Eng.* **2018**, *6* (11), 15083−15091.
(393) Qin, D.; Liu, Z.; Zhao, Y.; Xu, G.; Zhang, F.; Zhang, X. A sustainable route from corn stalks to N, P-dual doping carbon sheets toward high performance sodium-ion batteries anode. *Carbon* **2018**, *130*, 664−671.
(394) Wu, Q.; Wang, J.; Wang, H.; Si, Z.; Li, C.; Bai, J. Doped graphene encapsulated SnP_2O_7 with enhanced conversion reactions from polyanions as a versatile anode material for sodium dual-ion battery. *Electrochim. Acta* **2021**, *369*, 137657.
(395) Gao, X.; Dong, X.; Xing, Z.; Nie, C.; Zheng, G.; Ju, Z. Electrolyte Salt Chemistry Enables 3D Nitrogen and Phosphorus Dual-Doped Graphene Aerogels for High-Performance Potassium-Ion Batteries. *Adv. Mater. Technol.* **2021**, *6*, 2100207.
(396) Ge, L.; Wang, D.; Yang, P.; Xu, H.; Xiao, L.; Zhang, G. X.; Lu, X.; Duan, Z.; Meng, F.; Zhang, J.; An, M. Graphite N−C−P dominated three-dimensional nitrogen and phosphorus co-doped holey graphene foams as high-efficiency electrocatalysts for Zn−air batteries. *Nanoscale* **2019**, *11*, 17010−17017.
(397) Shao, Q.; Li, Y.; Cui, X.; Li, T.; Wang, H.; Li, Y.; Duan, Q.; Si, Z. Metallophthalocyanine-Based Polymer-Derived Co_2P Nanoparticles Anchoring on Doped Graphene as High-Efficient Trifunctional Electrocatalyst for Zn-Air Batteries. *ACS Sustainable Chem. Eng.* **2020**, *8* (16), 6422−6432.
(398) Zhang, G.; Xing, J.; Zhao, Y.; Yang, F. Hierarchical N, P co-doped graphene aerogels framework assembling vertically grown CoMn-LDH nanosheets as efficient bifunctional electrocatalyst for rechargeable Zinc-air battery. *J. Colloid Interface Sci.* **2021**, *590*, 476−486.
(399) Wen, Y.; Rufford, T. E.; Hulicova-Jurcakova, D.; Wang, L. Nitrogen and phosphorous co-doped graphene monolith for supercapacitors. *ChemSusChem* **2016**, *9*, 513−520.
(400) Xia, K.; Huang, Z.; Zheng, L.; Han, B.; Gao, Q.; Zhou, C.; Wang, H.; Wu, J. Facile and controllable synthesis of N/P co-doped graphene for high-performance supercapacitors. *J. Power Sources* **2017**, *365*, 380−388.
(401) Zhao, X.; Wang, S.; Wu, Q. Nitrogen and phosphorus dual-doped hierarchical porous carbon with excellent supercapacitance performance. *Electrochim. Acta* **2017**, *247*, 1140−1146.
(402) Wang, C.; Zhao, J.; Luo, S.; Yu, X. Improved Pseudocapacitive Performance of Graphene Architectures Modulating by Nitrogen/Phosphorus Dual-Doping and Steam-Activation. *Macromol. Res.* **2021**, *29*, 582−588.
(403) Wei, F.; Wei, Y.; Wang, J.; Han, M.; Lv, Y. N, P dual doped foamy-like carbons with abundant defect sites for zinc ion hybrid capacitors. *Chem. Eng. J.* **2022**, *450*, 137919.
(404) Cheng, H.; Yi, F.; Gao, A.; Liang, H.; Shu, D.; Zhou, X.; He, C.; Zhu, Z. Supermolecule self-assembly promoted porous N, P Co-doped reduced graphene oxide for high energy density supercapacitors. *ACS Appl. Energy Mater.* **2019**, *2* (6), 4084−4091.
(405) Li, G.; Li, Y.; Deng, J.; Lin, H.; Hou, X.; Jia, L. Ultrahigh rate capability supercapacitors based on tremella-like nitrogen and phosphorus co-doped graphene. *Mater. Chem. Front.* **2020**, *4*, 2704−2715.
(406) Sandhiya, M.; Sathish, M. Enhanced electrochemical performance of supercritical fluid treated N, P co-doped graphene by dual redox-additives. *J. Power Sources* **2022**, *540*, 231587.
(407) Zhao, Y.; Hao, H.; Song, T.; Wang, X.; Li, C.; Li, W. High energy-power density Zn-ion hybrid supercapacitors with N/P co-doped graphene cathode. *J. Power Sources* **2022**, *521*, 230941.
(408) Nazarian-Samani, M.; Haghighat-Shishavan, S.; Nazarian-Samani, M.; Kim, M.-S.; Cho, B.-W.; Oh, S.-H.; Kashani-Bozorg, S. F.; Kim, K.-B. Rational hybrid modulation of P, N dual-doped holey graphene for high-performance supercapacitors. *J. Power Sources* **2017**, *372*, 286−296.
(409) Wang, C.; Luo, S.; Yang, Y.; Ren, D.; Yu, X. Defect-Rich Graphene Architecture Induced by Nitrogen and Phosphorus Dual Doping for High-Performance Supercapacitors. *Energy Technology* **2020**, *8*, 1900685.
(410) Zhang, M.; Liu, H.; Ma, T.; Song, Z.; Shao, S. Ultrathin porous $Mn(PO_3)_2$ nanosheets and MoO_2 nanocrystal arrays on N, P-dual-doped graphene for high-energy asymmetric supercapacitor. *Chem. Eng. J.* **2021**, *403*, 126379.
(411) Wang, Z.; Tan, Y.; Yang, Y.; Zhao, X.; Liu, Y.; Niu, L.; et al. Pomelo peels-derived porous activated carbon microsheets dual-doped with nitrogen and phosphorus for high performance electrochemical capacitors. *J. Power Sources* **2018**, *378*, 499−510.
(412) Li, H.; Liu, T.; He, Y.; Song, J.; Meng, A.; Sun, C.; Hu, M.; Wang, L.; Li, G.; Zhang, Z.; Liu, Y.; Zhao, J.; Li, Z. Interfacial Engineering and a Low-Crystalline Strategy for High-Performance Supercapacitor Negative Electrodes: $Fe_2P_2O_7$ Nanoplates Anchored on N/P Co-doped Graphene Nanotubes. *ACS Appl. Mater. Interfaces* **2022**, *14* (2), 3363−3373.
(413) Deng, Y.; Wang, H.; Zhang, K.; Qiu, J.; Yan, L. Flexible Quasi-Solid-State High-Performance Aqueous Zinc Ion Hybrid Supercapacitor with Water-in-Salt Hydrogel Electrolyte and N/P-Dual Doped Graphene. *Adv. Sustainable Syst.* **2022**, *6*, 2100191.
(414) Rahimi-Aghdam, T.; Shariatinia, Z.; Hakkarainen, M.; Haddadi-Asl, V. Nitrogen and phosphorous doped graphene quantum dots: Excellent flame retardants and smoke suppressants for polyacrylonitrile nanocomposites. *J. Hazard. Mater.* **2020**, *381*, 121013.
(415) Feng, Y.; Wang, B.; Li, X.; Ye, Y.; Ma, J.; Liu, C.; Zhou, X.; Xie, X. Enhancing thermal oxidation and fire resistance of reduced graphene oxide by phosphorus and nitrogen co-doping: Mechanism and kinetic analysis. *Carbon* **2019**, *146*, 650−659.
(416) Feng, Y.; He, C.; Wen, Y.; Ye, Y.; Zhou, X.; Xie, X.; Mai, Y. W. Superior flame retardancy and smoke suppression of epoxy-based composites with phosphorus/nitrogen co-doped graphene. *J. Hazard. Mater.* **2018**, *346*, 140−151.
(417) Esrafili, M. D.; Mohammad-Valipour, R.; Mousavi-Khoshdel, S. M.; Nematollahi, P. A Comparative Study of CO Oxidation on Nitrogen-and Phosphorus-Doped Graphene. *ChemPhysChem* **2015**, *16*, 3719−3727.

https://doi.org/10.1021/acsomega.2c06010
ACS Omega 2022, 7, 45935−45961

(418) Han, C.; Chen, Z. Adsorption properties of O_2 on the unequal amounts of binary co-doped graphene by B/N and P/N: a density functional theory study. *Appl. Surf. Sci.* **2019**, *471*, 445−454.
(419) Cruz-Silva, E.; López-Urías, F.; Muñoz-Sandoval, E.; Sumpter, B. G.; Terrones, H.; Charlier, J. C.; Meunier, V.; Terrones, M. Electronic Transport and Mechanical Properties of Phosphorus and Phosphorus−Nitrogen-Doped Carbon Nanotubes. *ACS Nano* **2009**, *3*, 1913−1921.
(420) Yuan, B.; Xing, W.; Hu, Y.; Mu, X.; Wang, J.; Tai, Q.; Li, G.; Liu, L.; Liew, K. M.; Hu, Y. Boron/phosphorus doping for retarding the oxidation of reduced graphene oxide. *Carbon* **2016**, *101*, 152−158.
(421) Meng, J.; Tong, Z.; Sun, H.; Liu, Y.; Zeng, S.; Xu, J.; Xia, Q.; Pan, Q.; Dou, S.; Yu, H. Metal-Free Boron/Phosphorus Co-Doped Nanoporous Carbon for Highly Efficient Benzyl Alcohol Oxidation. *Adv. Sci.* **2022**, *9*, 2200518.
(422) Ma, G.; Huang, K.; Ma, J.-S.; Ju, Z.; Xing, Z.; Zhuang, Q.-C. Phosphorus and oxygen dual-doped graphene as superior anode material for room-temperature potassium-ion batteries. *J. Mater. Chem. A* **2017**, *5*, 7854−7861.
(423) Yu, X.; Kang, Y.; Park, H. S. Sulfur and phosphorus co-doping of hierarchically porous graphene aerogels for enhancing supercapacitor performance. *Carbon* **2016**, *101*, 49−56.
(424) Patel, M. A.; Luo, F.; Savaram, K.; Kucheryavy, P.; Xie, Q.; Flach, C.; Mendelsohn, F.; Garfunkel, E.; Lockard, J. V.; He, H. P and S dual-doped graphitic porous carbon for aerobic oxidation reactions: Enhanced catalytic activity and catalytic sites. *Carbon* **2017**, *114*, 383−392.
(425) Liu, H.; Zhang, M.; Ma, T.; Wang, Y. Ni and NiO in situ grown on sulfur and phosphorus co-doped graphene as effective bifunctional catalyst for hydrogen evolution. *J. Electroanal. Chem.* **2019**, *848*, 113306.
(426) An, M.; Du, L.; Du, C.; Sun, Y.; Wang, Y.; Yin, G.; Gao, Y. Pt nanoparticles supported by sulfur and phosphorus co-doped graphene as highly active catalyst for acidic methanol electrooxidation. *Electrochim. Acta* **2018**, *285*, 202−213.
(427) Jing, C.; Guo, X.; Xia, L.; Chen, Y.; Wang, X.; Liu, X.; Dong, B.; Dong, F.; Li, S.; Zhang, Y. Morphologically confined hybridization of tiny $CoNi_2S_4$ nanosheets into S, P co-doped graphene leading to enhanced pseudocapacitance and rate capability. *Chem. Eng. J.* **2020**, *379*, 122305.
(428) Zhang, M.; Wang, Y.; Liu, H.; Ma, T.; Xie, J.; Shao, S. Controllable synthesis of CoNb2O6 nanoparticles on multifunctional sulfur and phosphorus dual-doped graphene as advanced electrodes for hybrid supercapacitors. *Electrochim. Acta* **2019**, *309*, 104−115.
(429) Yu, X.; Pei, C.; Feng, L. Surface modulated hierarchical graphene film via sulfur and phosphorus dual-doping for high performance flexible supercapacitors. *Chin. Chem. Lett.* **2019**, *30*, 1121−1125.
(430) Chen, X.; Li, H.; Zhang, G.; Feng, S.; Yang, G.; Shi, L.; Liu, W.; Liu, G.; Pan, H. Au@Pt Hybrid Nanorods Encapsulated in B, S dual-doped Graphene as Highly Sensitive Immunosensing Platform for Electrochemical Determination of Aflatoxin B1. *Int. J. Electrochem. Sci.* **2020**, *15*, 6269−6289.
(431) Olaniyan, O.; Mapasha, R. E.; Momodu, D. Y.; Madito, M. J.; et al. Exploring the stability and electronic structure of beryllium and sulphur co-doped graphene: a first principles study. *RSC Adv.* **2016**, *6*, 88392−88402.
(432) Niu, F.; Liu, J. M.; Tao, L. M.; Wang, W.; Song, W. G. Nitrogen and silica co-doped graphene nanosheets for NO_2 gas sensing. *J. Mater. Chem. A* **2013**, *1*, 6130−6133.
(433) Zhou, X.; Zhao, C.; Wu, G.; Chen, J.; Li, Y. DFT study on the electronic structure and optical properties of N, Al, and N-Al doped graphene. *Appl. Surf. Sci.* **2018**, *459*, 354−362.
(434) Li, S.; Lu, Z.; Zhang, Y.; Ma, D.; Yang, Z. Mechanisms of direct hydrogen peroxide synthesis on silicon and phosphorus dual-doped graphene: a DFT-D study. *Phys. Chem. Chem. Phys.* **2017**, *19*, 9007−9015.
(435) Liu, H.; Tang, Y.; Zhao, W.; Ding, W.; Xu, J.; Liang, C.; Zhang, Z.; Huang, F. Facile Synthesis of Nitrogen and Halogen Dual-Doped Porous Graphene as an Advanced Performance Anode for Lithium-Ion Batteries. *Adv. Mater. Interfaces* **2018**, *5*, 1701261.
(436) Denis, P. A. Mono and dual doped monolayer graphene with aluminum, silicon, phosphorus and sulfur. *Comp. Theor Chem.* **2016**, *1097*, 40−47.
(437) Ullah, S.; Denis, P. A.; Sato, F. First-principles study of dual-doped graphene: towards promising anode materials for Li/Na-ion batteries. *New J. Chem.* **2018**, *42*, 10842−10851.
(438) Ullah, S.; Denis, P. A.; Sato, F. Adsorption and diffusion of alkali-atoms (Li, Na, and K) on BeN dual doped graphene. *Int. J. Quantum Chem.* **2019**, *119*, e25900.
(439) Hussain, A.; Ullah, S.; Farhan, M. A. Fine tuning the band-gap of graphene by atomic and molecular doping: a density functional theory study. *RSC Adv.* **2016**, *6*, 55990−56003.
(440) Olaniyan, O.; Maphasha, R. E.; Madito, M. J.; Khaleed, A. A.; Igumbor, E.; Manyala, N. A systematic study of the stability, electronic and optical properties of beryllium and nitrogen co-doped graphene. *Carbon* **2018**, *129*, 207−227.
(441) Denis, P. A.; Iribarne, F. Dual doped monolayer and bilayer graphene: The case of 4p and 2p elements. *Chem. Phys. Lett.* **2016**, *658*, 152.
(442) Safaei Ardakani, Y. S.; Moradi, M. A DFT/TDDFT study on dual doped bilayer graphene containing Se and X (Ga, P, S). *Eur. Phys. J. B* **2020**, *93*, 99.
(443) Chen, J.; Lin, C.; Zhang, M.; Jin, T.; Qian, Y. Constructing Nitrogen, Selenium Co-Doped Graphene Aerogel Electrode Materials for Synergistically Enhanced Capacitive Performance. *ChemElectroChem.* **2020**, *7*, 3311.
(444) Zhong, Y.; Xu, H.; Zhang, Q.; Song, X.; Hao, C. The Structural Design of Dual-Element-Doped Graphene for Iodine Reduction Reaction: Density Functional Theory Study. *ChemistrySelect* **2022**, *7*, e202200380.
(445) Dong, Q.; Zhuang, X.; Li, Z.; Li, B.; Fang, B.; Yang, C.; Xie, H.; Zhang, F.; Feng, X. Efficient approach to iron/nitrogen co-doped graphene materials as efficient electrochemical catalysts for the oxygen reduction reaction. *J. Mater. Chem. A* **2015**, *3*, 7767−7772.
(446) Zitolo, A.; Goellner, V.; Armel, V.; Sougrati, M. T.; Mineva, T.; Stievano, L.; Fonda, E.; Jaouen, F. Identification of catalytic sites for oxygen reduction in iron-and nitrogen-doped graphene materials. *Nat. Mater.* **2015**, *14*, 937−942.
(447) Niu, Y.; Huang, X.; Hu, W. Fe_3C nanoparticle decorated Fe/N doped graphene for efficient oxygen reduction reaction electrocatalysis. *J. Power Sources* **2016**, *332*, 305−311.
(448) Jiang, H.; Yao, Y.; Zhu, Y.; Liu, Y.; Su, Y.; Yang, X.; Li, C. Iron carbide nanoparticles encapsulated in mesoporous Fe−N-doped graphene-like carbon hybrids as efficient bifunctional oxygen electrocatalysts. *ACS Appl. Mater. Interfaces* **2015**, *7* (38), 21511−21520.
(449) Sibul, R.; Kibena-Põldsepp, E.; Ratso, S.; Kook, M.; Sougrati, M. T.; Käärik, M.; Merisalu, M.; Aruväli, J.; Paiste, P.; Treshchalov, A.; Leis, J.; Kisand, V.; Sammelselg, V.; Holdcroft, S.; Jaouen, F.; Tammeveski, K. Iron-and Nitrogen-Doped Graphene-Based Catalysts for Fuel Cell Applications. *ChemElectroChem.* **2020**, *7*, 1739−1747.
(450) Zhang, Z.; Huang, X.; Xu, H. Anchoring an Fe Dimer on Nitrogen-Doped Graphene toward Highly Efficient Electrocatalytic Ammonia Synthesis. *ACS Appl. Mater. Interfaces* **2021**, *13*, 43632−43640.
(451) Gao, X. X.; Zhou, X.; Ma, Y. F.; Wang, C. P.; Chu, F. A fluorometric and colorimetric dual-mode sensor based on nitrogen and iron co-doped graphene quantum dots for detection of ferric ions in biological fluids and cellular imaging. *New J. Chem.* **2018**, *42*, 14751−14756.
(452) Zhang, L.; Liang, P.; Man, X.; Wang, D.; Huang, J.; Shu, H.; Liu, Z.; Wang, L. Fe, N co-doped graphene as a multi-functional anchor material for lithium-sulfur battery. *J. Phys. Chem. Solids.* **2019**, *126*, 280−286.
(453) Zeng, Q. W.; Hu, R. M.; Chen, Z. B.; Shang, J. X. Single-atom Fe and N co-doped graphene for lithium-sulfur batteries: a density functional theory study. *Mater. Res. Express* **2019**, *6*, No. 095620.

https://doi.org/10.1021/acsomega.2c06010
ACS Omega 2022, 7, 45935−45961

(454) Ni, Y.; Chen, Z.; Kong, F.; Qiao, Y.; Kong, A.; Shan, Y. Space-confined synthesis of multilayer Cu−N-doped graphene nanosheets for efficient oxygen electroreduction. *Dalton Trans.* **2017**, *46*, 8586−8592.
(455) Zhu, G.; Liu, F.; Wang, Y.; Wei, Z.; Wang, W. Systematic exploration of N, C coordination effects on the ORR performance of Mn−N_x doped graphene catalysts based on DFT calculations. *Phys. Chem. Chem. Phys.* **2019**, *21*, 12826−12836.
(456) Luo, M.; Liang, Z.; Liu, C.; Qi, X.; Chen, M.; Sagar, R. U. R.; Yang, H.; Liang, T. Single−atom manganese and nitrogen co-doped graphene as low-cost catalysts for the efficient CO oxidation at room temperature. *Appl. Surf. Sci.* **2021**, *536*, 147809.
(457) Lee, B. H.; Hasan, M. T.; Lichthardt, D.; Gonzalez-Rodriguez, R.; Naumov, A. V. Manganese−nitrogen and gadolinium−nitrogen Co-doped graphene quantum dots as bimodal magnetic resonance and fluorescence imaging nanoprobes. *Nanotechnology* **2021**, *32*, No. 095103.
(458) Li, F.; Shu, H.; Hu, C.; Shi, Z.; Liu, X.; Liang, P.; Chen, X. Atomic mechanism of electrocatalytically active Co−N complexes in graphene basal plane for oxygen reduction reaction. *ACS Appl. Mater. Interfaces* **2015**, *7* (49), 27405−27413.
(459) Han, M.; Shi, M.; Wang, J.; Zhang, M.; Yan, C.; Jiang, J.; Guo, S.; Sun, Z.; Guo, Z. Efficient bifunctional Co/N dual-doped carbon electrocatalysts for oxygen reduction and evolution reaction. *Carbon* **2019**, *153*, 575−584.
(460) Liu, X.; Amiinu, I. S.; Liu, S.; Cheng, K.; Mu, S. Transition metal/nitrogen dual-doped mesoporous graphene-like carbon nanosheets for the oxygen reduction and evolution reactions. *Nanoscale* **2016**, *8*, 13311−13320.
(461) Du, Z.; Chen, X.; Hu, W.; Chuang, C.; Xie, S.; Hu, A.; Yan, W.; Kong, X.; Wu, X.; Ji, H.; Wan, L. J. Cobalt in nitrogen-doped graphene as single-atom catalyst for high-sulfur content lithium−sulfur batteries. *J. Am. Chem. Soc.* **2019**, *141* (9), 3977−3985.
(462) Zhang, L.; Liang, P.; Shu, H. B.; Man, X. L.; Du, X. Q.; Chao, C. L.; Liu, Z. G.; Sun, Y. P.; Wan, H. Z.; Wang, W. Design rules of heteroatom-doped graphene to achieve high performance lithium−sulfur batteries: both strong anchoring and catalysing based on first principles. *J. Colloid Interface Sci.* **2018**, *529*, 426−431.
(463) Xiao, M.; Zhu, J.; Li, G.; Li, N.; Li, S.; Cano, Z. P.; Ma, L.; Cui, P.; Xu, P.; Jiang, G.; Jin, H.; Wang, S.; Wu, T.; Lu, J.; Yu, A.; Su, D.; Chen, Z. Single atom iridium heterogeneous catalyst in oxygen reduction reaction. *Angew. Chem., Int. Ed.* **2019**, *58*, 9640.
(464) Zhou, Q.; Zhang, M.; Zhu, B.; Gao, Y. Investigation of the Stability and Hydrogen Evolution Activity of Dual-Atom Catalysts on Nitrogen-Doped Graphene. *Nanomaterials* **2022**, *12*, 2557.
(465) He, P.; Feng, H.; Wang, S.; Ding, H.; Liang, Y.; Ling, M.; Zhang, X. Electrocatalytic CO_2 reduction reaction on dual-metal- and nitrogen-doped graphene: coordination environment effect of active sites. *Mater. Adv.* **2022**, *3*, 4566−4577.
(466) Kharangarh, P. R.; Gupta, V.; Singh, A.; Bhardwaj, P.; Grace, A. N. An efficient pseudocapacitor electrode material with co-doping of iron (II) and sulfur in luminescent graphene quantum dots. *Diam. Relat. Mater.* **2020**, *107*, 107913.
(467) Gu, J.; Zhang, X.; Fu, L.; Pang, A. Study on the hydrogen storage properties of the dual active metals Ni and Al doped graphene composites. *Int. J. Hydrogen Energy* **2019**, *44*, 6036−6044.
(468) Ullah, S.; Denis, P. A.; Sato, F. Triple-Doped Monolayer Graphene with Boron, Nitrogen, Aluminum, Silicon, Phosphorus, and Sulfur. *ChemPhysChem* **2017**, *18*, 1864−1873.
(469) Razmjooei, F.; Singh, K. P.; Song, M. Y.; Yu, J. S. Enhanced electrocatalytic activity due to additional phosphorous doping in nitrogen and sulfur-doped graphene: a comprehensive study. *Carbon* **2014**, *78*, 257−267.
(470) Wang, W.; Wang, X.; Xing, J.; Gong, Q.; Wang, H.; Wang, J.; Chen, Z.; Ai, Y.; Wang, X. Multi-heteroatom doped graphene-like carbon nanospheres with 3D inverse opal structure: A promising bisphenol-A remediation material. *Environ. Sci.: Nano* **2019**, *6*, 809−819.
(471) Wang, Y.; Zhang, B.; Xu, M.; He, X. Tunable ternary (P, S, N)-doped graphene as an efficient electrocatalyst for oxygen reduction reaction in an alkaline medium. *RSC Adv.* **2015**, *5*, 86746−86753.
(472) Dou, S.; Shen, A.; Ma, Z.; Wu, J.; Tao, L.; Wang, S. N-, P-and S-tridoped graphene as metal-free electrocatalyst for oxygen reduction reaction. *J. Electroanal. Chem.* **2015**, *753*, 21−27.
(473) Wang, Y.; Xu, N.; He, R.; Peng, L.; Cai, D.; Qiao, J. Large-scale defect-engineering tailored tri-doped graphene as a metal-free bifunctional catalyst for superior electrocatalytic oxygen reaction in rechargeable Zn-air. *Appl. Catal., B* **2021**, *285*, 119811.
(474) Zheng, X.; Wu, J.; Cao, X.; Abbott, J.; Jin, C.; Wang, H.; Strasser, P.; Yang, R.; Chen, X.; Wu, G. N-, P-, and S-doped graphene-like carbon catalysts derived from onium salts with enhanced oxygen chemisorption for Zn-air battery cathodes. *Appl. Catal. B: Environ.* **2019**, *241*, 442−451.
(475) Xu, Y.; Wang, S.; Hou, X.; Sun, Z.; Jiang, Y.; Dong, Z.; Tao, Q.; Man, J.; Cao, Y. Coal-derived nitrogen, phosphorus and sulfur co-doped graphene quantum dots: A promising ion fluorescent probe. *Appl. Surf. Sci.* **2018**, *445*, 519−526.
(476) Li, Y.; Wen, H.; Yang, J.; Zhou, Y.; Cheng, X. Boosting oxygen reduction catalysis with N, F, and S tri-doped porous graphene: tertiary N-precursors regulates the constitution of catalytic active sites. *Carbon* **2019**, *142*, 1−12.
(477) Murugesan, B.; Pandiyan, N.; Arumugam, M.; et al. Two dimensional graphene oxides converted to three dimensional P, N, F and B, N, F tri-doped graphene by ionic liquid for efficient catalytic performance. *Carbon* **2019**, *151*, 53−67.
(478) Kundu, S.; Sarojinijeeva, P.; Karthick, R.; Anantharaj, G.; Saritha, G.; Bera, R.; Anandan, S.; Patra, A.; Ragupathy, P.; Selvaraj, M.; Jeyakumar, D.; Pillai, K. V. Enhancing the Efficiency of DSSCs by the Modification of TiO_2 Photoanodes using N, F and S, co-doped Graphene Quantum Dots. *Electrochim. Acta* **2017**, *242*, 337−343.
(479) Kundu, S.; Yadav, R. M.; Narayanan, T. N.; Shelke, M. V.; Vajtai, R.; Ajayan, P. M.; Pillai, V. K. Synthesis of N, F and S co-doped graphene quantum dots. *Nanoscale* **2015**, *7*, 11515−11519.
(480) Zhang, J.; Dai, L. Nitrogen, phosphorus, and fluorine tri-doped graphene as a multifunctional catalyst for self-powered electrochemical water splitting. *Angew. Chem., Int. Ed.* **2016**, *55*, 13296.
(481) Lin, H.; Chu, L.; Wang, X.; Yao, Z.; Liu, F.; Ai, Y.; Zhuang, X.; Han, S. Boron, nitrogen, and phosphorous ternary doped graphene aerogel with hierarchically porous structures as highly efficient electrocatalysts for oxygen reduction reaction. *New J. Chem.* **2016**, *40*, 6022−6029.
(482) Dong, F.; Cai, Y.; Liu, C.; Liu, J.; Qiao, J. Heteroatom (B, N and P) doped porous graphene foams for efficient oxygen reduction reaction electrocatalysis. *Int. J. Hydrog. Energy* **2018**, *43*, 12661−12670.
(483) Zhao, Y.; Huang, S.; Xia, M.; Rehman, S.; Mu, S.; Kou, Z.; et al. N-P-O co-doped high performance 3D graphene prepared through red phosphorous-assisted "cutting-thin" technique: A universal synthesis and multifunctional. *Nano Energy* **2016**, *28*, 346−355.
(484) Hu, R.; Li, Y.; Zeng, Q.; Shang, J. Role of active sites in N-coordinated Fe-Co dual-metal doped graphene for oxygen reduction and evolution reactions: A theoretical insight. *Appl. Surf. Sci.* **2020**, *525*, 146588.
(485) He, T.; Santiago, A. R. P.; Du, A. Atomically embedded asymmetrical dual-metal dimers on N-doped graphene for ultra-efficient nitrogen reduction reaction. *J. Catal.* **2020**, *388*, 77−83.
(486) Zhou, Y.; Yang, W.; Utetiwabo, W.; Lian, Y.; Yin, X.; Zhou, L.; Yu, P.; Chen, R.; Sun, S. Revealing of active sites and catalytic mechanism in N-coordinated Fe, Ni dual-doped carbon with superior acidic oxygen reduction than single-atom catalyst. *J. Phys. Chem. Lett.* **2020**, *11* (4), 1404−1410.
(487) Wu, C.; Yang, W.; Wang, J. J.; Li, H.; Gates, I. D. Methane activation on dual-atom catalysts supported on graphene. *Chem. Commun.* **2021**, *57*, 12127−12130.
(488) Qiao, X.; You, C.; Shu, T.; Fu, Z.; Zheng, R.; Zeng, X.; Li, X.; Liao, S. A one-pot method to synthesize high performance multielement co-doped reduced graphene oxide catalysts for oxygen reduction. *Electrochem. Commun.* **2014**, *47*, 49−53.

https://doi.org/10.1021/acsomega.2c06010
ACS Omega 2022, 7, 45935−45961

(489) Feng, M.; Zhang, Q.; Sun, S.; Zhang, X.; Hu, S. In-situ synthesis of Fe, N, S co-doped graphene-like nanosheets around carbon nanoparticles with dual-nitrogen-source as efficient electrocatalyst for oxygen reduction reaction. *Int. J. Hydrog. Energy* **2021**, *46*, 8002−8013.
(490) Molina-García, M. A.; Rees, N. V. "Metal-free" electrocatalysis: Quaternary-doped graphene and the alkaline oxygen reduction reaction. *Appl. Catal., A* **2018**, *553*, 107−116.
(491) Nguyen, G. D.; Toma, F. M.; Cao, T.; Pedramrazi, Z.; Chen, C.; Rizzo, D. J.; Joshi, T.; Bronner, C.; Chen, Y.-C.; Favaro, M.; Louie, S. G.; Fischer, F. R.; Crommie, M. F. Crommie, Bottom-Up Synthesis of N = 13 Sulfur-Doped Graphene Nanoribbons. *J. Phys. Chem. C* **2016**, *120* (5), 2684−2687.

https://doi.org/10.1021/acsomega.2c06010
ACS Omega 2022, 7, 45935−45961